Journal of Nanobiotechnology

REVIEW

Open Access

Recent advances of photoresponsive nanomaterials for diagnosis and treatment of acute kidney injury

Shijie Yao[1], Yinan Wang[2], Xiaozhou Mou[4*], Xianghong Yang[1*] and Yu Cai[3,4*]

Abstract

Non-invasive imaging in the near-infrared region (NIR) offers enhanced tissue penetration, reduced spontaneous fluorescence of biological tissues, and improved signal-to-noise ratio (SNR), rendering it more suitable for in vivo deep tissue imaging. In recent years, a plethora of NIR photoresponsive materials have been employed for disease diagnosis, particularly acute kidney injury (AKI). These encompass inorganic nonmetallic materials such as carbon (C), silicon (Si), phosphorus (P), and upconversion nanoparticles (UCNPs); precious metal nanoparticles like gold and silver; as well as small molecule and organic semiconductor polymer nanoparticles with near infrared responsiveness. These materials enable effective therapy triggered by NIR light and serve as valuable tools for monitoring AKI in living systems. The review provides a concise overview of the current state and pathological characteristics of AKI, followed by an exploration of the application of nanomaterials and photoresponsive nanomaterials in AKI. Finally, it presents the design challenges and prospects associated with NIR photoresponsive materials in AKI.

Keywords Acute kidney injury, Near-infrared, Nanomaterials, Fluorescent probe, Diagnosis and treatment

*Correspondence:
Xiaozhou Mou
mouxz@zju.edu.cn
Xianghong Yang
jyy623@163.com
Yu Cai
caiyu@hmc.edu.cn
Full list of author information is available at the end of the article

Graphical Abstract

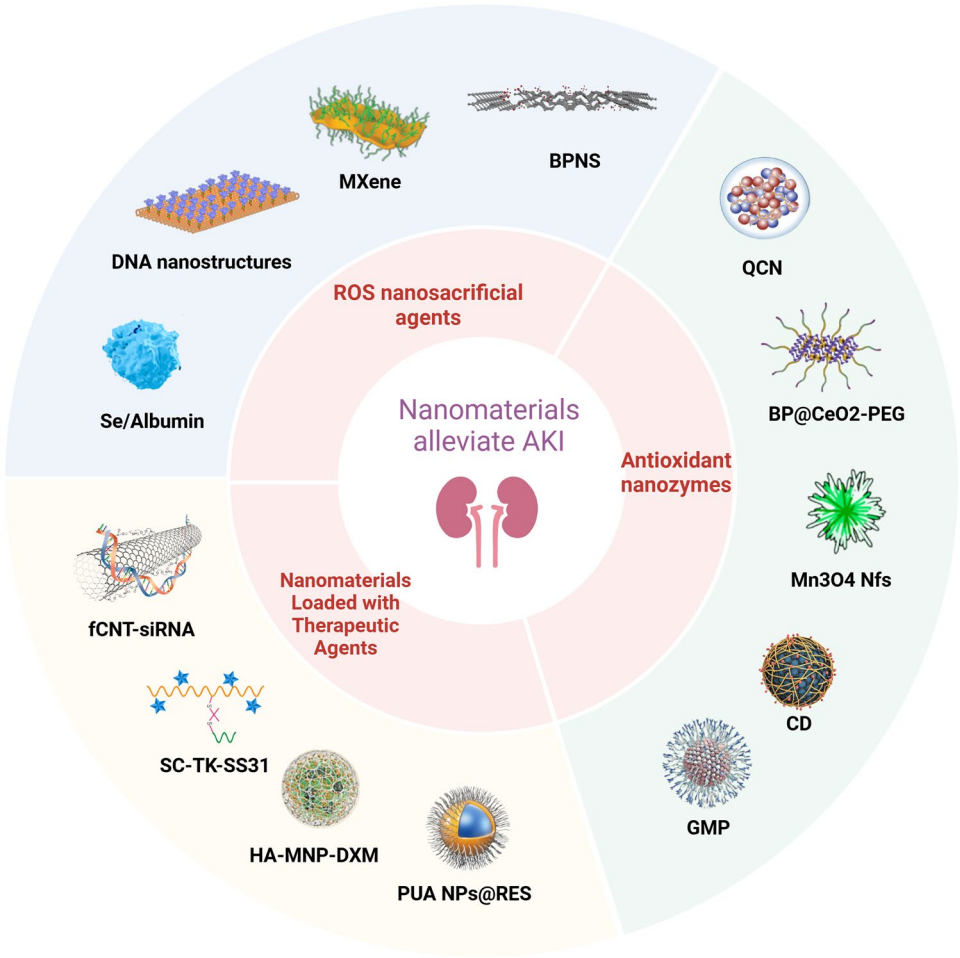

Introduction

Acute kidney injury (AKI) is a serious health problem that manifests as a rapid decline in kidney function, leading to the accumulation of metabolic products in the body and disorders of water, electrolytes, and acid–base balance [1, 2]. The AKI is based on a sustained elevation in serum creatinine (sCr) levels (a marker of renal excretory function) for at least 7 days, accompanied by decreased urine output (oliguria) as an indicator of urine quantification. Currently, the Kidney Disease Improving Global Outcomes (KDIGO) criteria are widely used for diagnosing AKI in adults [3–5].

The occurrence of AKI not only results in short-term renal impairment, but also elevates the risk of developing chronic kidney disease (CKD), which is characterized by persistent structural and functional damage to the kidneys caused by various etiologies (with a history of kidney injury lasting more than 3 months). However, it should be noted that AKI and CKD are not entirely mutually exclusive. Additionally, both conditions share common risk factors such as advanced age, diabetes and hypertension [6]. In clinical practice, patients may exhibit changes in renal function and structure without fully meeting the definition or staging criteria for either AKI or CKD. To address this issue, the 2012 KDIGO Task Force on Clinical Practice Guidelines for Acute Kidney Disease proposed an operational definition for acute kidney disease (AKD), which includes renal functional and structural abnormalities present for less than three months (Table 1). The AKI is defined as a subset of AKD. The updated definition and staging criteria can be applied to patients who do not meet the diagnostic criteria for both AKI and CKD, but exhibit renal functional abnormalities and structural anomalies. This definition elucidates the transitional phase from AKI to CKD in individuals with AKI [7]. The relationship between these three conditions can be summarized as follows (Fig. 1a). First of all, in terms of the defined

Table 1 Criteria for defining AKI, AKD, CKD and NKD

	NKD*	AKI	AKD	CKD
Duration	NA	≤ 7 days	< 3 months	> 3 months
Functional criteria	GFR ≥ 60 ml/min/1.73 m^2, stable GFR (no decrease by 35% within 3 months), stable sCr (no increase by 50% within 3 months or increase by 0.3 mg/dl within 2 days), no oliguria for ≥ 6 h	Increase in sCr by ≥ 50% within 7 days or increase in sCr by ≥ 0.3 mg/dl (26.5 µmol/l) within 2 days or oliguria for ≥ 6 h	AKI or GFR < 60 ml/min/ 1.73 m^2 or decrease in GFR by ≥ 35% over baseline or increase in sCr by > 50% over baseline	GFR < 60 ml/min/1.73 m^2
AND/OR	AND	OR	OR	OR
Structural criteria	No marker of kidney damage	Not defined	Elevated marker of kidney damage (albuminuria, haematuria or pyuria are most common)	Elevated marker of Kidney damage (albuminuria is most common)

course and duration of illness, AKD encompasses AKI while remaining distinct from CKD. However, AKI/AKD can also manifest in individuals with underlying CKD, resulting in simultaneous fulfillment of the criteria for both AKI/AKD and CKD. Consequently, there exists a reciprocal relationship between CKD and these two conditions, whereas Non-Kidney Disease (NKD) remains independent from all three. After onset of AKI, if treated early enough it may restore normal renal function. However, if abnormality persists beyond seven days but less than ninety days it will be defined as AKD [8, 9]. If injury continues there will be further progression to CKD leading eventually to chronic renal failure and uremia. The ongoing advancement of AKI and the exploration of interventions that impede its progression require further investigation (Fig. 1b). It should also be noted that the relationship between these conditions is not always one-way progressive. The starting point can be AKD or CKD rather than AKI. Additionally, AKD can develop into AKI reversely instead of CKD [10]. Similarly, patients with CKD may also experience episodes of AKI or AKD.

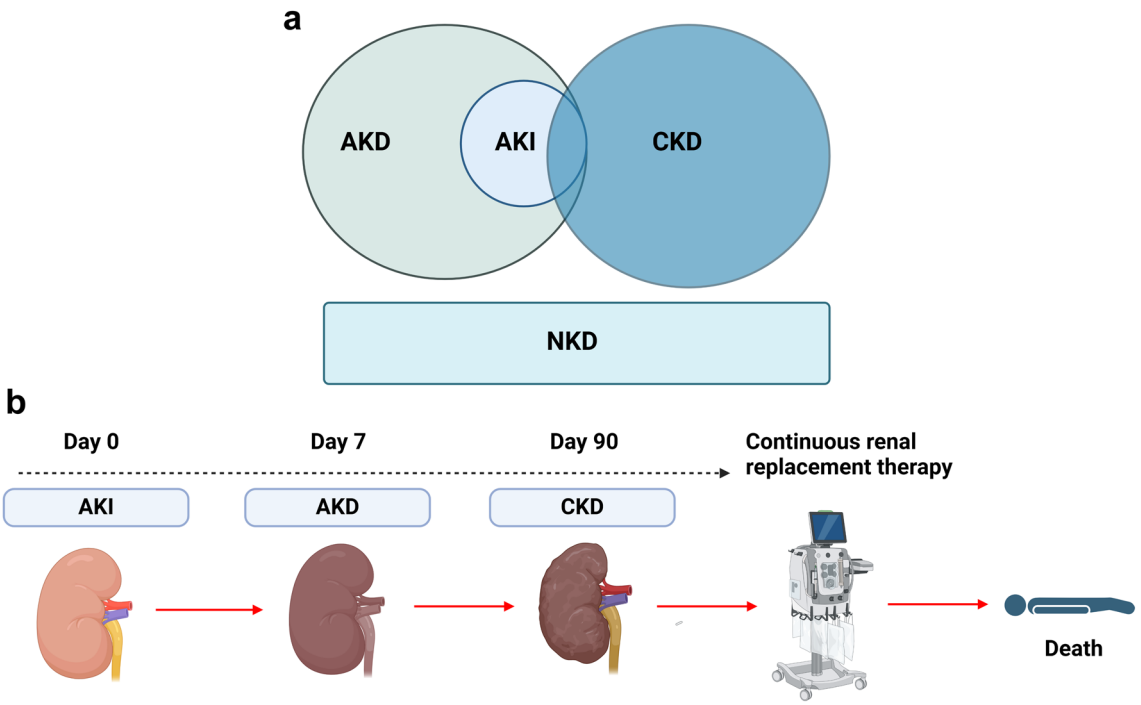

Fig. 1 **a** Relationship between AKI, AKD, CKD, and NKD. **b** The development of AKI over time and the outcomes that would result

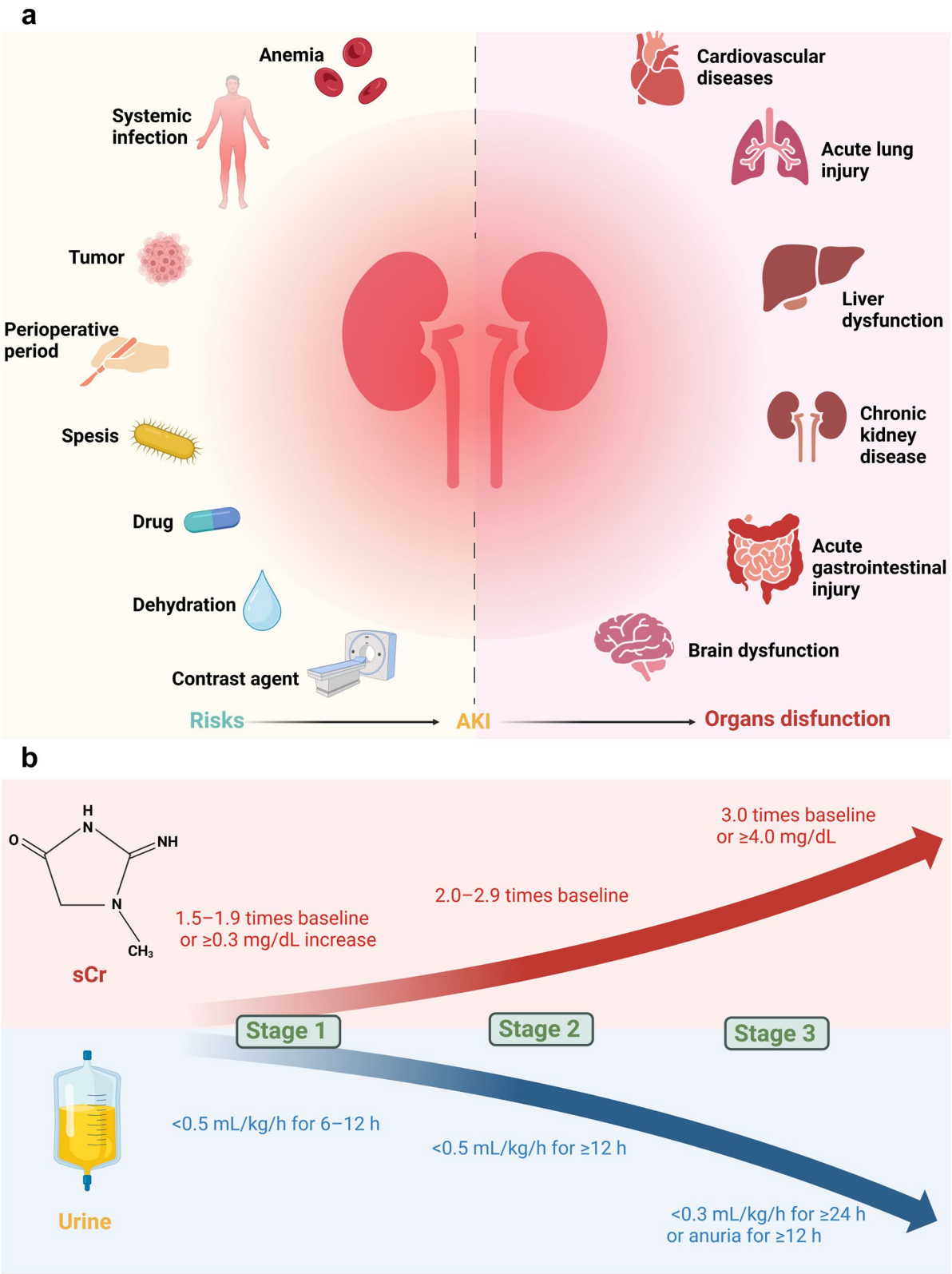

Fig. 2 **a** Etiology of AKI and distal multi-organ dysfunction caused by AKI. **b** Staging of AKI according to current KDIGO

Causes of AKI are often multifactorial, encompassing environmental, socioeconomic, cultural, nursing process, and patient-related factors [11]. Risk factors for AKI include exposure to systemic infections, critical illnesses, shock, trauma, burns, cardiac surgeries, nephrotoxic medications, and contrast agents. Susceptibility factors include dehydration, volume depletion advanced age, female gender, CKD, diabetes mellitus, tumor, anemia, etc. [12–16]. Additionally, the development of AKI predisposes patients to multiorgan dysfunction such as cardiovascular disease, acute lung injury, cerebral dysfunction, hepatic dysfunction, and systemic inflammation which subsequently increases the mortality rate through systemic or organ-specific, hemodynamic fluid, and immunologic imbalances (Fig. 2a) [17]. The grading of AKI is based on the 2012 KDIGO AKI guidelines (Fig. 2b). Clinically the typical course of AKI can be divided into three phases. The initial phase: the presentation in this phase encompasses a range of etiologies, including infection, ischemia, and nephrotoxicity, including infection, ischemia, and nephrotoxicity. However, there is no evident renal parenchymal injury observed at this time. Typically, such conditions persist for a duration ranging from several hours to a few days. The timely implementation of appropriate measures can effectively prevent AKI at this stage. However, the current clinical practice often lacks the ability to diagnose AKI due to its insidious onset, resulting in delayed initiation of optimal treatment. Maintenance phase: typically lasts from a few days to several weeks or even months, during which significant kidney damage occurs and glomerular filtration rate (GFR) decreases. Patients may exhibit oliguria or anuria, progressive elevation of blood creatinine and urea nitrogen levels, as well as disturbances in water, electrolyte, and acid–base balance. Severe cases may present with impaired consciousness, agitation, coma or even fatality. Recovery phase: there is a gradual increase in GFR leading to the restoration of renal function and gradual improvement in urine output. However, some patients may experience residual renal function impairment and structural damage that could eventually progress into CKD [18].

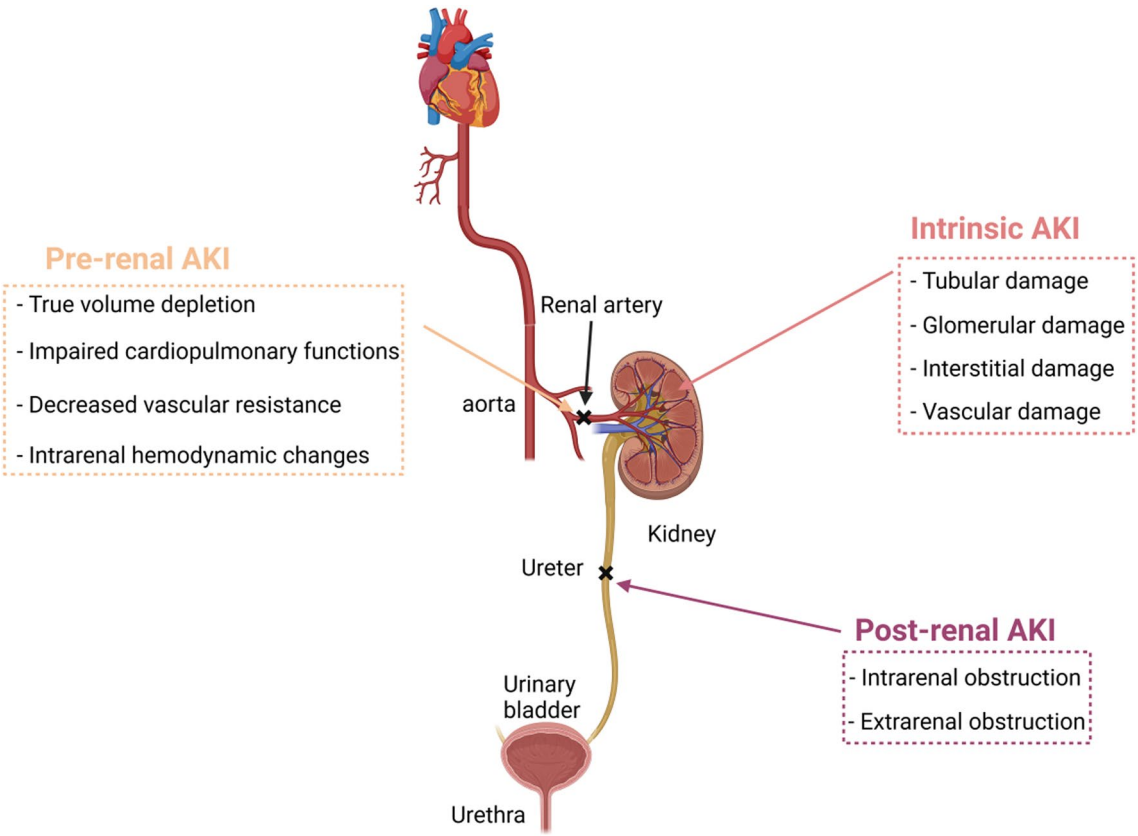

Fig. 3 Etiology of AKI, including pre-renal, intrinsic renal, and post-renal

Epidemiology of AKI

The morbidity and mortality rate of AKI is significantly high, affecting individuals with or without pre-existing kidney disease. As a clinical syndrome, its incidence continues to rise annually in both developing and developed countries. Globally, there are approximately 13.3 million new cases of AKI reported each year, resulting in nearly 1.7 million deaths due to AKI and its complications [19]. Hospitalized patients also commonly experience AKI, accounting for about 10–15% of cases and even up to 50% in intensive care units (ICUs) [20–22]. The prevention and treatment of AKI require substantial resources in both developed and developing nations, placing a significant burden on families and society as a whole; for instance, dialysis costs alone exceed 6% of the overall health insurance budget in the United States [23].

According to current epidemiological studies, AKI can be classified into two categories: community-acquired AKI (CA-AKI) and hospital-acquired AKI (HA-AKI). CA-AKI refers to the occurrence of AKI prior to hospital admission. The primary risk factors for CA-AKI are CKD, pneumonia, and urinary tract obstruction in that order. On the other hand, HA-AKI is commonly associated with intensive care, CKD, and cardiac surgery as major risk factors in that order. CKD is a shared significant risk factor for both types of AKI. In rural or underserved areas with limited healthcare infrastructure, the etiology of AKI is commonly attributed to CA-AKI. Young individuals, previously healthy individuals, or those with susceptible diseases are more prone to developing AKI. Common causes include infection-induced or toxin-induced diarrhea, hemolytic uremic syndrome, and post-infectious acute glomerulonephritis. In regions with higher levels of medical conditions, mild AKI is less prevalent in general wards, while severe AKI primarily affects critically ill patients in ICUs. It is often attributed to one or more etiologies, including postoperative hypoperfusion-induced renal ischemia, hemorrhage, dehydration, shock, sepsis, nephrotoxic effects of medications, and pigment damage induced by myoglobin or hemoglobin [24]. Overall, the prevalence of AKI is higher among men than women and increases with age.

The statistical data from various AKI epidemiologic studies at home and abroad generally exhibit significant variation, likely attributed to disparities in the diagnostic criteria and indexes employed, the selected baseline creatinine values, as well as the patient populations, geographic regions, and observation time points [12, 25]. Nevertheless, it is indisputable that AKI currently represents a crucial global public health concern and a prevalent complication among critically ill patients. Moreover, its incidence continues to escalate annually while significantly impacting patient prognosis.

Etiology of AKI

Contrary to the previous notion that AKI is a self-healing disease. Recent research has demonstrated that AKI can result in incomplete renal regeneration, persistent chronic inflammation, and progressive fibrosis, leading to the chronic impairment of organ function. There are multiple etiologies for AKI, which can be classified into three primary categories: pre-renal, renal, and post-renal. Among these causes, pre-renal accounts for approximately 55%, renal for about 40%, and post-renal for around 5% (Fig. 3).

Pre-renal kidney injury

Maintaining an optimal GFR in the kidneys requires adequate renal perfusion. Causes such as renal ischemia or renal vasoconstriction can result in a reduction in renal blood flow, leading to a state of hypoperfusion of renal blood flow, thereby compromising normal GFR maintenance and causing oliguria, which plays a pivotal role in pre-renal AKI. It is important to note that pre-renal AKI must be attributed to true blood volume depletion or fluid volume depletion, such as hemorrhagic shock, severe vomiting, profuse sweating, and burns. In the case of a young and healthy adult, several hours of volume depletion may not have long-term health consequences; however, at this juncture, they may meet the criteria for AKI. Another factor that can induce changes in renal blood flow is medication usage which has the potential to alter renal blood flow significantly, particularly certain antihypertensive medications (e.g., diuretics and angiotensin-converting enzyme inhibitors). These medications can either decrease vascular volume or constrict the renal vasculature. Initially, these factors do not result in any damage to the renal parenchyma or functional alterations, and compensatory mechanisms are activated by the body's self-regulatory system. However, if left untreated, persistent reduction in renal blood flow can progress to acute tubular necrosis (ATN). Generally speaking, pre-renal AKI is primarily caused by volume insufficiency, impaired cardiopulmonary function, renal vascular disease and alterations in renal hemodynamics [26].

Renal AKI

The renal AKI primarily refers to the decline in renal function caused by various lesions in the renal parenchyma or due to delayed removal of pre-renal factors and subsequent disease progression. Common causes include ATN, acute interstitial nephritis (AIN) and glomerulonephritis. ATN is mainly caused by renal ischemia, sepsis

and nephrotoxins [27]. Sepsis is a systemic inflammatory response syndrome triggered by infection that increases the risk of multiple organ failure. It is often associated with persistent pre-renal factors, such as hypotension or infectious shock leading to renal under perfusion [28, 29]. Meanwhile the release of inflammatory mediator and the influence of toxin in vivo can also further aggravate the progress of AKI. Endotoxemia can activate vasoactive hormones, induce nitric oxide (NO·) synthase production, release cytokines, and activate neutrophils. Sepsis can also lead to apoptosis and cell death through complement system activation and intrinsic cellular immunity [30, 31]. Other causes of AKI include rhabdomyolysis-induced AKI and AKI caused by certain medications or radiographic contrast agents. Rhabdomyolysis results in hemolysis and muscle breakdown. Myoglobin, creatine kinase and lactate dehydrogenase are important substances released during muscle damage that can obstruct renal tubules, cause damage and inflammation. Myoglobin also induces renal vasoconstriction which reduces kidney perfusion pressure and GFR. Hemoglobin and myoglobin can further break down into methemoglobin which directly damages the renal tubules [32, 33].

Post-renal AKI

The condition is primarily observed in cases of acute urinary tract obstruction resulting from various causes and can be categorized as either functional or organic. Obstruction may manifest in any segment of the urinary system, leading to an increase in pressure above the site of obstruction, potentially causing pyelonephrosis as well. Etiologies encompass prostatic hyperplasia, renal calculi, and tumor compression. A significant decline in GFR may indicate bilateral urinary tract obstruction or unilateral urinary tract obstruction in patients with a solitary functioning kidney. This is most attributed to prostatic hyperplasia or prostate cancer. Although unilateral or incomplete obstruction in a healthy individual can result in AKI, their sCr levels typically remain within normal range due to robust compensatory function exhibited by the contralateral kidney.

It is crucial to acknowledge that the pathophysiology of AKI is intricate, involving a complex interplay between pre-renal factors and renal dysfunction, making it challenging to discern the dominant factor. Consequently, the simultaneous possibility of overlapping and crossover effects among pre-renal, renal, and post-renal factors necessitates careful consideration.

Pathophysiology of AKI

The unique anatomical structure of the kidney, combined with a multitude of etiological factors, gives rise to a complex pathophysiological mechanism underlying AKI [34, 35]. This susceptibility primarily stems from hypoxia and the accumulation of detrimental toxins.

The kidneys exhibit a notably high perfusion rate, with a renal blood flow of approximately 1.2 L per minute, which is essential for maintaining a heightened GFR. The kidneys receive 20% of the cardiac blood supply and possess selective distribution of blood flow. The renal arteries terminate at the glomeruli and transition into small arteries, forming a capillary network within the glomeruli where filtration and purification of substances occur. Physiologically, the vasculature of the renal microcirculation consists of two separate yet interconnected vessels: the glomerular capillary network and the peritubular capillary network [36]. This structural arrangement results in blockages in upper segments of the renal vasculature inevitably causing ischemia in downstream vessels since these arterioles lack inter-arterial anastomoses and cannot be compensated by other renal arteries [37]. The oxygen delivery efficiency will gradually decrease due to the diffuse shunt between parallel arteriovenous vessels in the cortex with opposite blood flow direction and between ascending and descending branches of the medullary straight small vessels, simultaneously [38]. Functionally, while blood primarily flows through most organs to provide oxygenation, it flows through kidneys mainly for blood purification [39, 40]. Na + -K + -ATPase located in proximal tubules plays a crucial role in actively reabsorbing sodium ions as well as transporting glucose molecules, amino acids and other solutes; being responsible for majority (80%) of renal oxygen demand [41]. Consequently, substantial amounts of oxygen are required to fuel kidney's reabsorption processes [42]. Overall, the intricate anatomical structure and distinctive physiological function render kidneys highly vulnerable to hypoxia [43].

Accumulation of toxic substances in the bloodstream can also result in AKI. These harmful substances can be categorized into two main groups: exogenous toxins, such as nephrotoxic compounds and pathogen-associated molecular patterns (PAMPs), and endogenous toxins, including inflammatory factors and damage-associated molecular patterns (DAMPs) [44]. PAMPs are inherent molecular structures found in various pathogens like bacteria, viruses, fungi, and parasites; for instance, lipopolysaccharides in bacteria, double-stranded RNA in viruses, and DNA in parasites. DAMPs are a class of substances released into the interstitial space or bloodstream following tissue or cellular stimulation caused by injury, hypoxia, stress, etc. These substances encompass various molecules such as small metabolites including nucleic acids and ATP, as well as calcium network proteins like calreticulin [45, 46]. Because of the unique physiological structure of the

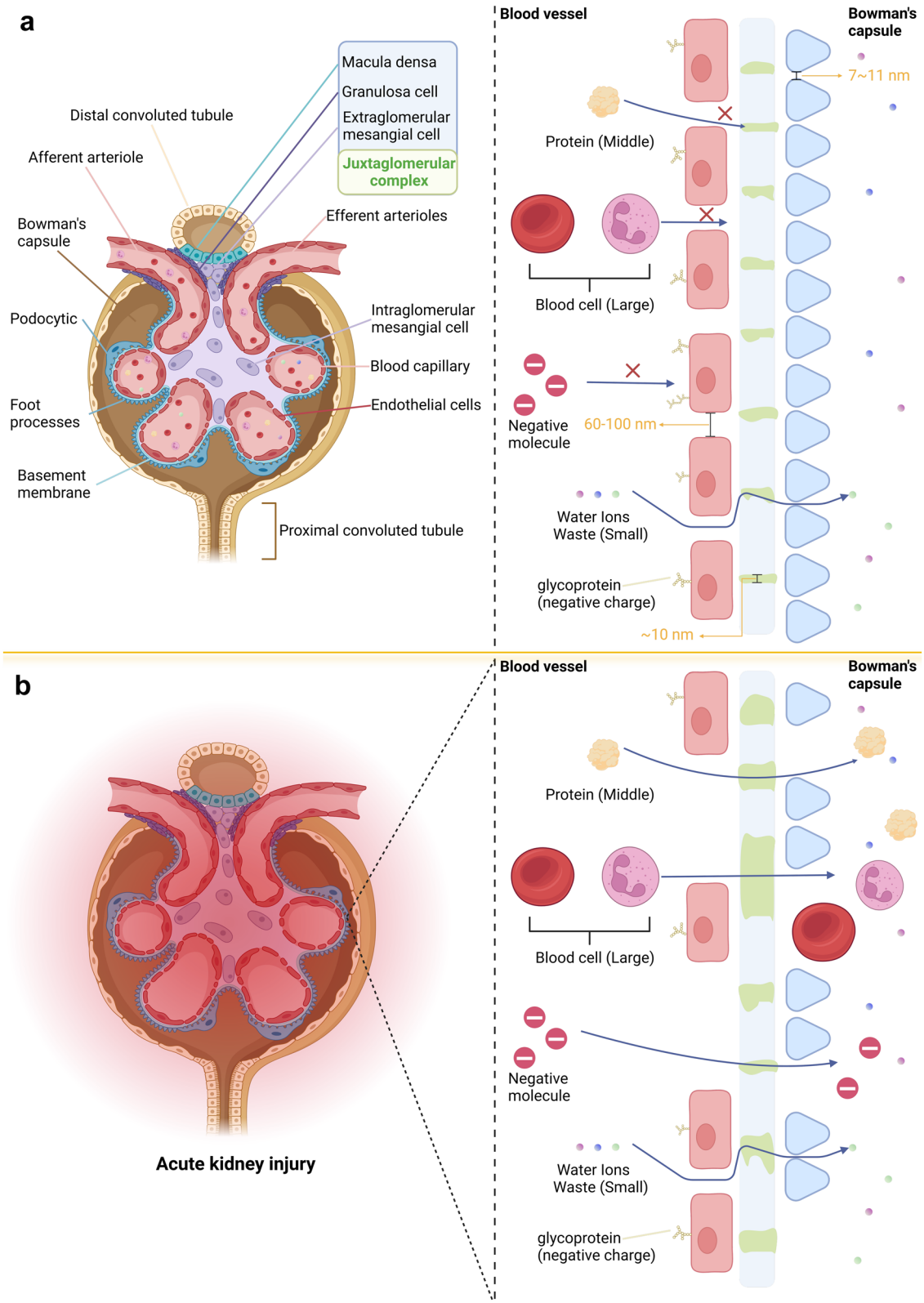

Fig. 4 **a** Basic structure of the renal corpuscle and schematic diagram of the glomerular filtration barrier. **b** Schematic representation of the glomerular filtration barrier after injury

Table 2 Various antioxidant enzymes in the body

Enzymes	Target	Reaction
Superoxide dismutase (SOD)	O_2^-	$2O_2^- + 2H^+ \rightarrow H_2O_2 + O_2$
Catalase (CAT)	H_2O_2	$2H_2O_2 \rightarrow 2H_2O + O_2$
Glutathione peroxidase (GPx)	H_2O_2	$2GSH + H_2O_2 \rightarrow GSSG + 2H_2O$
Myeloperoxidase (MPO)	H_2O_2	$H_2O_2 + Cl^- \rightarrow HOCl^- + OH$

kidneys, their high blood supply makes them vulnerable to harmful substances and leads to a vicious cycle [47]. The glomeruli bear the brunt of damage when harmful substances accumulate in the kidneys. AKI occurs due to damage to the glomerular basement membrane and podocytes, resulting in an enlarged barrier gap. Consequently, molecules that could have been blocked rush through the filtration membrane into renal tubules where they further accumulate within tubular epithelial cells. This accumulation leads to oxidative stress (OS), inflammation and even apoptosis within renal tubules [48–52]. Such processes constitute one of the primary causes for renal tubular damage and dysfunction (Fig. 4a, b).

The pathophysiology of AKI is intricate, with multiple overlapping pathological processes. However, the role of OS as a pivotal mechanism in the pathogenesis of AKI is evident across various etiologies. When the kidneys are exposed to various harmful stimuli such as ischemia-hypoxia and nephrotoxic substances, excessive production of reactive oxygen species (ROS) and reactive nitrogen radicals (RNS) occurs in different kidney cells including fibroblasts, endothelial cells, vascular smooth muscle cells, tethered cells, renal tubular cells and podocytes.[53–55]. These ROS and RNS are oxygen/nitrogen-containing free radicals or molecules generated by cellular organelles that can cause oxidative damage to lipids, proteins and DNA through their reactivity, which in turn leads to cell and tissue damage [56]. Examples of ROS include superoxide anion (O_2·-), hydroxyl radical (·OH), hydrogen peroxide (H_2O_2), etc., while RNS encompass NO·, nitrogen dioxide (NO_2·) and peroxynitrite (ONOO-), etc. To counteract the detrimental effects caused by excess ROS accumulation within the body, there exist two intrinsic scavenging systems: antioxidant enzymes system and non-enzymatic system. Antioxidant enzymes comprise superoxide dismutase (SOD), catalase (CAT) and glutathione peroxidase (GSH-Px). SOD facilitates the decomposition of superoxide through the reaction: $2O_2^- + 2H^+ \rightarrow H_2O_2 + O_2$. The enzyme CAT facilitates the decomposition of H_2O_2 through the reaction: $2H_2O_2 \rightarrow 2H_2O + O_2$. In the presence of glutathione, GSH-Px breaks down H_2O_2 into H_2O (Table 2) [57]. Another group is the non-enzymatic antioxidant system, which comprises vitamin C, vitamin E, glutathione, melatonin, carotenoids, and trace elements such as copper, zinc, and selenium (Se). However, during AKI, an abrupt surge of ROS and RNS exhausts these antioxidant enzymes, disrupting cellular structural integrity and function ultimately leading to cellular damage and even death. Therefore, it is crucial to comprehend the production mechanism of ROS in the kidney.

Renal injury and repair are a complex and multifaceted process involving intricate interactions among microvessels, tubules, inflammatory factors, as well as various signaling pathways [58, 59]. Mitochondria and NADPH oxidase (NOX) are the primary sources of ROS in cells. Notably, the kidney exhibits a mitochondrial density second only to that of the myocardium; thus, endogenous ROS in the kidney have an intimate association with mitochondria [60]. More and more researches suggest that aberrations in mitochondrial function play a pivotal role in the mechanisms underlying AKI and incomplete renal repair following AKI. The literature has documented that in a glycerol-induced mouse model of AKI, disruption of mitochondrial respiration and ultrastructural abnormalities were observed in kidneys just three hours after glycerol injection—prior to any evidence of renal injury. This implies that pathological changes in mitochondria can be detected before renal dysfunction becomes apparent [61]. Furthermore, post-AKI tissue analysis reveals varying degrees of swelling and fragmentation within mitochondria along with disruptions in mitochondrial ridges, cytochrome C (Cytc) release and ROS production. Similar mitochondrial damage has also been observed in other AKI animal models such as sepsis models and glycerol models.

Mitochondria play a crucial role in sustaining the vital activities of the cell. They are responsible for various functions, including ROS production, calcium ion storage and participation in apoptosis. Most importantly, mitochondria serve as the primary site for aerobic respiration through the tricarboxylic acid cycle with oxidative phosphorylation. This process generates energy that fuels the Na+-K+-ATPase, facilitating the transportation of specific ions and ensuring the maintenance of an optimal ion concentration gradient across the cell membrane. (Fig. 5a). In the kidney, substances are filtered by passive transport, which comprises podocytes, tethered cells, and endothelial cells. The primary function of these cells is blood filtration, involving the removal of small molecules (such as glucose, urea, water, and salt) while retaining large molecules (like proteins). The reabsorption of ions in other regions of the kidney, such as the proximal tubule, loop of Henle, distal tubule and collecting ducts,

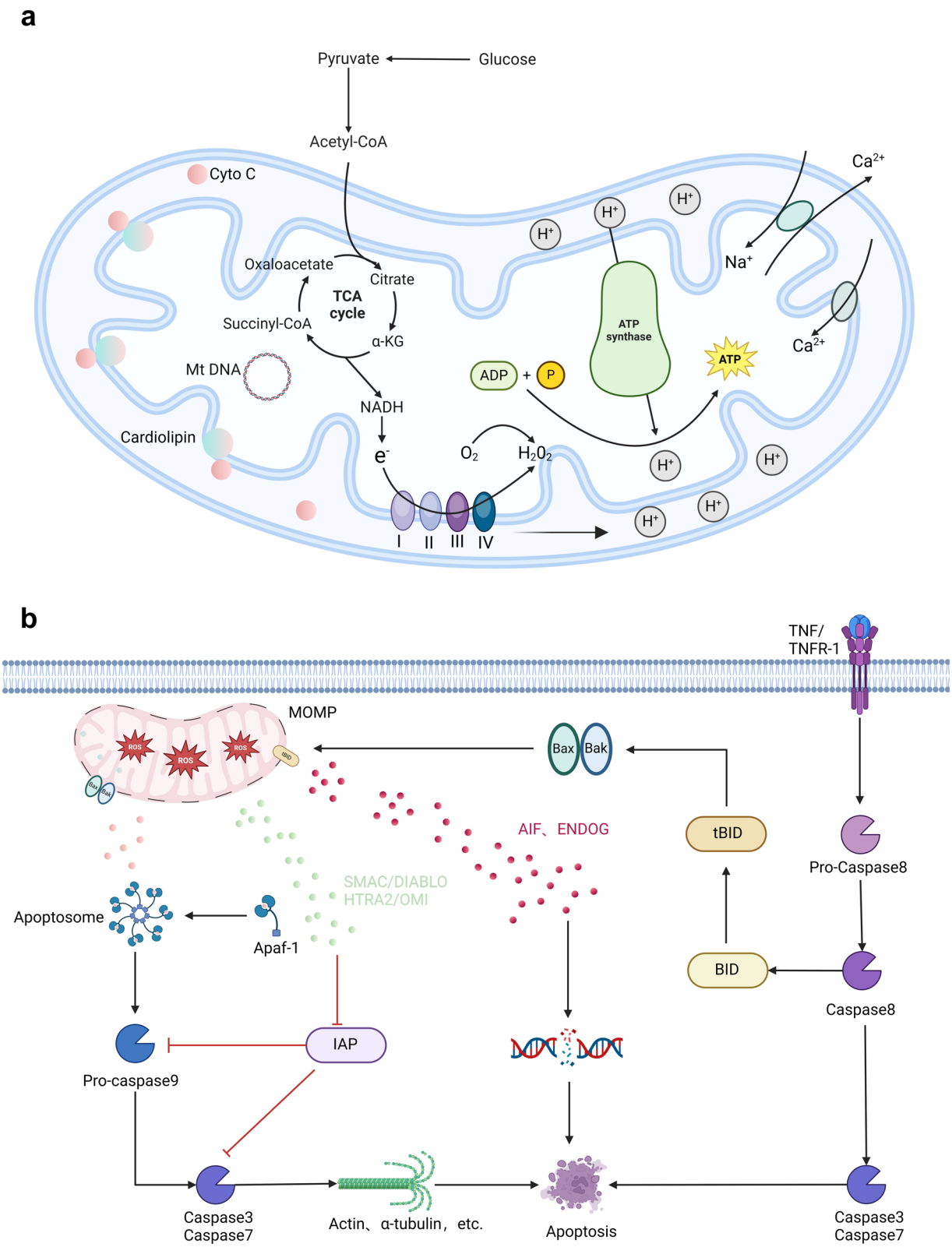

Fig. 5 **a** Basic structure of mitochondria. **b** Endogenous and exogenous apoptotic pathways in mitochondria

necessitates active transport. The proximal tubule renal cell demands a higher energy expenditure compared to other renal cells, as it is responsible for reabsorbing 80% of the glomerular filtrate, including ions, glucose, and essential nutrients. Consequently, this particular cell type possesses a higher number of mitochondria making it more susceptible to injury caused by ROS accumulation [62].

Mitochondrial damage is a common characteristic of renal diseases. For instance, following ischemia/reperfusion (I/R), there is an immediate surge in ROS production, leading to direct oxidative harm to mitochondrial proteins and lipids [63]. Inflammation represents a cascade of protective response reactions triggered by tissue damage, with mitochondria serving as the central hub for pro-inflammatory signaling. Dysregulation of the inflammatory response induced by mitochondrial components or products has been demonstrated to contribute to a range of human diseases, spanning from those driven by excessive inflammation to those resulting from insufficient inflammatory responses. The onset of inflammation is typically initiated by the activation of pattern recognition receptors (PRRs) expressed by both immune and non-immune cells. PRRs are a group of receptors found in the mammalian immune system that specifically recognize and bind to PAMPs and DAMPs. The injury-induced changes in cell permeability enable DAMPs, which would otherwise be inaccessible to these subcellular regions under normal conditions, to enter the cell and bind to the PRR, thereby triggering inflammation [45, 46]. The mitochondria possess their own unique pattern of damage-associated molecules in the form of formyl peptides and mitochondrial DNA (mtDNA). The activation of inflammatory vesicles by these DAMPs molecules subsequently triggers inflammation. The inflammasome, a complex composed of multiple proteins, primarily mediates the host's immune reaction to microbial infection and cellular damage. It is synthesized in bone marrow cells and serves as a crucial component of the innate immune system. Furthermore, regarded as a trigger of inflammation within the body, once activated, it stimulates inflammatory cells to undergo extensive secretion of inflammatory mediators, thereby initiating or exacerbating the inflammatory response. The NLRP3 inflammasome is currently the most extensively studied inflammasome [64]. When NLRP3 detects damage signals, such as mtDNA, extracellular ATP, RNA viruses, etc., it triggers intracellular potassium ion (K^+) efflux. K^+ efflux is an essential prerequisite for the activation of NLRP3. Following NLRP3 activation, conformational changes ensue [65]. Additionally, it interacts with the adaptor protein apoptosis-associated speck-like protein (ASC) to form inflammasome complexes. ASC recruits and activates caspase-1, which in turn activates immature pro-IL-1β and pro-IL-18. Consequently, active IL-1β and IL-18 are secreted by cells to induce an inflammatory response [66, 67].

Mitochondria can regulate cell death, including apoptosis and necrosis. Apoptosis refers to the genetically regulated, autonomous, and orderly process of cell death that maintains internal environmental stability. The process of apoptosis differs from necrosis in that it is an active rather than passive phenomenon. It entails a cascade of gene activation, expression, and regulation, representing a form of programmed cell death that actively strives for enhanced adaptation to the survival environment [68]. The level of apoptosis can be classified into endogenous and exogenous apoptosis. Endogenous apoptosis is initiated through mitochondrial outer membrane permeability (MOMP). Under normal circumstances, Cytc is primarily localized in the intermembrane space of mitochondria or anchored to the mitochondrial membrane via binding with cardiolipin. However, upon stimulation by endogenous apoptotic factors such as DNA damage, hypoxia, I/R injury, and ionizing radiation, the cytoplasm undergoes the formation of Bax/Bak oligomeric complexes. The Bax/Bak oligomeric complexes will insert into the outer mitochondrial membrane pore, resulting in altered mitochondrial osmotic pressure, loss of transmembrane potential, and increased mitochondrial membrane permeability. This process leads to the release of Cytc from the mitochondria into the cytoplasm, where it binds to apoptotic protease activating factor-1 (Apaf-1) to form an apoptotic complex. The apoptotic complex is capable of activating the Caspase-9 precursor, which subsequently triggers a cascade reaction involving Caspase-3 and Caspase-7. This cascade leads to the cleavage of over 100 cellular substrates, including α-tubulin, Actin, poly ADP-ribose polymerase (PARPA), Lamin, etc., ultimately resulting in apoptotic cell death. Inhibitor of apoptosis proteins (IAPs) can suppress the activation of Caspase-3 and Caspase-7 to inhibit apoptosis [69]. However, SMAC/DIABLO and HTRA2/OMI are released from the mitochondria into the intracellular space and bind to IAPs, thereby disinhibiting the effect of IAPs and indirectly promoting apoptosis [70–73]. Additionally, with changes in mitochondrial membrane potential, AIF and ENDOG are also released into the cytosol and then be transported to the nucleus. Once in the nucleus, AIF and ENDOG can initiate chromatin condensation and DNA fragmentation, ultimately leading to apoptosis. This signaling pathway is commonly known as the "caspase-dependent apoptosis pathway". Correspondingly, the initiation of the exogenous apoptotic pathway typically occurs because of the activation of death receptors on the cell membrane by corresponding ligands, such as members of TNF receptor family. Upon

activation of these receptors, they can induce self-cleavage of Caspase-8 zymogen to generate active Caspase-8, thereby initiating a downstream cascade reaction involving Caspases. Secondly, activated Caspase-8 cleaves the Bcl-2 family pro-apoptotic protein Bid, leading to the generation of carboxylated fragment tBID that can be translocated to mitochondria. Subsequently, tBID binds to the mitochondrial membrane and induces the release of pro-apoptotic substances such as Cyt C from mitochondria, thereby initiating apoptotic responses (Fig. 5b) [68, 74–77].

Overall, OS resulting from mitochondrial injury is a key factor in the development of AKI. Failure to restore mitochondrial function following various injuries may contribute to the progression of AKI to CKD. Therefore, targeting mitochondria as a therapeutic approach for restoring mitochondrial function and facilitating recovery from AKI is necessary. However, the precise roles and mechanisms by which mitochondria participate in renal injury and repair during different forms of regulated necrosis remain insufficiently elucidated.

Early diagnosis and treatment of AKI

The accurate diagnosis of AKI in its early stages is crucial, given the high incidence and mortality rates associated with this condition as well as its complex pathophysiology. This enables timely implementation of renal protection interventions to prevent the progression of acute kidney injury into more severe complications. Current clinical diagnostic methods lack the ability to detect AKI in its early stage due to their reliance on measurements of sCr and blood urea nitrogen (BUN), which are not sensitive indicators for renal dysfunction. These two markers only exhibit significant changes when 75% of renal function has been lost [78]. Furthermore, these two indicators are also influenced by various other factors, such as patients' improper dietary habits and excessive food intake. Additionally, it should be noted that these two indicators solely reflect changes in renal function and do not accurately represent the extent of tubular damage. Inulin clearance is the gold standard for assessing GFR but its practical clinical application has certain limitations. Recent studies have demonstrated that bedside GFR determination based on visual fluorescence injection is a safe, rapid, accurate and reproducible method, but more validation studies are needed to further demonstrate the clinical applicability of this method [79]. As previously mentioned, there is not necessarily a problem with kidney function when the kidney structure is damaged. Therefore, early diagnosis of AKI is crucial. However, it remains challenging to promptly diagnose AKI in clinical practice. The emergence of new biomarkers has made this possible. Currently, commonly used biomarkers include kidney injury molecule 1 (KIM-1), liver-type fatty acid binding protein (L-FABP), neutrophil gelatinase-associated lipocalin (NGAL), soluble urokinase plasminogen activator receptor (suPAR), and triggering receptors expressed on myeloid cells (TREM). Although there have been numerous studies on the use of biomarkers for early diagnosis and prognosis of AKI, unfortunately their potential has not been fully tapped. These biomarkers have limited value in diagnosing, assessing risk, and predicting outcomes for AKI.

Meanwhile, currently there is a lack of effective pharmacological interventions for the treatment of AKI, with hemodialysis or kidney transplantation being the primary therapeutic approaches. In addition to these therapies, supportive measures such as optimizing intravascular volume status, providing comprehensive nursing care, maintaining fluid balance, and preventing and managing complications are also employed. However, these treatments still present several limitations including high financial burden, poor patient adherence, and elevated rates of adverse events [80]. Therefore, there is an urgent need for a nanomaterial that can serve both diagnostic and therapeutic purposes in AKI.

Progress in the application of nanomaterials in AKI

The pathogenesis of renal diseases is highly intricate, primarily attributed to the multitude of factors contributing to AKI, including I/R, surgical procedures, nephrotoxic medications, sepsis, and other etiologies. This complexity poses a significant challenge in the current management of AKI [81–84]. These factors are all associated with reactive oxygen and nitrogen species (RONS), thus prompt elimination of RONS is advantageous for the recovery of AKI [85, 86]. Currently available drugs in clinical practice possess certain clearance capabilities. However, they are constrained by various factors resulting in suboptimal therapeutic outcomes, [87–89] such as limited water solubility, inadequate renal targeting, and heightened drug toxicity.

In recent years, there has been significant advancement in the integration of nanomaterials with medicine. It has been reported that the size of nanomaterials plays a crucial role in cell targeting and uptake. Nanomaterials with diameters less than 500 nm are easily taken up by cells, and the smaller the size of the nanomaterial, the larger the active surface area and the higher the surface-to-volume ratio, which implies an increased potential for interaction with cells and enhanced efficiency [90]. Particularly for the kidney, the size of nanomaterials is a critical factor determining their interaction. The normal glomerular filtration barrier (GFB) allows passage of small molecules such as water molecules and ions, as well

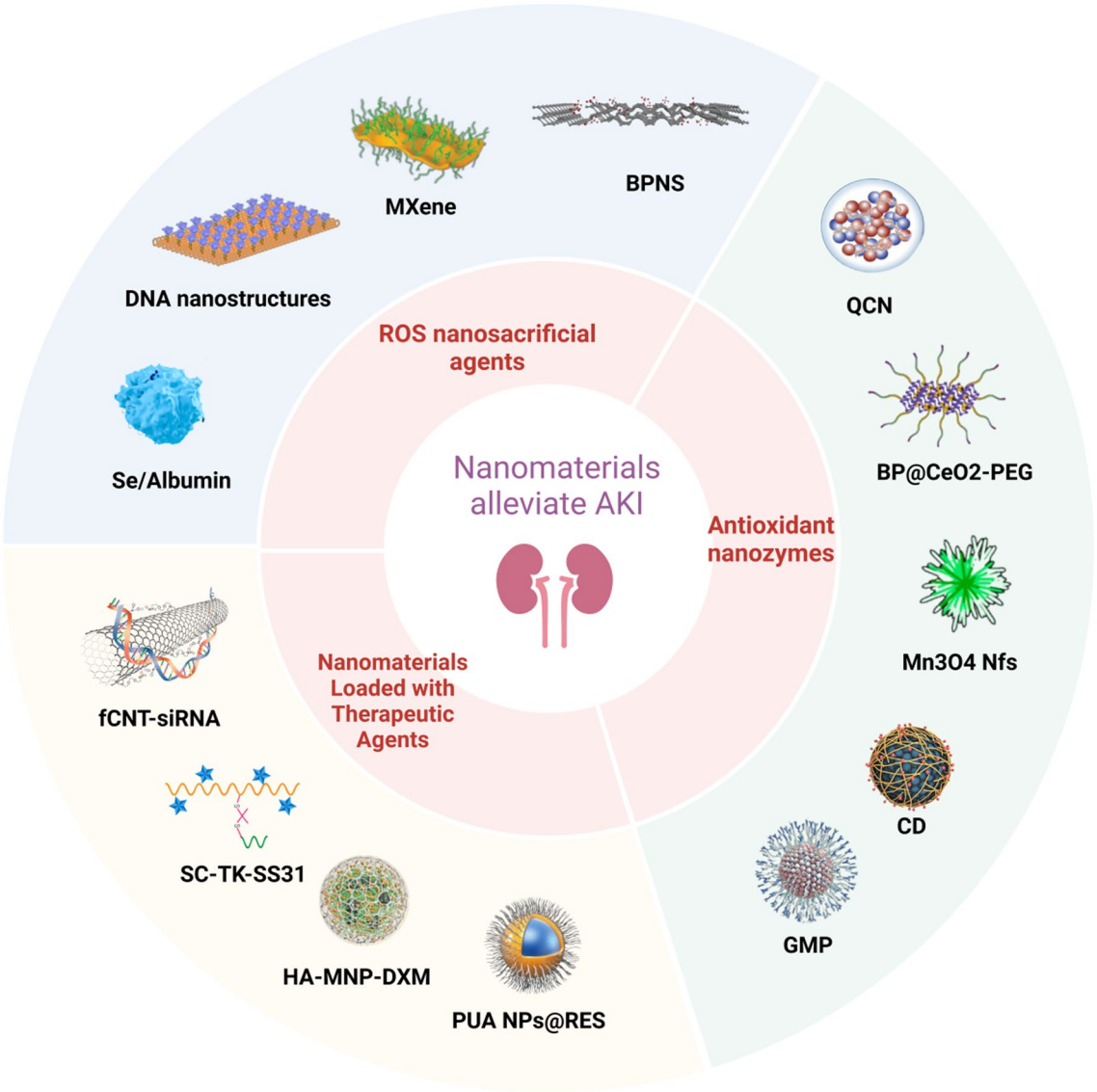

Fig. 6 Application of various nanomaterials in AKI

as nanomaterials smaller than 7 nm in size. Therefore, smaller-sized nanomaterials have greater favorability to directly pass through the GFB to reach renal tubular epithelial cells [91]. However, it is important to note that nanomaterials ranging from 3 to 7 nm exhibit an enhanced glomerular filtration as their size decreases. Conversely, nanomaterials smaller than 2 nm result in a reduced GFR due to stronger interactions between the glycosylation products of glomerular endothelial cells and the glomerular basement membrane (GBM) [92]. Furthermore, by modifying their shape, size, thickness, surface potential, and surface modifiers, nanomaterials can be tailored to prolong their half-life in the bloodstream while efficiently targeting therapeutic agents to specific tissues in a sustained and controlled manner. Additionally, these modified nanomaterials can protect active substance payloads (e.g., small molecule drugs) from premature degradation and elimination in vivo while improving solubility and preventing capture by the reticuloendothelial system. Nanomaterials can be specially designed to enhance renal targeting and optimize in vivo distribution of renoprotective agents [93–96], showcasing the extensive therapeutic potential of nanomaterials for AKI. Currently, diverse

compositions of nanomaterials with varying sizes and morphologies have been tailored for AKI therapy, including ROS nanosacrificial agents, nanoenzymes, and nanocarriers loaded with therapeutic agents (Fig. 6).

The current design of targeted nanomaterials for AKI can be categorized into two main approaches: passive targeting and active targeting. Passive targeting relies on the inherent physicochemical properties of the material, including its size, shape, and surface charge. On the other hand, active targeting involves modifying nanoparticles (NPs) with substances like hyaluronic acid and kidney-targeting peptides to enhance their affinity towards specific cell surfaces. By employing meticulous design in both the physical attributes and surface modifications of these nanomaterials, they can effectively deliver anti-inflammatory and antioxidant drugs to the site of renal injury for efficient and safe treatment.

Passive targeting

Size

For AKI, the passive targeting of nanomaterials is primarily influenced by factors such as the material's size, shape, and surface charge. In terms of size, small-sized NPs like nanoenzymes can easily traverse the filtration membrane to reach renal tubular epithelial cells due to their dimensions being below the GFR (< 7 nm). Conversely, large-sized NPs are unable to pass through due to stringent size screening imposed by GFB. However, in cases of AKI where glomerulus damage occurs and there is an enlargement in the gap between endothelial cells, basement membrane, and podocytes, significant structural changes and increased permeability allow for larger materials to pass through and deliver NPs to various renal cells. In recent years, most nanomaterials designed for AKI have been within a range of tens to hundreds of nanometers in size, mostly below 200 nm. Nevertheless, it has also been observed that NPs around 400 nm can accumulate in the kidney contradicting previous knowledge [97]. Considering the possibility that these NPs may be endocytosed by endothelial cells surrounding renal tubules leading to their long-term accumulation in proximal tubules, Han et al. developed polymer-based mesoscale NPs measuring 300–400 nm. These NPs exhibited localization within renal tubules following intravenous injection with over 26-fold selectivity towards tubular cells compared to other organs [98].

Shape

The biodistribution in vivo and the ability to pass through the GFB are also influenced by the morphology of nanomaterials. These morphologies primarily include spherical, tubular, rectangular, orthotetrahedral, and triangular shapes [99]. This is particularly applicable to sheet nanomaterials such as DNA rectangular origami and black phosphorus nanosheets (BPNS), which exhibit excellent renal targeting. Wang et al. discovered that the unique physical geometry of BPNS, including their size, shape, and charge properties, ensured their specific accumulation in mouse kidneys while exhibiting high ROS scavenging ability and minimal cytotoxicity in vivo. Such simultaneous achievement is challenging for other nanomedicines composed of metal NPs or polymers [100]. Carbon nanotubes (CNTs) with lengths ranging from 200 to 300 nm and molecular weights between 350 and 500 kDa (30–50 KDa for plasma proteins) can also be effectively filtered through intact GBM [101]. The enhanced renal targeting observed with these morphologies compared to spherical NPs may be attributed to the fact that on a three-dimensional scale, sheet nanomaterials can vertically traverse cellular interstitial spaces. These findings suggest that the specific aspect ratio of NPs plays a crucial role in facilitating their targeted diffusion across the GFB.

Surface charge

In addition to size and shape, the potential of NPs is one of the crucial factors influencing renal targeting. The charge of GFBs primarily originates from anionic proteoglycans in the basement membrane and negatively charged acetylheparin sulfate embedded in the surface of endothelial cells and the glycocalyx of podocytes [102, 103]. Consequently, positively charged NPs are more likely to traverse through the GFB and be eliminated by the kidneys. Conversely, negatively charged NPs face electrostatic repulsion, making them less prone to pass through the GFB [104–106]. However, certain recent studies have demonstrated that some strongly negatively charged NPs can be cleared by the kidneys more rapidly than weakly negatively charged ones [107], which contradicts prevailing perception. Therefore, further research is needed to draw more definitive conclusions.

Active targeting

Active targeting is primarily achieved through the surface modification of nanomaterials, which enables them to possess corresponding binding sites with the kidney. In comparison to passive targeting, active targeting results in higher accumulation within the target tissue and lower off-target toxicity.

Many studies have been conducted to enhance renal targeting by designing glycoprotein-bound peptides on the plasma membrane of proximal renal tubules, which were subsequently combined with nanomaterials. He et al. modified nanomaterials with the renal-targeting peptide LTHVVWL (PEG-LTH) [80]. In the mouse AKI

model, the fluorescence intensity of LTH-modified NPs was 1.6–1.8 times higher compared to NPs without LTH modification. Furthermore, in terms of biodistribution, NPs without LTH modification exhibited abundant distribution in the liver and spleen. The targeting efficiency of LTH-modified NPs was significantly superior to that of passive single targeting due to their ability to preferentially recognize the highly expressed Kim-1 receptor in injured proximal tubules facilitated by LTH peptide assistance. The aggregation of NPs at the renal site ensured drug availability for subsequent treatment purposes. However, some accumulation of NPs in the liver and spleen can be attributed to their capture by mononuclear phagocytes during toxin filtration from blood circulation as part of their physiological function within these organs' mononuclear phagocyte system (MPS). Similarly, other strategies such as hyaluronic acid and salivary acid have also been designed based on overexpression of specific proteins on renal tubular epithelial cell surfaces during AKI [108, 109].

In recent years, the wrapping of NPs with biofilms has emerged as a prominent research area. This approach enhances the blood half-life, tissue specificity, and biocompatibility of NPs. Examples include using platelet membrane or neutrophil membrane [110, 111]. In a recent study by Liu et al., they successfully demonstrated the targeting ability of renal cell membranes to the kidney [112], which is relatively uncommon compared to other types of cell membranes used in previous studies. By encapsulating NPs with renal cell membranes, not only can their accumulation in the kidney be increased but also the inherent properties of renal cell membranes contribute to improved biocompatibility, enhanced biodistribution, and reduced phagocytosis by the reticuloendothelial system.

The strengths of active targeting and passive targeting in renal targeting have not been thoroughly researched and compared, despite their unique advantages. Additionally, the synergistic effect achieved by combining these advantages to surpass their individual benefits has not been explored. It is insufficient to assume that simply mixing them together will result in stronger targeting. Furthermore, the current study only examines the phenotype without investigating the underlying mechanism of NPs targeting renal tubular epithelial cells or exploring the pathway of NPs uptake.

ROS nanosacrificial agents

In recent years, ROS nanosacrificial agents have gained widespread usage as active reducing agents for AKI treatment, including DNA Origami, Mxene and other nanosacrificial agents. These sacrificial agents protect endogenous biomolecules by rapidly reacting with ROS.

DNA

DNA can serve as an efficient scavenger of ROS due to its abundance of nucleophilic groups and high reactivity towards electrophilic ROS. Moreover, DNA possesses excellent inherent biocompatibility and biodegradability, being rapidly degraded by nuclease in vivo. Additionally, exogenous DNA can directly interact with RONS to mitigate cellular damage and alleviate AKI [113, 114]. Cai et al. engineered radiolabeled DNA origami nanostructures (DON) with rectangular, triangular, and tubular shapes [99]. These nanostructures exhibited preferential accumulation in the kidneys of healthy mice as well as rhabdomyolysis-induced AKI mice, with the rectangular DON demonstrating nephroprotective properties. The authors propose that this DON structure holds great potential for active drug delivery (e.g., Rec-don for AKI treatment) and as a carrier for NAC or other small molecule drugs. Subsequently, Per-Olof Berggren et al. developed a nanoscale cytokine based on precisely arranged interleukin 33 (IL-33) nano-arrays on rectangular DNA origami platforms to selectively deliver IL-33 to the kidneys for mitigating AKI [115]. Nanorafts carrying accurately quantified amounts of IL-33 primarily accumulated in the kidney for up to 48 h. Prolonged release of IL-33 from Nanoraft induced rapid expansion of type 2 intrinsic lymphoid cells (ILC2s) and regulatory T cells (Tregs), resulting in superior therapeutic effects compared to free IL-33 treatment alone. Thus, their study suggests that nanofolds could serve as structurally well-defined delivery platforms for cytokine immunotherapy targeting ischemic AKI and other renal diseases.

MXene

MXene materials are a type of transition metal carbide/nitride with a two-dimensional layered structure. They consist of transition metal carbides, nitrides, or carbon-nitrides that have a thickness of several atomic layers. These materials possess many advantages commonly found in 2D nanomaterials, such as extreme thinness, large specific surface area, high surface-to-volume ratio, and mechanical toughness. Due to the similarity between their nanosheet framework and the previously reported sheet DNA framework, MXenes preferentially accumulate in the kidneys of AKI mice and can be efficiently taken up by the kidneys. Additionally, they serve as carriers for drug molecules and exhibit great potential in the biomedical field as promising therapeutic nanomedicine [116]. Despite these excellent physicochemical properties that make MXenes suitable for various applications, there are still some drawbacks

when used in vivo including poor water dispersibility, slow degradation rate, and toxicity. Therefore, surface modification and functionalization are necessary to enhance the properties of MXene materials and provide them with new functions. Yang et al. proposed a novel artificial non-enzymatic antioxidant MXen nanoplatform for effective treatment of AKI in live animals [117]. Ti3C2-PVP nanosheets (TPN) were synthesized through polyvinylpyrrolidone (PVP) surface modification, demonstrating broad-spectrum redox-mediated ROS scavenging activity against oxidative stress-induced injury in both in vitro and in vivo experiments. Furthermore, the TPNs exhibited enhanced biocompatibility and physiological stability without causing significant toxicity in vitro and in vivo.

Other nanosacrificial agents

Many inorganic non-metallic elements also exhibit different valence states and demonstrate antioxidant activity. Among them, Se, phosphorus, and carbon are essential physiological elements. NPs based on these elements are currently being utilized for the treatment of AKI with exceptional therapeutic efficacy and minimal side effects. Cao et al. have developed a novel composite nanoparticle known as Se/albumin nanomaterials (SA NPs) [118]. In vivo experiments have confirmed that SA NPs effectively treat and prevent cisplatin-induced AKI by inhibiting oxidation and ferroptosis. BPNS are two-dimensional semiconductor materials composed of an equal number of phosphorus atoms (P), which possess strong RONS scavenging ability due to the easy oxidation of phosphorus by RONS to form non-toxic phosphate ions. Additionally, BPNS exhibit excellent biosafety properties, making them highly promising for biomedical applications including AKI therapy [119–122]. Wang et al. have developed a novel renal therapy based on BPNS [100]. These BPNS can act as ROS scavengers for treating AKI in mice. In vivo analyses conducted in mice have demonstrated that the remarkable advantages of BPNS-directed renal therapy lie in its lamellar structure, high ROS scavenging capacity, and minimal cytotoxicity within living organisms—attributes that are challenging to achieve simultaneously with other nanomedicines made from metal NPs or polymers. The unique physical geometry of BPNS such as their size, shape, and charge ensure targeted delivery to the kidneys in mice during treatment procedures. Carbon quantum dots (CDs) represent innovative carbon nanomaterials consisting of dispersed spheroidal carbon particles with extremely small sizes (below 10 nm) along with fluorescent properties. It exhibits excellent biocompatibility and minimal cytotoxicity. CDs also have a high accumulation and long-term retention in the kidneys. Moreover, CDs are abundant in oxygen functional groups, enabling its utilization as an antioxidant to exert antioxidative activity and eliminate ROS [123–126]. Ren et al. developed and synthesized kidney-cleavable quantum dot-drug conjugates (QDCs) [126]. These drug conjugates consist of CDs, DFO with iron chelating capacity, and polyethylene glycol (PEG) with prolonged in vivo retention. They possess remarkable ROS scavenging activity, favorable renal biodistribution, and can be employed to mitigate chemotherapeutic drug induced AKI. The inclusion of CDs within QDCs not only confer a high degree of renal specificity for DFO but also effectively scavenges pathologically unstable iron species within the kidney, thereby obstructing the source of ROS production and exerting potent antioxidant effects while preventing renal oxidative damage caused by excessive ROS generation. In a cisplatin-induced AKI mouse model, QDCs effectively safeguard against oxidative damage in the kidneys while inhibiting ferroptosis and apoptosis.

Nanoenzymes

Antioxidant nanoenzymes possess renewable active centers that imitate endogenous antioxidant enzymes for continuous RONS detoxification. In contrast to nanosacrificial agents, nano-enzymes are not scavenged but rather efficiently eliminate RONS from the body in an ongoing manner [127]. These nanomaterials can be divided into two categories: (1) enzymes or catalytic groups modified onto nanomaterial surfaces wherein primary catalysis is derived from the enzyme itself. Through assistance from nanomaterials, these modified enzymes or their enzymatic moieties attain remarkable stability and durability. (2) Nanomaterials inherently exhibit enzymatic properties enabling them to facilitate biocatalytic reactions akin to natural enzymes [128]. Nevertheless, there remains ambiguity on the definition of nanoenzymes.

Metal and metal-based nanoenzymes

Nano cerium oxide (CeO_2) is an inorganic metal oxide that exhibits chemical catalytic activity like peroxidase (POD) and oxidase (OXD). Its unique physicochemical properties enable nano CeO_2 to find extensive applications, including UV-absorbent materials, catalysts, and biomedicine. Recently, there have been numerous studies demonstrated the antioxidant, antitumor, antibacterial, and neuroprotective effects of CeO_2 NPs. The antioxidant effect of CeO_2 is attributed to its cyclic conversion between Ce^{3+} and Ce^{4+}, enabling it to function as both an oxidation and reduction catalyst. CeO_2 can scavenge ·OH, O_2^- and H_2O_2 in solution, thereby exerting its antioxidant role. When the ratio of

Ce (III)/Ce (IV) in CeO_2 is high, it tends to exhibit SOD-mimicking activity: $O_2^- + Ce^{3+} + 2H^+ \rightarrow H_2O_2 + Ce^{4+}$; $O_2^- + Ce^{4+} \rightarrow O_2 + Ce^{3+}$. Conversely, when the ratio of Ce(III)/Ce(IV) is low, it tends to display CAT-like activity: $2Ce^{4+} + H_2O_2 \rightarrow Ce^{3+} + O_2 + 2H^+$ [129–131]. Yang et al. developed a pH-selective "oxidation cycle gas pedal" based on black phosphorus/cerium-catalyzed tunable nanoenzymes (BP@CeO_2-PEG) [132]. The BP@CeO_2-PEG nanoenzymes exhibited diverse catalytic activities, including CAT, SOD, and ·OH antioxidant capacity (HORAC). Importantly, it also demonstrated pH-selective catalytic activity. Consequently, BP@CeO_2-PEG effectively and persistently scavenged ROS, thereby mitigating cisplatin (DDP)-induced AKI. In the neutral renal environment, BP@CeO_2-PEG nanoenzymes can enhance their catalytic "oxidation cycle" by increasing the Ce^{3+}/Ce^{4+} ratio and promoting ATP regeneration, leading to efficient elimination of DDP-induced ROS. Furthermore, BP@CeO_2-PEG nanomolecules can inhibit oxidative stress-induced apoptosis of tubular epithelial cells through suppression of the PI3K/Akt signaling pathway. However, in the acidic tumor microenvironment, the presence of H^+ impedes the conversion of Ce^{4+} to Ce^{3+}, disrupting the oxidative cycle and compromising ROS scavenging ability therefore ensuring DDP's anti-tumor effect.

Similarly, numerous other metals, such as ultra-small gold (Au), Argentum (Ag), copper (Cu), platinum (Pt), manganese (Mn), iridium (Ir) and ruthenium (Ru) NPs, have been developed for the treatment of AKI. These NPs are frequently passively targeted to renal tissues to eliminate various RONS due to their multiple antioxidant enzyme properties [133, 134]. Jiang et al. fabricated PVP-coated bimetallic nanoenzymes doped with diverse metals including Ru, Mn, Fe, Cu, Ni, Zn and Au using Pt as a catalyst [135]. They assessed the free radical scavenging activity of these metallo-nano-enzymes which led to the identification of a potent in vitro antioxidant capacity in RuPt nano-enzyme. The subsequent modification of the compound involved quercetin coordination (QCN), which enabled obtained QCN to effectively scavenge a wide range of ROS both in vivo and in vitro, thereby exerting a therapeutic effect against glycerol-induced and DDP-induced AKI. The protective effect of QCN on H_2O_2-induced HEK293 cells was attributed to its excellent biocompatibility and antioxidant properties. On the other hand, nanoenzymes composed of small-sized RuPt particles played a protective role in preventing AKI occurrence. As a nano-antioxidant, QCN has great potential for mitigating the effects of rhabdomyolysis and DDP-induced AKI. Guo et al. synthesized Mn3O4 nanoflowers (Nfs) with dual abilities to scavenge ROS and adsorb cfDNA for AKI treatment [136]. Importantly, Mn3O4 Nfs exhibited both SOD and CAT activities, enabling cascade ROS scavenging. Mn3O4 Nfs provided effective protection against both DDP-induced and I/R-induced AKI mouse models. Additionally, Mn3O4 Nfs allowed T1 magnetic resonance imaging (MRI) for monitoring renal function during AKI treatment, providing a nano-enzymatic therapeutic strategy for treating AKI.

Non-metallic nanoenzymes

For non-metallic substances, their participation in the catalytic process is challenging due to the absence of empty orbitals. However, advancements in nanoscience have enabled the modification of non-metallic materials' surface and nanostructure, thereby allowing them to exhibit catalytic activity. Carbon nanomaterials such as fullerenes, CNTs, graphene, graphene oxides (GO), CDs and graphene quantum dots (GQDs) have gained widespread usage across various research fields owing to their exceptional physical and chemical properties. Xu et al. developed metal-free and phenolic functionalized CDs that mimic intracellular antioxidant defense systems [137]. These CDs demonstrate SOD, GPX and CAT activities. The SOD activity of the CDs was found to be remarkably high (18,187 U/mg). The bond dissociation of phenol on the CDs was significantly lower than that of natural GPx's selenocysteine residue, facilitating peroxide intermediate formation for initiating GPx-like reactions. Consequently, CDs possess excellent mimetic activity resembling intracellular antioxidant systems while exhibiting selective enrichment in the kidney and inhibiting iron metamorphosis. They exhibit significant therapeutic effects in AKI mice models. Phenolic functionalized CNTs prepared herein hold immense potential for nanocatalytic treatment against DDP-induced AKI.

In addition, several other antioxidant nanoenzymes, such as melanin NPs, Prussian blue nanoenzymes and molybdenum (Mo)-based polyoxidized metal clusters (POM) have also been reported [133, 138]. Overall, despite the advantages of low cost, high stability and durability possessed by nanoenzymes that overcome many disadvantages of natural enzymes, there are still some challenges to address. For instance, the catalytic activity of most nanoenzymes remains significantly lower than that of their corresponding natural enzymes. Furthermore, poor substrate selectivity is a common issue faced by nanoenzymes. Although certain nanomaterials exhibit multi-enzyme activities like natural enzymes', these activities sometimes interfere with each other. Researchers have dedicated considerable efforts to studying the catalytic mechanisms of nanoenzymes; however, only a few mechanisms have been reported thus far while many others remain unclear. Understanding the catalytic

kinetics and mechanisms can potentially aid in regulating the activity of nanoenzymes.

Nanomaterials loaded with therapeutic agents

Due to the unique physiological structure and function of the kidneys, certain traditional drugs such as amphotericin and NAC exhibit suboptimal renal accumulation, thereby diminishing their therapeutic efficacy. Additionally, some drugs suffer from poor water solubility, low bioavailability and heightened adverse reactions and side effects, posing challenges for clinical medication in AKI. In recent years, there has been rapid progress in combining nanomaterials with medicine as a promising approach to address these issues. Loading drugs onto nanomaterials offers a viable solution by enabling effective drug delivery. These drug-loaded nanomaterials can be broadly classified into three categories: nucleic acid nanomaterials, protein nanomaterials and small molecule drug nanomaterials.

Nucleic acid nanomaterials

RNA interference (RNAi) is considered a significant technological advancement that holds promise for novel therapeutic strategies through gene regulation. One of the mechanisms of interference involves sequence-specific targeting of messenger RNA (mRNA) using complementary small interfering RNAs (siRNAs), resulting in mRNA degradation. Although RNAi has immense potential for treating various diseases, its realization has been hindered primarily by challenges such as poor tissue and cell specificity, adverse off-target effects, and limited serum stability in vivo. However, with advancements in nanomedicine, these barriers to in vivo siRNA utilization can be overcome by integrating siRNAs with nanomaterials [139–142]. Michael R. McDevitt et al. employed an ammonium-functionalized carbon nanotube (fCNT) platform to specifically deliver Trp53- and Mep1b-targeted siRNAs to proximal renal tubular cells for prophylactic mitigation of AKI in an animal model [143]. Compared to the delivery of siRNA alone, fCNT facilitated enhanced siRNA delivery to renal tubular cells and effectively reduced the expression levels of several target genes including Trp53, Mep1b, Ctr1 and EGFP.

MicroRNAs (miRNAs) are short non-coding RNAs that participate in the post-transcriptional regulation of target gene expression by binding to the 3′ untranslated region (3′UTR) of downstream target genes, leading to their degradation or repression. The utilization of miRNAs for kidney disease treatment represents a fascinating and emerging area of research. MiRNAs function as key regulators of gene expression and play critical roles in various molecular processes across multiple organs, including the kidney. However, one limitation associated with miRNAs is their high susceptibility to enzymatic degradation and instability within the systemic circulation. To enable successful clinical application of miRNAs, it is imperative to design a stable drug delivery system. Nanoparticle-based drug delivery systems offer an intriguing approach for targeted delivery of therapeutic drugs to specific body regions [144–146]. Zhang et al., through electrostatic interactions, encapsulated miR-500a-3p within cationic liposomes on their surface to enhance therapeutic efficacy against AKI [147]. Their study demonstrated that miR-LIP directly regulates the expression levels of RIPK3 and MLKL (a necrosis regulator), thereby mitigating the severity of kidney injury. Compared to DDP-treated HK2 cells, miR-LIP effectively modulated MLKL phosphorylation levels. Similar results were observed for RIPK3 as well. Additionally, miR-LIP was found to regulate inflammatory responses in renal tubular cells. Western blot analysis revealed that the phosphorylation of P-65 was the primary instigator of the inflammatory response, and miR-LIP significantly attenuated CDDP-induced NF-kB phosphorylation.

Protein nanomaterials

Several pro-inflammatory mechanisms have been observed following the development of AKI, including elevated levels of cytokines such as TNF-α, IL-18 and IL-1β, as well as activation of pro-inflammatory pathways like NF-κB and Toll-like receptor. Inflammatory factors play a crucial role in initiating and progressing fibrosis, leading to renal tubular epithelial cell activation and infiltration by inflammatory cells. Recently, there has been renewed interest in certain proteins or peptides with anti-inflammatory and tissue protective properties in the kidney through their binding to nanocarriers. Liu et al. developed a self-assembling peptide/heparin (SAP/Hep) hydrogel [148]. This SAP/Hep hydrogel encapsulates two drugs, TNF-α neutralizing antibody (anti-TNF-α) and hepatocyte growth factor (HGF). The physical mixing of these substances leads to an accelerated release of anti-TNF-α and a sustained release of HGF. This mechanism facilitates tissue repair following I/R injury. Compared to SAP or Free-drug alone, the combination of SAP/Hep demonstrated superior efficacy in reducing inflammation and apoptosis, improving renal function and tubular regeneration, as well as attenuating chronic fibrosis after I/R injury. SS-31 peptide is an inhibitor of cardiolipin POD that specifically targets mitochondria and possesses therapeutic properties for I/R injury. Du et al. synthesized a renal-targeted chitosan drug carrier called SC, which exhibits rapid and efficient accumulation in AKI kidneys, particularly within the renal tubules [149]. The mitochondria-targeted antioxidant SS31 was synthesized

as a precise stepwise-targeted prodrug (SC-TK-SS31) by conjugating it to SC through a ROS-responsive TK linker. SC-TK-SS31 accumulates in AKI kidneys (organs), subsequently localizes within renal tubules (tissues), and finally internalizes into injured renal tubular cells (cells). The reactive release of SS31 within these cells further targets the mitochondria (organelles), alleviating mitochondrial damage and ultimately ameliorating AKI. Based on its precise accumulation and sensitive release mechanism, SC-TK-SS31 significantly enhances the therapeutic effect of SS31.

Small molecule drug nanomaterials

The clinical application of certain small molecule drugs, such as resveratrol (RES) and curcumin, is severely limited due to their inadequate water solubility, weak renal targeting, and low bioavailability. Combining nanomaterials with small molecule drugs can provide a promising solution to address these challenges. Zhang et al. developed a HA-based self-assembled melanin NPs covalently linked with DXM (HA-MNP-DXM) for the treatment of I/R-induced AKI. This system effectively scavenges excessive RONS while attenuating inflammatory damage [150]. Upon targeting the lesion microenvironment, the assembled NPs degrade into ultrasmall melanin NPs and release free DXM. The HA-MNP-DXM NPs exhibit excellent antioxidant properties, targeted delivery capabilities and demonstrate significant accumulation in the renal tissue of an AKI mouse model. Importantly, administration of HA-MNP-DXM NPs improves renal function and mitigates tubular apoptosis through anti-inflammatory and antioxidant mechanisms. Zheng et al. reported a novel nanomedicine for the treatment of AKI utilizing polyursolic acid (PUA) as a bioactive nanocarrier and RES as a model drug [151]. PUA NPs effectively encapsulate hydrophobic antioxidant and anti-inflammatory drugs, such as RES, demonstrating excellent stability and displaying potent in vitro antioxidant and anti-inflammatory effects. Moreover, PUA NPs significantly enhance the renal accumulation of RES while exerting their inherent antioxidant properties, thereby further enhancing the therapeutic efficacy of RES in AKI treatment. Su et al. developed Garcinic acid NPs (GA-NPs) modified with PEG [152]. These GA-NPs exhibit prolonged drug retention time within the body in both DDP-induced

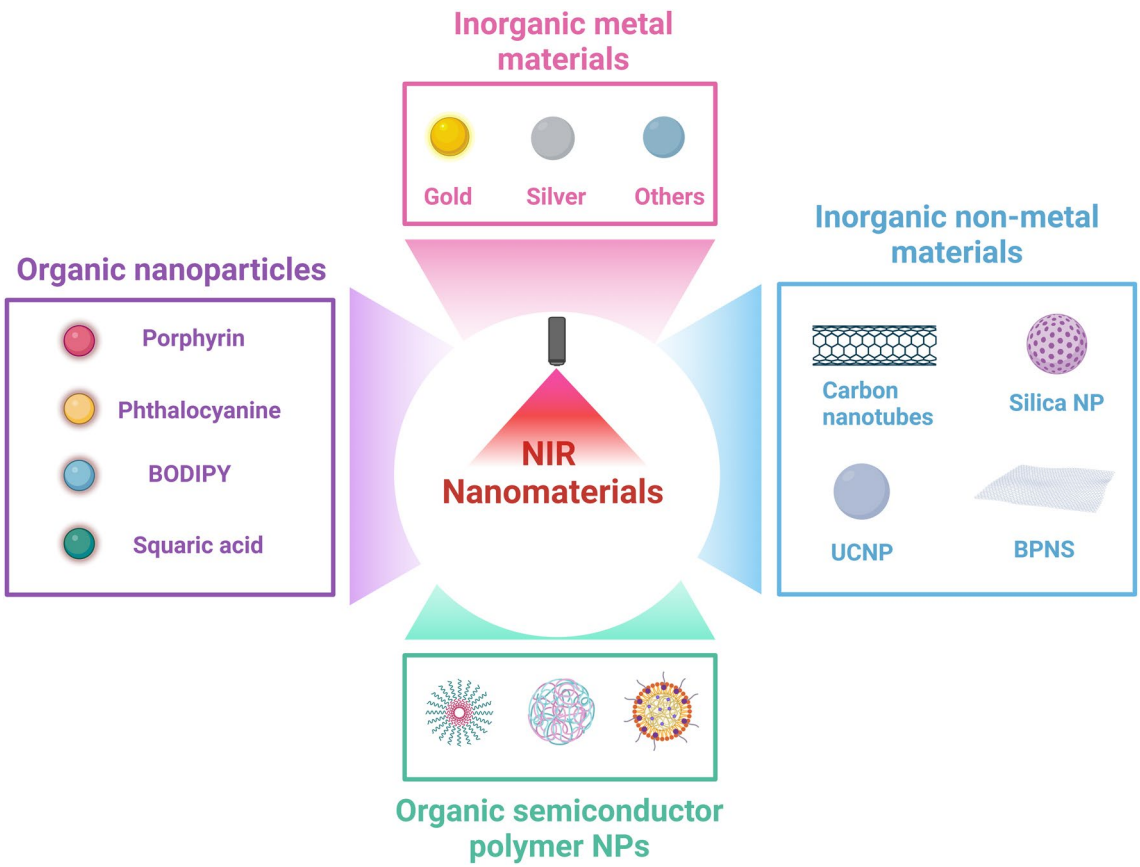

Fig. 7 Different types of NIR Photoresponsive nanomaterials

and rhabdomyolysis-induced AKI models, consequently augmenting the therapeutic effect of garcinia cambogia extract. Collectively, these examples highlight the promising potential of nanomaterials loaded with small molecule drugs for AKI therapy.

However, there are several limitations in the therapeutic application of nanomedicine for AKI. On the one hand, a lack of comprehensive understanding regarding the physiological structure of the kidneys and the pathological mechanisms of AKI among nanoresearchers has resulted in the development of materials that deviate from clinical relevance. Consequently, these materials often remain at conceptual stages, lacking effective solutions to safety, efficacy, and administration protocol-related issues. On the other hand, biomedical researchers solely focused on biological aspects lack sufficient interdisciplinary knowledge in nanomaterials, leading to an inadequate recognition of the therapeutic potential of nanomaterials in AKI [23].

Application of optical diagnosis and treatment in AKI

Most of the nanomaterials currently utilized for AKI treatment only possess therapeutic effects and lack diagnostic capabilities. Additionally, early diagnosis plays a crucial role in determining the prognosis of AKI. To address this issue, integrating nanomaterials with optical imaging techniques holds great promise. The commonly employed medical imaging modalities in clinical practice today primarily involve tomography methods such as MRI, X-ray computed tomography (CT) and positron emission tomography (PET). These techniques rely on deep-penetrating radiation, including electromagnetic waves and moving subatomic particles to capture both structural and functional information about the imaged object. Subsequently, collected data is processed using computer algorithms to construct spatial signal distributions within the human body [153]. This method has certain limitations, including the presence of ionizing radiation, limited spatial resolution and low temporal resolution. In recent years, optical imaging diagnosis and treatment have made significant advancements compared to traditional imaging methods. It does not possess the drawbacks associated with tomography but offers several advantages such as high sensitivity, high SNR, superior spatial and temporal resolution, and cost-effectiveness. Consequently, it has witnessed an increasing utilization in disease diagnosis and treatment. Among these optical imaging methods is NIR imaging diagnosis and treatment which holds great promise for both basic science research and clinical practice. The most widely used biomedical fluorescence imaging technique operates in the NIR-I window (700–1000 nm) [154], although there is a growing focus on imaging in the NIR-II window (1000–1700 nm) [155]. Compared to NIR-I imaging, NIR-II imaging offers enhanced imaging depth and resolution while minimizing light scattering and absorption. In recent years, there has been a growing interest in combining NIR technology with nanomaterials for disease treatment. Currently, reported nanomaterials for therapeutic applications encompass both inorganic and organic materials. In terms of inorganic materials, this includes nonmetallic compounds such as carbon (C), silicon (Si), phosphorus (P), upconversion nanoparticles (UCNPs), and composite nanomaterials known as MXenes. Additionally, precious metal NPs like Au and silver, along with other metal NPs including iron (Fe), Cu, tungsten (W), and niobium (Nb) are also considered inorganic options. On the other hand, organic NIR nanomaterials mainly consist of small molecules that respond to NIR light and polymer NPs based on organic semiconductors referred to as SPNPs. Examples of these include indocyanine green (ICG), phthalocyanine NPs, borondipyrromethane (BODIPY) NPs, among others (Fig. 7).

Inorganic non-metallic materials

Carbon NPs primarily encompass CNTs, graphene nanomaterials, and carbon dots (CDs) among others. They exhibit excellent biocompatibility, water solubility, low biotoxicity, and stable optical properties while continuously and consistently generating localized thermal effects under NIR light irradiation [156]. For instance, CDs represent a novel class of fluorescent carbon nanomaterials typically characterized by their sub-10-nm size. These CDs are commonly composed of amorphous and crystalline carbon nuclei adorned with diverse oxygen-containing functional groups on the surface such as hydroxyl and carboxyl groups [157]. Currently, there is only one study available on the direct utilization of carbon dots for AKI imaging. In 2022, Tian et al. synthesized NIR-CDs through one-pot pyrolysis using glutathione and urea as precursors [158]. The resulting NIR-CDs exhibited NIR fluorescence (696 nm), ultra-small size (1.8 ± 0.3 nm), low toxicity, and high renal clearance (97.84%). This NIR-CDs can be employed for imaging analysis of impaired renal function, providing valuable insights into novel applications of NIR-CDs in this context. Most other studies primarily focus on the direct treatment of AKI using CDs alone. For instance, wu et al. developed a novel selenium-doped carbon point (SeCD) [159]. SeCD effectively eliminates broad-spectrum ROS and significantly enhances GPX4 expression by releasing selenium, thereby considerably mitigating iron-induced apoptosis and cisplatin-related AKI in renal tubular epithelial cells without compromising the efficacy

of cisplatin chemotherapy. In general, their applications primarily encompass the following aspects: Firstly, they can serve as fluorescent probes for precise disease localization, enabling early diagnosis and disease monitoring, and even facilitating integrated diagnosis and treatment. Secondly, they can function as targeted drug carriers for site-specific drug delivery and lesion treatment. Thirdly, they can act as photosensitizers (PS) or sound sensitizers to generate heat and energy upon light activation or ultrasonic stimulation, allowing non-invasive disease therapy.

As previously mentioned, black phosphorus (BP) is a distinctive allotrope of phosphorus with a layered structure that exists in single- and multilayer forms. Compared to graphene, BP exhibits remarkable prospects in the field of photodynamic therapy (PDT) and photothermal therapy (PTT), owing to its exceptional efficiency in generating singlet oxygen ($^1O_2$) and strong NIR light absorption capability [160]. Tian et al. investigated the synthesis and surface modification of BPQDs with renal clearance capability [161]. The resulting PEG-BPQDs exhibited an ultra-small hydrodynamic diameter of 1.74 ± 0.23 nm and demonstrated strong PA signals upon near infrared excitation. Real-time monitoring of kidney injury can be achieved by utilizing PEG-BPQDs as a PA imaging agent. However, BP is highly susceptible to oxidation in the presence of air, leading to a reduction in its photothermal conversion performance due to the formation of insulating phosphorus oxide on its surface. Despite demonstrating favorable biocompatibility and light stability in biomedical applications, practical utilization of BP faces two main challenges. Firstly, achieving large-scale and uniform production remains unattainable. Secondly, there is a need for further research on fine functional modification strategies to enhance its targeting efficiency in disease tissues.

UCNPs are lanthanide metals, transition metals, or actinide doped ions fixed in the main lattice of an inorganic crystal. It has the characteristics of deep tissue excitation, high resolution, minimal light damage, light stability and a variety of excitation wavelengths [162]. UCNPs are different from traditional contrast agents. Conventional contrast agents exhibit Stokes shift luminescent emission, which emits longer wavelengths and lower energies after they are illuminated by a laser [163]. UCNPs can convert low-energy photons (such as NIR light) into ultraviolet or visible light. This is an anti-Stokes shift. In recent years, researchers have mainly used UCNPs for PDT, as well as for cell, tissue, animal imaging, and biological detection. Compared to conventional fluorophores, organic dyes have excitation wavelengths in the ultraviolet and visible light regions. So it's limited by the depth of the organization. UCNPs can overcome this shortcoming by using the anti-Stokes shift for upconversion photoluminescence imaging in the NIR range. Zhou et al. proposed an upconversion luminescence (UCL) sensing system utilizing upconversion nanoparticles, which consists of three components: mesoporous silicon dioxide ($mSiO_2$) coated UCNPs (NaYF4: 20 mol% Yb, 1.8 mol% Er, 0.5 mol% Tm) as the carrier and energy donor. This system is capable of monitoring endogenous CO fluctuations such as hypoxia, acute inflammation or ischemic injury and evaluating HO-1 expression in vitro and in vivo, providing a valuable tool for detecting disease-associated ions and biomolecules [164]. However, UCNPs still exhibit certain limitations, including a low energy transfer efficiency between UCNPs and PS, as well as elevated tissue temperatures. Additionally, there are challenges in imaging such as limited imaging modes and weak fluorescence intensity. The composite nanomaterial MXenes has been previously discussed (refer to Sect. 6.3.2).

Inorganic metal materials

Au NPs are particles of gold with diameters ranging from 1 to 100 nm. As a crucial member of the nanotechnology family, Au NPs possess several advantages including low toxicity, facile surface modification, strong biocompatibility, unique optical properties, and the ability to finely adjust their size, shape, and surface characteristics [165]. Notably, they exhibit local surface plasmon resonance (LSPR), which refers to the collective oscillation of electrically conductive band electrons in metal NPs when exposed to electromagnetic excitation from incident light [166]. These exceptional optical properties have led to widespread applications in photoacoustic imaging for cancer detection, atherosclerotic plaque visualization, brain function analysis, and image-guided therapy. By accumulating at lesion sites and combining with photoacoustic imaging technology, high-contrast and high-resolution images can be obtained. Liu et al. designed renal-clearable NIR-II emitting AuNPs co-coated with both pH-responsive 2,3 dimethylaleic anhydride (DMA) modified β-mercaptoethylamine (CA) ligand (CA-DMA) and ionized 2-diethylami- noethanethiol hydrochloride (DAT) groups (p-AuNPs), which incorporated both charge-reversal and self-assembly abilities toward renal acidic microenvironments to enhance renal tubular interactions and retention of the particles, thereby generating amplified fluorescence signals in the injured kidneys [167].

Silver NPs are a type of precious metal nanomaterials that can be synthesized easily and at a low cost. They exhibit various shapes, including spherical, rod-like, and tetrahedral structures. By altering the synthesis

conditions, controlled self-assembly and nanostructure regulation of silver NPs can be achieved. Moreover, they possess exceptional optical properties such as strong surface plasmon resonance effects, which render them highly suitable for applications in optical sensing, imaging, and therapy [168–170]. Currently, there is no existing literature reporting the direct utilization of silver NPs for NIR diagnosis and treatment of AKI. However, it has been scientifically demonstrated that silver NPs possess anti-inflammatory properties, antibacterial activity, and regenerative potential. For example, Mou et al. proposed a novel approach for the preparation of highly biocompatible Ag/pda nanoplatforms for wound treatment utilizing AgNPs and pda [171]. This nanoplatform not only exhibits broad-spectrum antibacterial properties against diverse planktonic bacteria, but also possesses the ability to disrupt bacterial biofilm formation by dismantling the biofilm structure under 808 nm laser irradiation. Furthermore, this nanoplatform demonstrates anti-inflammatory effects and facilitates wound healing through regulation of macrophage polarization. We anticipate an increased research investment and clinical translation of silver NPs in the NIR diagnosis and treatment of renal conditions in the future.

Other metal nanoparticles

Mo based NPs, as outstanding representatives of transition metal semiconductors, have set off a research upsurge in the field of phototherapy due to their excellent biocompatibility, high PCE and excellent NIR absorption characteristics. However, the utilization of these transition metal NPs in NIR phototherapy for AKI is relatively uncommon, primarily limited to therapeutic applications. For instance, Cai et al. reported the discovery of molybdenum-based polyoxometalate (POM) nanoclusters that exhibit preferential renal uptake, making them promising nanoantioxidants for renal protection [133]. POM nanoclusters demonstrate a broad spectrum of antioxidant activities against various reactive oxygen species. Additionally, dynamic PET imaging revealed their remarkable affinity for renal accumulation.

Organic nanoparticles

Organic NPs primarily consist of organic small molecules and organic semiconductor polymer NPs that exhibit NIR response. Small molecule photothermotropic agents, such as porphyrin, phthalocyanine, BODIPY, and squaraine dye, are commonly used. However, despite their relatively excellent light stability and PCE, these dyes have certain limitations. For instance, porphyrins are a class of macromolecular heterocyclic compounds formed by connecting the α-carbon atoms of four pyrrole subunits via a methyl-bridge (=CH–). The absorption peaks of porphyrins may include 1627.83 cm^{-1} (benzene ring stretching), 1311.48 cm^{-1} (amide bond stretching), 1088.6 cm^{-1} (benzene ring bending inside), and 892.472 cm^{-1} (benzene ring bending outside) [172, 173]. The infrared spectrum characteristics of porphyrins can be influenced by various factors such as the type and location of substituents and the choice of solvents; therefore, it is essential to comprehensively consider these factors when analyzing and interpreting the infrared spectrum to obtain accurate results [174]. Akimitsu Narita et al. reported that the fusion of π-extended porphyrins with one or two nanographene units (GPP-1 and GPP-2) can serve as a new class of NIR-responsive organic reagents, which show absorption of ≈1000 and ≈1400 nm in the NIR window. Under 808 nm and 1064 nm laser irradiation, the PCE reached 60% and 69%, respectively [175]. However, porphyrins exhibit inherent drawbacks such as low aqueous solubility and facile self-aggregation, which impede their drug absorption in phototherapy. Moreover, their limited tissue penetration restricts their application to superficial diseases exclusively. It is noteworthy that sodium porphyrin (Photofrin®) stands as the pioneering clinically approved PS [176]. In the course of long-term treatment, it exhibits reduced incidence of adverse effects, excellent reproducibility, and absence of drug resistance. However, its current application is primarily limited to cancer patients rather than those with kidney injury. Additionally, it is associated with cutaneous photosensitivity issues and metabolic disorders.

Similarly, phthalocyanine is a compound possessing an extensive conjugated system comprising 18 electrons. Its structural composition bears striking resemblance to that of porphyrins, which are abundantly present in the natural world. Phthalocyanine has exhibited remarkable potential in the fields of bioimaging and disease treatment [176]. Wang et al. prepared a unique nano-sized hypoxia-sensitive coassembly (Pc/C5A@EVs) by molecular recognition and self-assembly [177]. The coassembly consists of macrocyclic amphiphilic C5A, commercial dye sulfonated aluminum phthalocyanine, and mesenchymal stem cell-excreted extracellular vesicles (MSC-EVs). The administration of Pc/C5A@EVs in a mouse model of renal injury enhances their in vivo circulation time, facilitates targeted delivery to the kidney through integrin receptors α4β1 and αLβ2, and enables hypoxia-sensitive NIR fluorescence imaging. Although it exhibits superior thermal stability, a high extinction coefficient, and strong absorption in the NIR region, its wide application in the biomedical field is limited due to its slow metabolic rate in vivo, propensity for aggregation, inadequate targeting ability, suboptimal "normal open" photosensitivity, and unsatisfactory therapeutic efficacy.

Organic semiconductor polymer NPs possess an alternating structure of single, double, or triple bonds along their main chain, endowing them with semiconductor properties. Organic semiconductor polymer NPs are polymers that exhibit extended conjugation through donor–acceptor connections, thereby enhancing their light absorption capabilities. Additionally, they demonstrate remarkable characteristics such as strong photostability, rapid radiation transition rates, and a large Stokes shift [178]. The emission wavelength of such materials is generally limited to less than 900 nm due to the challenges in molecular design and synthesis. Hence, the advancement of NIR two region imaging holds greater significance.

The application of NIR light-responsive nanomaterials in AKI holds significant therapeutic potential given the current challenges associated with this condition. However, currently there is a paucity of studies focusing solely on nanomaterial therapy in AKI, let alone the utilization of combined NIR and nanomaterials for optical diagnosis in AKI. Such reports are scarce. This paper will then provide a concise introduction to optical bioimaging modalities, elucidating their underlying physical principles, relative advantages, and synergistic capabilities. Additionally, it will outline the current advancements and applications of NIR diagnosis and treatment for AKI, while addressing potential future challenges pertaining to NIR photoresponsive nanomaterials. These insights are expected to offer novel perspectives for the diagnosis and treatment of AKI.

Physical mechanisms of fluorescence imaging

Fluorescence is a prevalent luminescent phenomenon observed in nature, arising from the interaction between photons and molecules. It involves the emission of light at a different wavelength (emitted light) by a fluorescent molecule upon absorption of specific wavelength light (excitation light). This process primarily entails internal electron transfer, which can be illustrated using the Jablonslc molecular energy level diagram. According to the law of conservation of energy, during energy transformation, its magnitude remains constant and energy cannot be created or destroyed. When a molecule in its ground state receives external energy (such as light, electrical, or chemical stimuli), electrons surrounding the nucleus transition from the ground state energy level S0 to higher-energy excited states (first or second excited state). However, an electron in an excited state is unstable and subsequently returns to its ground state through radiative and non-radiative decay processes. Radiative decay occurs via photon emission to release energy (including fluorescence, phosphorescence and delayed fluorescence processes), while non-radiative decay does not involve photon emission but rather dissipates excess energy as heat or undergoes internal conversion into other forms [179, 180].

Application of NIR imaging in clinical settings

The visible spectrum spans from 350 to 700 nm, while the NIR window is further divided into NIR-I (700 nm-1000 nm) and NIR-II (1000 nm-1700 nm), with the latter being subdivided into NIR-IIa (1000 nm-1400 nm) and NIR-IIb (1500 nm-1700 nm). Compared to visible light, NIR-I has deeper tissue penetration depth and relatively lower levels of light scattering and absorption. Additionally, in vivo imaging using NIR exhibits higher signal-to-background (SBR) ratio. These properties collectively enable high sensitivity and resolution imaging within the NIR-I window. Conventional fluorescence imaging primarily utilizes the visible and NIR-I windows [181–184].

Over the past 50 years, the U.S. Food and Drug Administration (FDA) has granted approval for clinical use to two primary NIR fluorophores. These include ICG, which emits at approximately 800 nm, and methylene blue (MB), which emits at around 700 nm. Both ICG and MB have been utilized in NIR fluorescence-based intraoperative imaging to visualize anatomical structures such as blood vessels, lymphatic vessels, gastrointestinal tract, bile ducts, ureters, cardiac perfusion function imaging, and image-guided surgical resection of diseased tissue [185–189]. Moreover, NIR laser technology has been extensively employed in the medical field for the last three decades with well-established safety measures and methodologies. Henceforth, it holds great promise for clinical applications [190–192]. However, there is a scarcity of reports on the application of NIR in AKI and particularly limited clinical usage.

NIR-II fluorescence imaging is a technique that utilizes the emission of fluorescence within this spectral range to visualize anatomical structures, biomolecules, and functional activities in biological tissues. In comparison to NIR-I imaging, NIR-II not only possesses similar properties as NIR-I but also demonstrates enhanced tissue penetration capabilities due to reduced scattering and autofluorescence. This inherent advantage facilitates high-resolution fluorescence imaging of deep tissues such as subcutaneous lymph nodes, neurons in deep brain regions, deep-seated tumors, and abdominal cavity intestines. The ability to image these deep tissues in vivo is of utmost importance since many diseases cannot be fluorescently imaged due to their depth [193, 194]. The development of NIR-II nanomaterials holds great potential for applications in pigs, monkeys, and humans [195–197]. Existing contrast agents for NIR-II imaging encompass CNTs [198, 199], quantum dots (QDs) [200, 201], small molecules [202–204], fluorescent proteins [205, 206], rare earth NPs (RENPs) [207–209], and Au

Table 3 A summary of NIR-I and NIR-II fluorescent probes for AKI in recently year

Probe	Size	Analyte	Spectral Region	λex	λem	Kidney-targeting strategy	Refs.
FDOCl-22	/	HOCl	NIR-I/PA	620 nm	680 nm	/	[222]
KNP-1	/	ONOO–	NIR-I	640 nm	679 nm	Nile red derivative	[219]
NFP-ONOO	/	ONOO–	NIR-I	500 nm	654 nm	/	[220]
NRN	/	ONOO–/GSH	NIR-I	683 nm	766 nm	GFR decline	[221]
Kim-TDF17	10.10 nm	/	NIR-I	745 nm	790 nm	Kim-1/DNA structure	[223]
NIR-CDs	1.8 ± 0.3 nm	/	NIR-I	420 nm	696 nm	GFR decline	[158]
1-DPA_2	/	caspase-3	NIR-I	790 nm	808 nm	phosphatidylserine	[224]
DDAV	/	Vanin-1	NIR-I	605 nm	660 nm	/	[225]
DSMN	/	$SO3^{2-}$	NIR-I	580 nm	710 nm	/	[226]
NAC-AuNCs	~2 nm	ONOO–	NIR-II	808 nm	1050 nm	AuNC aggregation/GFR decline	[227]
TPPTS-AuNPs	4.3 ± 1.0 nm	GSH	NIR-II	488 nm	1026 nm	small size/Zeta potential	[228]
MHA/Cystm-Au NCs	2.82 ± 0.04 nm	1064 nm laser	NIR-II	1000 nm	1045 nm	GFR decline	[229]
GNP-KTP5-ICG	5.8 nm	ROS	NIR-II	805 nm	1105 nm	KTP	[230]
PEG3-HC-PB	/	H_2O_2	NIR-II/3D-MSOT	808 nm	950 nm	renal clearance	[231]
BOD-II-NAG	30 ± 10 nm	NAG	NIR-II	710 nm	1000 nm	small size	[232]
PLK3-LIP	187 nm	/	NIR-II	1080 nm	/	PLK3	[233]
CB[7]/CRGD-AuNPs	3.3 ± 0.5 nm	/	NIR-II	488 nm	1050 nm	small size/Zeta potential	[234]
$Au_{24}Cd_1$ clusters	1.9 nm	ROS	NIR-II	808 nm	1020 nm	GFR decline	[235]
BPQDs	3.5 nm	ROS	NIR-II	808 nm	1050 nm	small size/Zeta potential	[236]
rDONs@AuNR dimer	60 nm	miR-21	NIR-II/PA	1060 nm	/	DNA structure	[237]
CDIA	58.3 ± 1.9 nm	•OH	NIR-I/PA	650 nm	720 nm	Low molecular weight chitosan	[238]

nanoclusters (AuNCs) [210, 211]. The field of NIR-II fluorescence imaging technology has made significant advancements in the past decade. Several novel NIR-II contrast agents have emerged, including molecularly engineered NIR-II dyes [212–214], genetically engineered NIR-II fluorophores [205, 215], NIR-II J aggregates [216, 217], and rare-earth downconversion NPs [207, 218]. These fluorophores exhibit bright NIR-II emission along with excellent biocompatibility and a wide range of functionalities. However, there is still limited reporting on the application of NIR-II contrast agents in AKI. Therefore, this paper aims to describe the recent advances in utilizing photoresponsive materials within the NIR spectrum for diagnosing and treating AKI (Table 3).

NIR diagnosis and treatment of AKI

NIR-I diagnosis

Extensive research indicates that OS triggered by the overexpression of ROS is closely related to the various pathological changes of AKI. ONOO- is one of the more prominent ROS. Therefore, establishing an efficient, sensitive, and real-time analytical method to detect changes in ONOO- is crucial for the accurate diagnosis and treatment of AKI. Li et al. developed a kidney-targeted NIR fluorescence probe—KNP-1, which is activated only in the presence of ONOO- [219]. With the progression of AKI, ONOO- gradually increases. More importantly, it allows the observation of the upregulation of ONOO- at least 24 h earlier than the clinical popular methods of sCr and BUN, demonstrating its clinical significance in the early detection of AKI (Fig. 8a, b). Additionally, Jiang et al. designed a highly sensitive NIRF probe (NFP-ONOO) [220]. This probe also exhibits good imaging capabilities in the physiological environment of

(See figure on next page.)

Fig. 8 **a** Early diagnosis of AKI by designing inherently kidney-targeted NIR fluorescent probes and detecting $ONOO^-$ rise during AKI. **b** The probe's mechanism for detecting $ONOO^-$. Reproduced from ref [219] with permission. Copyright (2020) Springer. **c** The mechanism of $ONOO^-$ production in ferroptosis-mediated AKI. Reproduced from ref [220] with permission. Copyright (2023) Springer. **d** The NRN probe attenuates fluorescence by responding to $ONOO^-$, while reduced glutathione reduces it to restore fluorescence. The probe enables diagnosis and treatment of DIAKI by simultaneously detecting two redox biomarkers in the kidney. Reproduced from ref [221] with permission. Copyright (2022) Springer

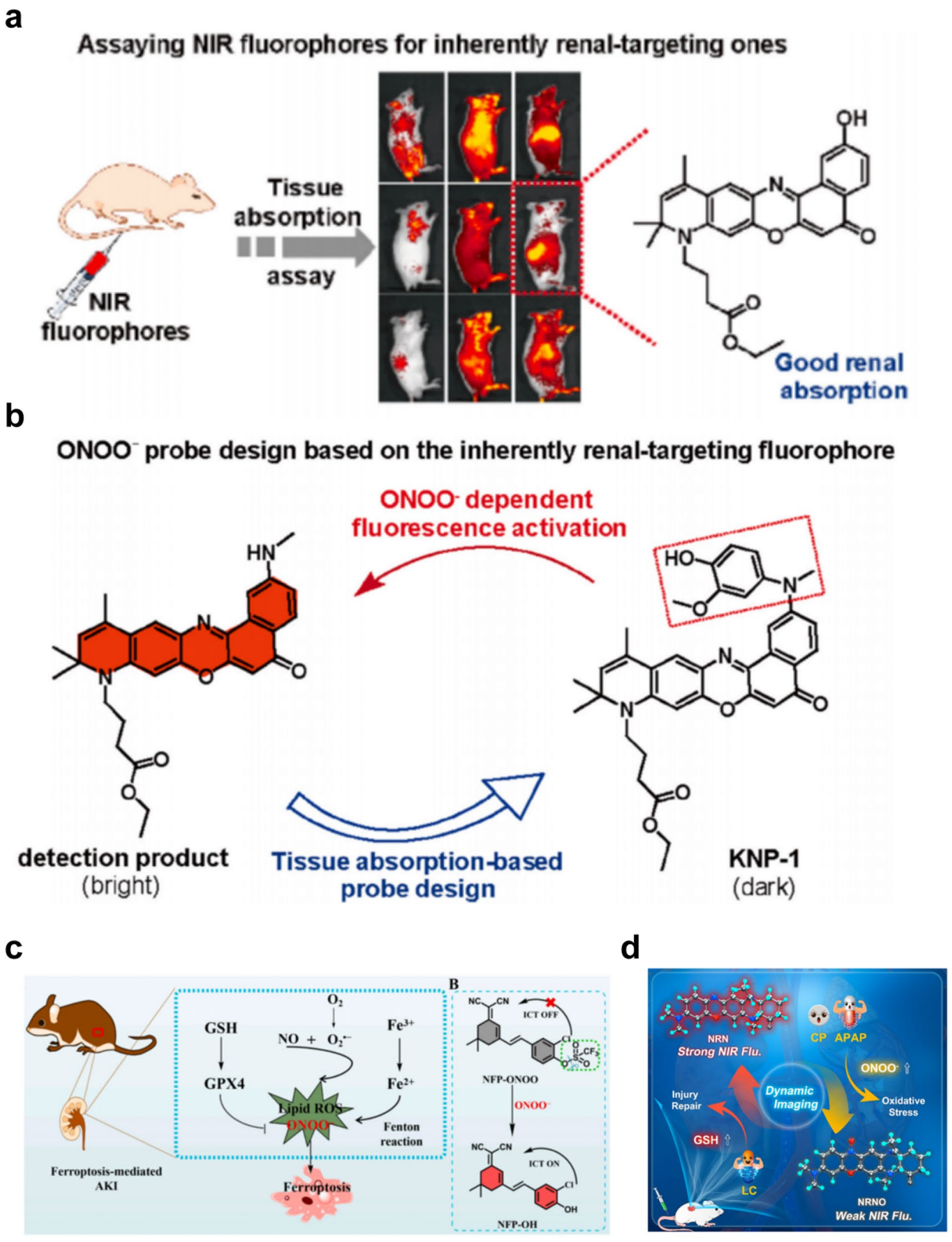

Fig. 8 (See legend on previous page.)

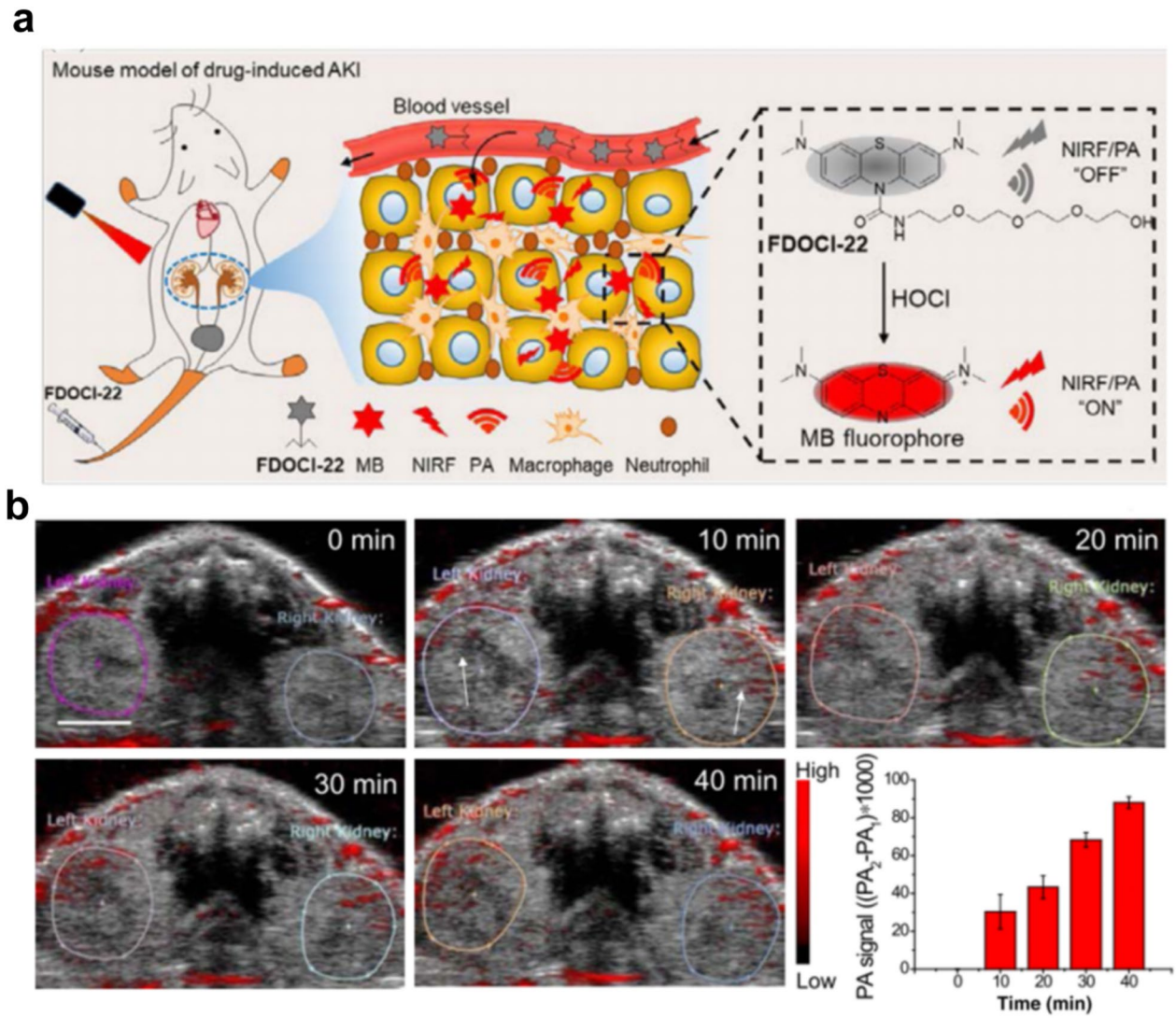

Fig. 9 **a** FDOCI-22 reacts with HOCl and provides early diagnosis of AKI by NIR and PA imaging. **b** Renal PA imaging maps of mice at different times after intravenous injection of FDOCI-22 in a cisplatin-induced AKI mouse model. (200 μL × 0.5 mM); the histogram is the PA intensity of kidneys at different time points (PA2: PA intensity at different time points; PA1: PA intensity at 0 min; n = 3 per group). Reproduced from ref [222] with permission. Copyright (2020) Springer

ONOO-, and reveals the dynamic changes of ONOO- flux in an AKI model mediated by ferroptosis. NFP-ONOO can serve as a reliable tool to aid in the diagnosis and treatment of AKI mediated by ferroptosis (Fig. 8c). Cheng et al. also reported a reversible NIRF probe based on ONOO-/GSH changes, which has a large Stokes shift (83 nm) and exhibits good selectivity and sensitivity with detection limits of 418 nM and 0.28 mM, respectively [221] (Fig. 8d).

Recent research indicates that numerous ROS-activated probes have been developed for diagnosing related diseases. However, many of them rely only rely

(See figure on next page.)

Fig. 10 **a** Design and characterization of the engineering TDF nanodevice (Kim-TDF). The stepwise assembly of Kim-TDF was verified by polyacrylamide gel electrophoresis (PAGE). In vivo schematic diagrams of Kim-TDF in normal kidney and renal injury conditions. Reproduced from ref [223] with permission. Copyright (2022) Springer. **b** An illustrative diagram detailing the process of synthesizing NIR-CDs with both NIRF and ultra-small dimensions. These NIR-CDs are subsequently employed in imaging studies to track the renal clearance pathway and assess kidney function effectively. Reproduced from ref [158] with permission. Copyright (2022) Springer

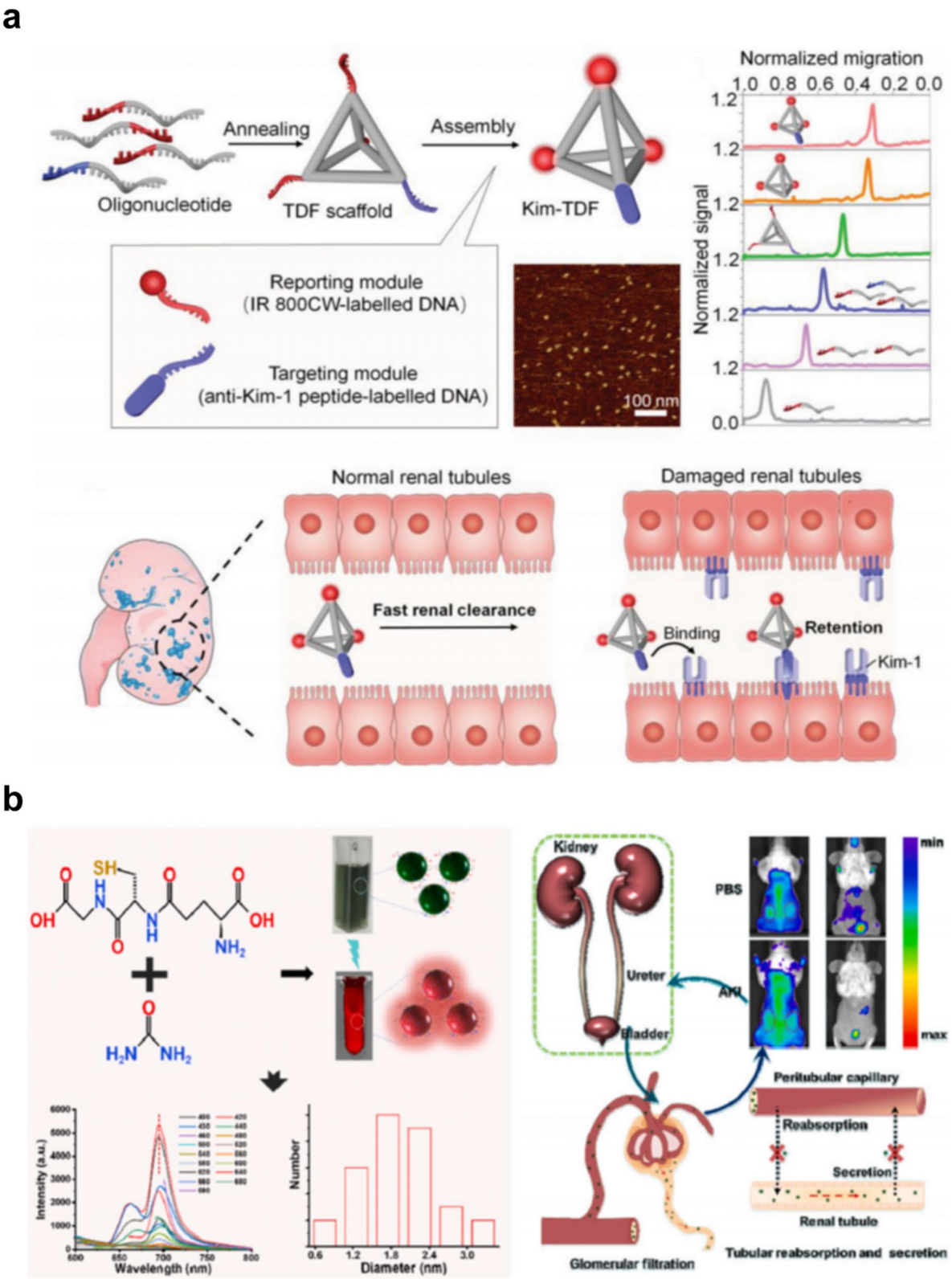

Fig. 10 (See legend on previous page.)

on fluorescence imaging as the sole indicator. Therefore, it is imperative to incorporate various imaging modalities for comprehensive diagnostic purposes. As shown in Fig. 9a, Yi et al. developed a NIR probe with MB as the fluorophore [222]. Building on their preliminary work, they designed and synthesized the HOCl-activated probe FDOCl-22 through structural modification. FDOCl-22 is completely soluble in water. Upon the addition of HOCl, it exhibits significant changes in its NIR emission and absorption spectra, demonstrating high selectivity and sensitivity. With the addition of different concentrations of HOCl, the fluorescence intensity of FDOCl-22 significantly increases in the 640–800 nm range. The absorption of FDOCl-22 in the 550–700 nm range also significantly increases, with the maximum absorption peak at 664 nm (an 80-fold increase) after adding 10 μM HOCl. Simultaneously, MB is a good agent for photoacoustic (PA) imaging (Fig. 9b). The advantages of PA imaging include increased penetration depth and spatial resolution within the body. In this study, FDOCl-22 serves as a tool for detecting early AKI and assessing the extent of AKI damage by combining NIR fluorescence (NIRF) and PA imaging. The PA signal begins to be detected 10 min after the injection of FDOCl-22, and then gradually increases in 40 min. However, the PA signal in the kidneys of healthy mice does not change, even 40 min after the injection of FDOCl-22.

Recent studies have shown that dense DNA nanostructures possess inherent kidney-targeting capabilities, making them promising candidates for treating renal diseases such as AKI. As shown in Fig. 10a, Xia et al. developed a nanodevice based on a tetrahedral DNA scaffold (Kim-TDF) for in vivo NIR imaging and identification of the kidneys in AKI [223]. The nanodevice features three components: 1. A kidney-targeting DNA framework 2. A KIM-1 module for AKI targeting 3. NIR fluorophores for NIR imaging. The design of this nanomaterial allows it to generate intense NIRF specifically in KIM-1-rich kidneys, enabling the early detection of AKI. Real-time kidney imaging is essential for monitoring the progress of kidney-related diseases and evaluating the renal toxicity of nano-probes. CDs, widely employed as nano-probes for image-guided disease diagnosis, are favored for their small size, tunable photoluminescent properties, and low biotoxicity. As shown in Fig. 10b, Tian et al. synthesized NIR-CDs using glutathione and urea as precursors through a one-pot pyrolysis method [158]. The prepared NIR-CDs exhibit NIR fluorescence (696 nm), ultra-small size (1.8 ± 0.3 nm), low toxicity, and a high renal clearance rate of up to 97.84%. In healthy kidneys, due to the high clearance rate of NIR-CDs, they can be quickly metabolized within the kidney. However, in the context of renal damage, as the extent of the injury increases, the residence time of NIR-CDs in the body is prolonged. Therefore, NIR-CDs can be used to monitor impaired kidney function. Overall, in vivo imaging studies support the feasibility of using NIR-CDs for real-time monitoring of kidney function.

Renally clearable and target-responsive NIR fluorescence imaging probes hold broad prospects for in vivo diagnosis of AKI. However, designing a renal-clearable imaging probe that is simultaneously responsive to multiple molecular targets to enhance sensitivity and specificity for the early detection of AKI is challenging. As shown in Fig. 11a, Ye et al. developed a NIR fluorescent probe (1-DPA2) that combines receptor-mediated binding with enzyme-triggered fluorescence activation, targeting phosphatidylserine (PS) and caspase-3 (CASP-3), two fundamental biomarkers of apoptosis [224]. 1-DPA2 can target externalized PS and active caspase-3, producing enhanced 808 nm NIRF and a high SBR, enabling the earliest detection of cisplatin-induced AKI in mice.

Vanin-1 is a type of amidase with a specific function of hydrolyzing a carbamoyl bond in D-pantetheine. It plays a crucial role in various physiological and biological processes such as OS regulation and the accumulation of inflammation in various pathological states. It is widely expressed in different organs, especially in the kidney and intestine. Given Vanin-1's significant functions and the increasing evidence, urinary Vanin-1 is considered a predictive biomarker for various kidney diseases. As shown in Fig. 11b, Ma et al. developed an enzyme-activated NIR fluorescent probe, DDAV, for the ultra-sensitive and highly specific detection of Vanin-1 activity in various complex biological systems [225]. DDAV can diagnose kidney injury early by detecting urinary Vanin-1

(See figure on next page.)

Fig. 11 **a** Schematic design of caspase-3 activatable NIR fluorescent probe. In the early stage of AKI, phosphatidylserine (PS) is flipped from the inner membrane to the outer membrane, and 1-DPA2 is retained in the renal tubule by binding to the flipped PS. At the same time, caspase-3 can cleave 1-DPA2 and then intense NIR fluorescence appears. Reproduced from ref [224] with permission. Copyright (2021) Springer. **b** A depiction illustrating the process of DDAV mediated by Vanin-1, accompanied by the absorption and fluorescence spectra depicting the response of DDAV towards Vanin-1. Reproduced from ref [225] with permission. Copyright (2022) Springer. **c** In the drug-induced AKI mouse model, DSMN can diagnose AKI by detecting SO_2. Reproduced from ref [226] with permission. Copyright (2023) Springer

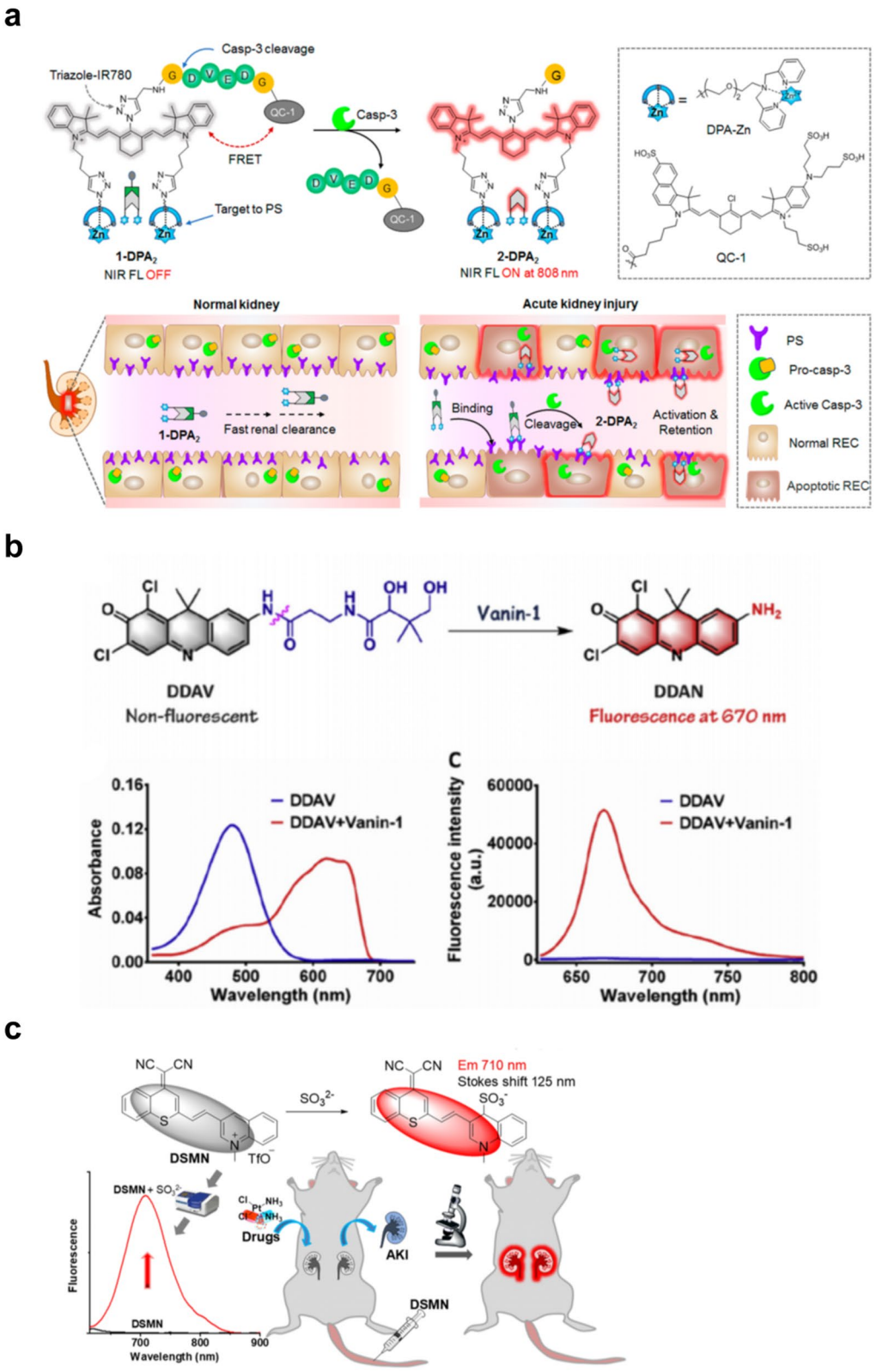

Fig. 11 (See legend on previous page.)

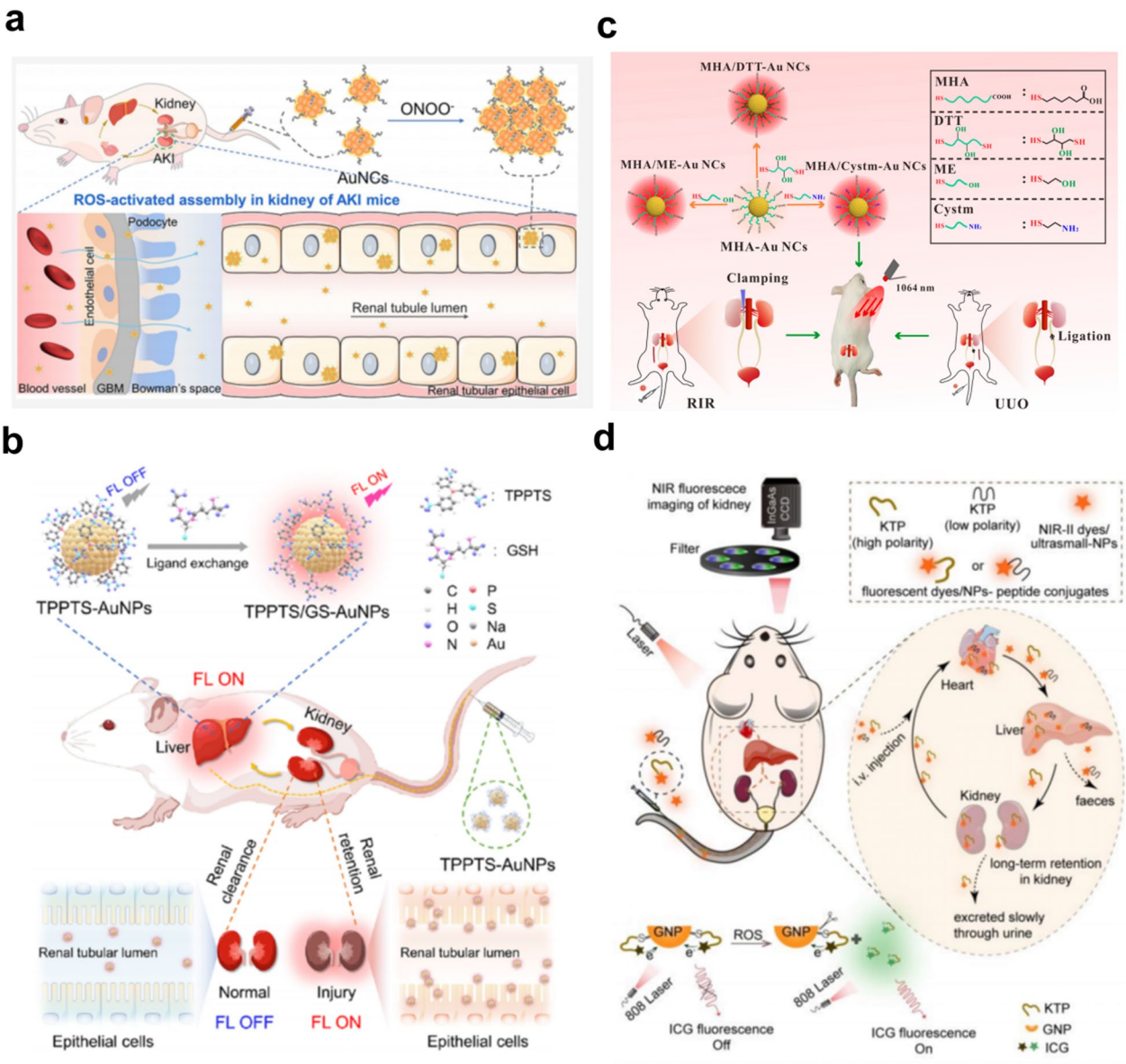

Fig. 12 **a** The $ONOO^-$-activated AUCN is applied for efficient NIR-II fluorescence imaging of AKI. Reproduced from ref [227] with permission. Copyright (2023) Springer. **b** TPPTS-AuNPs can be activated by GSH in the liver, while early imaging can be performed in metabolic acidosis-induced kidney injury. Reproduced from ref [228] with permission. Copyright (2023) Springer. **c** Schematic Diagram of the Dual-Ligands Stabilized Au NCs and NIR-II window fluorescence imaging in animal models of renal ischemia–reperfusion (RIR) and unilateral ureteral obstruction (UUO). Reproduced from ref [229] with permission. Copyright (2023) Springer. **d** Illustrations presenting the metabolic pathways of various dye-KTP conjugates in vivo and their application in noninvasive kidney monitoring within the NIR-II window. Reproduced from ref [230] with permission. Copyright (2021) Springer

activity and allows for real-time imaging of Vanin-1 both in vivo and in vitro.

Up to now, only a few NIR probes have been reported for detecting biomarkers related to AKI, such as ROS and some relevant enzymes. Although some fluorescent probes have been used to detect SO_2 in living systems, very few have associated SO_2 with AKI. As shown in Fig. 11c, Feng et al. developed a new NIR probe for AKI detection related to SO_2, DSMN [226]. DSMN exhibits high sensitivity and selectivity towards SO_2, providing rapid and significant fluorescence changes at 710 nm. Moreover, DSMN is primarily concentrated in the kidneys and can detect changes in SO_2 in the kidneys of AKI mice. The SO_2 marker is different from some of the previous markers, and this should be the first NIRF probe that is kidney-targeted and detects SO_2 levels.

NIR-II diagnosis

Currently, second NIR window (NIR-II, 1000–1700 nm) fluorescence imaging has demonstrated broad prospects in clinical translation, including biomedical basic research. In comparison to first NIR window (NIR-I, 700–1000 nm), NIR-II imaging exhibits significant improvements in imaging sensitivity, penetration depth, and spatial resolution.

Ultra-small Au nanoclusters (AuNCs) possess unique particle sizes (< 3 nm), discrete energy levels, and intriguing photoluminescence properties. They find widespread applications in various in vivo imaging scenarios, such as protein tracking, tumor imaging, and organ damage monitoring. As shown in Fig. 12a, Yang et al. developed a ROS-responsive NIR-II phosphorescent imaging based on AuNCs [227]. They found that NaC-AUNC exhibits excellent response sensitivity and selectivity to $ONOO^-$. Based on the reduction in GFR in the damaged kidneys and the in-situ aggregation triggered by $ONOO^-$, they successfully conducted NIR-II imaging of AKI in mice. This approach proves superior to clinical blood analysis in diagnosing AKI. As shown in Fig. 12b, Liu et al. also developed a straightforward in vivo ligand exchange strategy to obtain kidney-clearable, activatable luminescent Au NPs (AuNPs) [228]. They coated the Au NPs with trisodium triphenylphosphine trisulfonate (TPPTS), which can undergo ligand exchange with GSH, and then get activated in the NIR-II (1026 nm). The TPPTS-AuNPs, after in vivo GSH exchange, demonstrated enhanced cellular interactions with acidic renal tubular epithelial cells. This shows tremendous potential for high sensitivity (CI, ~ 3.9) and long-term (> 6.5h) non-invasive monitoring of early kidney injury caused by acidosis. As shown in Fig. 12c, Xiao et al. synthesized a series of dual-ligand stabilized AuNCs using mercaptohexanoic acid (MHA) or cysteamine (Cystm) as ligands [229]. These nanoclusters exhibit good renal clearance, along with NIR-II excitation and emission, high quantum yield (QY), as well as excellent photostability and biocompatibility. Under 1064 nm excitation, the Au NCs demonstrated deeper tissue penetration, higher imaging resolution, and better SBR compared to NIR-I excitation. These exceptional characteristics make the MHA/Cystm-Au NCs suitable for high-resolution fluorescence imaging to detect AKI caused by renal ischemia–reperfusion (RIR) and unilateral ureteral obstruction (UUO). Hydrophilic peptides can alter the biological metabolic pathways of organic molecules and ultrasmall NPs. Small particle organic molecules, which are rapidly cleared by the liver or kidneys, are often filtered out by the glomeruli. When bound to highly polar peptides, such as KTP5, they are reabsorbed by the tubules, leading to renal accumulation. As shown in Fig. 12d, Zhang et al. designed a ROS-responsive, activatable NIR-II probe based on a kidney-targeting peptide [230]. The results showed that the probe has a good hepatic and renal clearance rate, and the probe coupled with peptides can accumulate and retain in the kidneys, allowing for long-term in vivo monitoring of the kidneys and ex vivo urine detection. However, the specific mechanisms underlying the metabolic pathway changes and renal retention induced by KTP5 remain unclear.

NIR-II fluorophores typically possess long linkages and hydrophobicity, making them challenging to be cleared by the kidneys, thus limiting their application in renal disease detection and imaging. To fully leverage the advantages of heptamethine cyanine dyes while overcoming their relatively poor photostability, efforts have been made to design an NIR-II probe for dual-modal imaging detection and imaging of AKI. As shown in Fig. 13a, Wu et al. developed the Peg3-HC-PB probe, which features renal clearance, water solubility, biomarker-activatable, and good photostability [231]. For this probe, its fluorescence (900 – 1200 nm) is quenched due to the presence of electron-withdrawing groups, showing weak absorption with a peak at 830 nm. Meanwhile, in the presence of overexpressed H_2O_2 in the renal region of AKI, the phenylboronic groups are converted to phenolic groups, thereby enhancing the NIR-II fluorescence emission (900 – 1200 nm) and absorption (600 – 900 nm), ultimately generating a significant photoacoustic signal and NIR-II fluorescence emission for imaging. The probe can detect contrast-agent-induced and ischemia/reperfusion-induced mouse AKI using real-time three-dimensional multispectral optoacoustic tomography (3D-MSOT) and NIR-II fluorescence dual-modal imaging techniques in response

(See figure on next page.)

Fig. 13 **a** In previous studies, Heptamethine Cyanine Dyes with hydrophilic groups located at one or both ends have been reported. Despite the introduction of these hydrophilic groups, these dyes maintain hepatic clearance. Chemical Structure and Features of the Probe PEG3-HC-PB and the Chromophore PEG3-HC-POH (the Activated Probe) Resulting from the Probe's Response to the Biomarker H2O2, as well as the Probe's Utilization in Detecting Contrast-Agent- and Ischemia/Reperfusion-Induced AKI by NIR-II Fluorescent and Optoacoustic Dual-Mode Imaging. Reproduced from ref [231] with permission. Copyright (2023) Springer. **b** Mechanism of NAG detection by BOD-I-NAG-NP and BOD-II-NAG-NP in vivo. Reproduced from ref [232] with permission. Copyright (2021) Springer

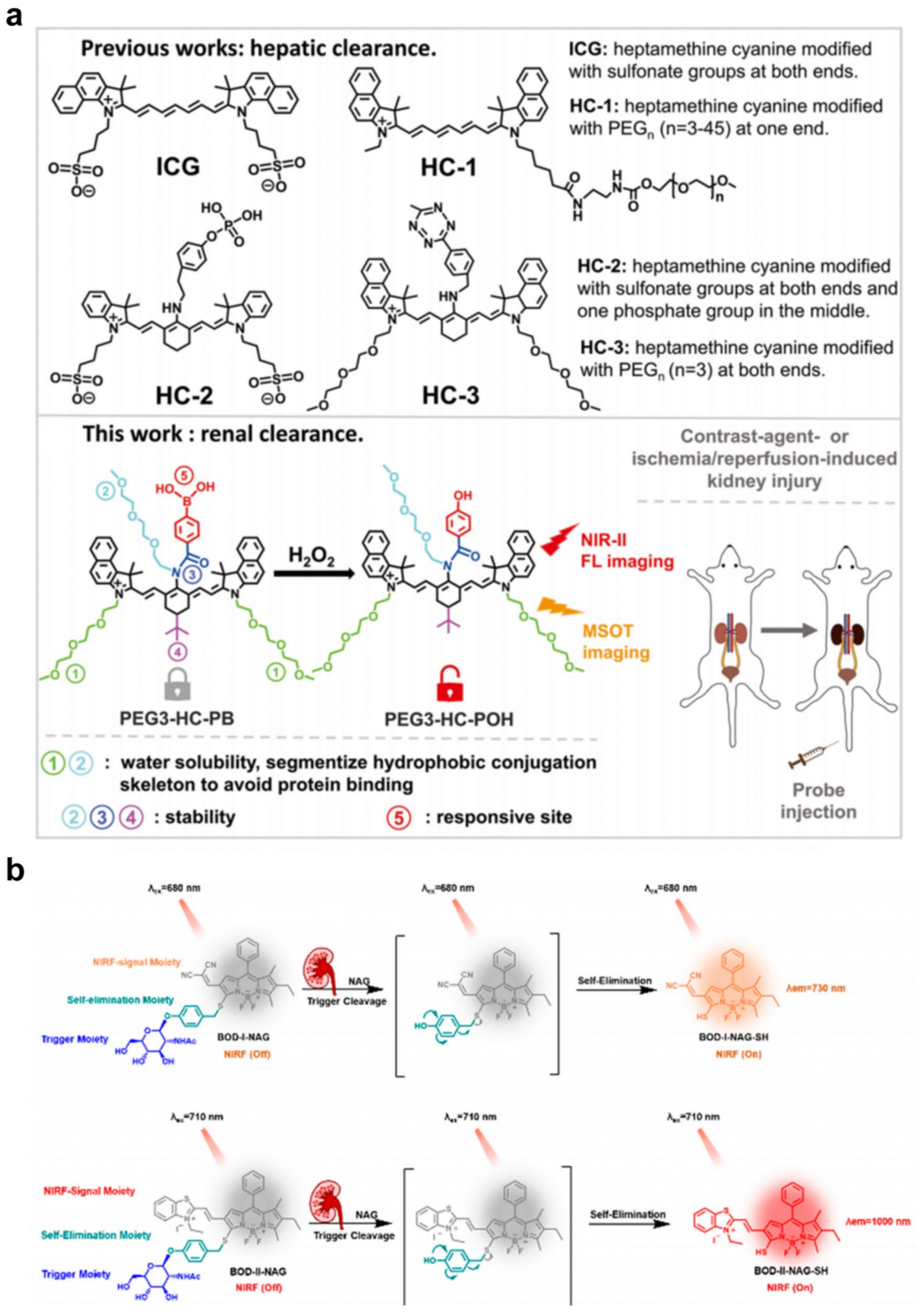

Fig. 13 (See legend on previous page.)

to the biomarker H_2O_2. Thus, this probe serves as a practical tool for AKI detection.

In recent years, N-acetyl-β-D-glucosaminidase (NAG) has gained attention as a specific and sensitive biomarker for the occurrence of kidney injury. Urinary NAG is secreted by lysosomes when the epithelial cells of the proximal renal tubules are damaged. Therefore, an increase in urinary NAG content is an important clinical indicator of kidney damage. However, urinary enzyme analysis still has many limitations in the diagnosis of AKI and CKD, such as low detection sensitivity, cumbersome detection procedures, and significant background interference. As shown in Fig. 13b, Gu et al. developed a NAG-activatable fluorescent nanoprobe (BOD-II-NAG-NP) that emits in the NIR-II window [232]. NAG, as a biomarker for renal diseases, can specifically activate BOD-II-NAG-NP to release NIR-II fluorescence signals, enabling in vivo imaging of renal dysfunction in live mice. Importantly, this active imaging mechanism allows BOD-II-NAG-NP to detect the onset of drug-induced AKI at least 32 h in advance non-invasively compared to most existing detection methods, suggesting that BOD-II-NAG-NP could become an optical imaging agent for early diagnosis of AKI. Additionally, the NIR-II fluorescence generated by BOD-II-NAG-NP can penetrate the thicker fat layers of diabetic nephropathy mice and provide high-resolution in vivo imaging, indicating that BOD-II-NAG-NP has clinical potential in the precise diagnosis of kidney disease.

Phototherapy

Polo-like kinase (PLK) is a conserved serine/threonine kinase. Previous studies have reported that PLK can negatively regulate the expression of HIF-1α under hypoxic conditions, acting as a tumor suppressor. Therefore, it is considered that PLK may also be related to inflammation and hypoxia in ischemia–reperfusion and AKI. Liposomes can encapsulate a variety of therapeutic agents, such as drugs, proteins, oligonucleotides, and genetic material. To further enhance the controllability of the drug and reduce its side effects, a type of liposome containing NIR absorbers has been developed. This liposome can be triggered by NIR light, which then releases the internal drug, thereby improving the local therapeutic effect. As shown in Fig. 14a, Gu et al. developed a lipid-based NP containing a PLK3 inhibitor that can be triggered by 1080 nm NIR light (PLK3-LIP) [233]. The results indicate that PLK3-LIP can inhibit renal inflammation.

Cucurbit[n]uril (CB[n]) is a type of supramolecular host molecule, featuring two hydrophilic carbonyl oxygen entrances and one hydrophobic cavity. This characteristic makes CB[n] suitable for various applications such as molecular recognition, cellular imaging, drug delivery, and disease treatment. As shown in Fig. 14b, Wang et al. designed a NIR II NP using Au NPs as carriers, incorporating CB [7]/CRGD (peptide) [234]. Through surface chemical modification, they selectively targeted the liver and kidneys by adjusting the ratio of CB [7] to CRGD. Simultaneously, the NPs loaded with dexamethasone (DXM) increased the accumulation of DXM in the kidneys, thereby achieving a better therapeutic effect.

Combined NIR diagnosis and treatment

As shown in Fig. 15a, Zhang et al. developed a monoatomic Cd-doped, monoatomic-engineered Au cluster [235]. Exhibiting exceptional brightness and long-term photostability in the NIR-II, the monoatomic Cd enhancement in the Cd-Au bonds, formation energy, and stable cluster structure contribute to its sustained stability for up to one month without decay, along with excellent 1 h photostability (no photobleaching), Much longer than clinically approved for ICG (< 5min). In vivo imaging demonstrates that, even 72 h after injury, the Au clusters can monitor AKI and can be used for prolonged monitoring and assessment of AKI progression. Moreover, the Au clusters themselves exhibit biological activity, alleviating inflammation and OS associated with AKI.

NIR-II fluorescent nano-probes based on inorganic materials, including rare-earth-doped NPs, single-walled CNTs, cadmium sulfide quantum dots, Au nano-clusters and so on, have attracted increasing attention in the field of biomedical imaging. However, these materials often exhibit challenges in terms of degradation or lack therapeutic functionalities. BP represents a novel non-metallic two-dimensional material that has gained attention for various biological applications due to its excellent

(See figure on next page.)

Fig. 14 **a** Preparation of a novel liposome-mediated biomimetic delivery system with NIR-II triggered release and NIR light irradiation to kidney resulted in an excellent effect for reduced immune cell infiltration and renal inflammation. Mechanistically, inhibiting PLK3 suppressed the degradation of HIF-1α and ROS-induced OS. This protection shielded renal tubular epithelial cells from apoptosis and halted macrophage activation, thereby mitigating renal inflammation. Reproduced from ref [233] with permission. Copyright (2022) Springer. **b** A schematic diagram depicting the use of CB[7]-mediated ultrasmall luminescent Au nanocarriers for targeted delivery to specific organs, along with the therapeutic application of DXM-02AuNPs in mice with cisplatin-induced AKI. Reproduced from ref [234] with permission. Copyright (2023) Springer

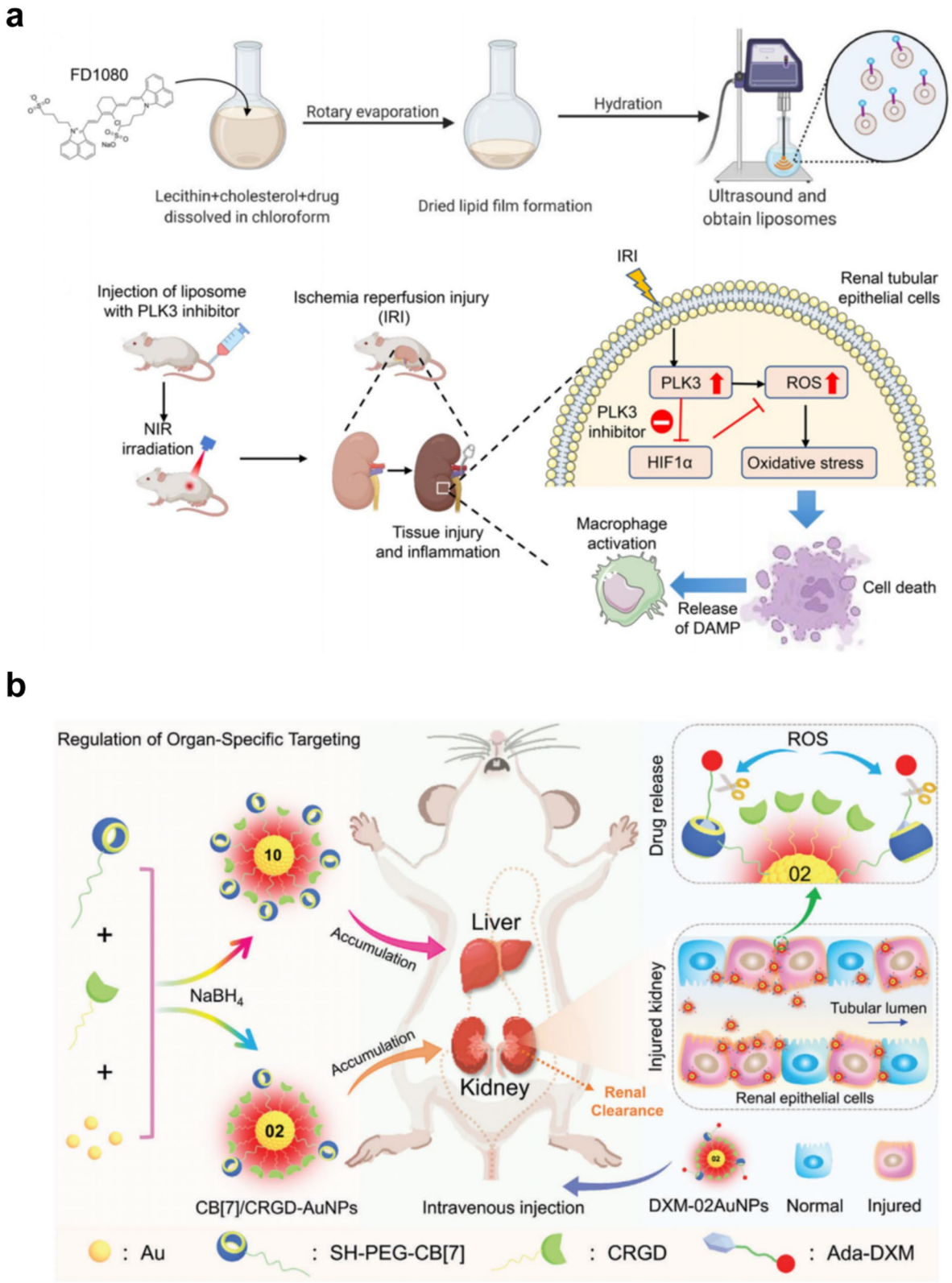

Fig. 14 (See legend on previous page.)

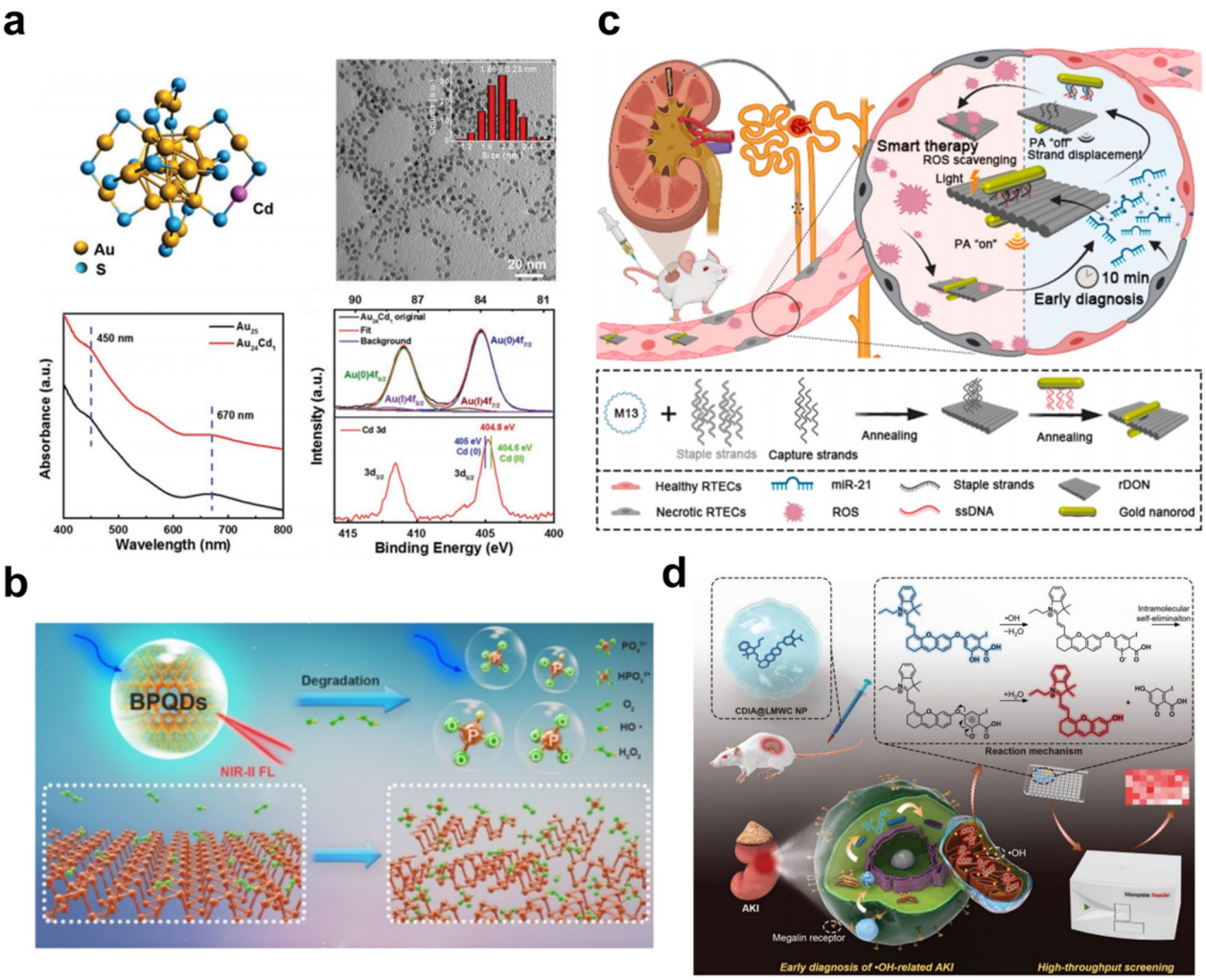

Fig. 15 **a** Structural schematic, TEM image, UV–Vis absorption spectrum, and XPS image of $Au_{24}Cd_1$ clusters. Reproduced from ref [235] with permission. Copyright (2023) Springer. **b** An illustrative representation of the NIR-II fluorescence emission of BPQDs upon excitation with an 808 nm laser. BPQDs undergo degradation into phosphate, phosphite, and other phosphorus oxide compounds triggered by water, oxygen, or ROS, resulting in decreased NIR-II fluorescence intensity. Reproduced from ref [236] with permission. Copyright (2021) Springer. **c** An illustrated depiction of a DNA origami plasmonic nanoantenna designed for the early detection and targeted treatment of AKI. Following intravenous administration, the rDONs@AuNR dimer exhibited preferential accumulation in the kidneys. Reproduced from ref [237] with permission. Copyright (2022) Springer. **d** Schematic diagram to indicate the design of a NIR fluorescent/photoacoustic probe, CDIA, for monitoring •OH in AKI and demonstration of the strategy for HTS of antioxidant natural products to attenuate AKI. Reproduced from ref [238] with permission. Copyright (2023) Springer

biocompatibility and optical properties. These applications include PDT, drug delivery systems photoacoustic imaging and so on. As shown in Fig. 15b, Liao et al. were the first to develop a new class of biodegradable NIR-II fluorescent-emitting BP quantum dots (BPQD) [236]. The prepared BPQD exhibited strong emissions in the range of 900–1350 nm under 808 nm laser irradiation. Additionally, BPQD can degrade under physiological conditions, demonstrating excellent ROS scavenging capabilities. Upon contact with ROS, BPQD degrades into phosphates, thereby attenuating NIR-II fluorescence emission. The accumulation and metabolism of BPQD can be studied through real-time detection of NIR-II fluorescence signals.

DNA nanofold structures exhibit inherent renal targeting properties. As shown in Fig. 15c, He et al. have developed a novel microRNA (miRNA)-21-responsive DNA nanofold nanoantenna for the early diagnosis and treatment of AKI [237]. This nanoantenna is composed of two miniature Au nanorods connected by a rectangular DNA nanofold structure, displaying significant absorption in the NIR window. In AKI mice, the nanoantenna interacts

with upregulated miR-21, suppressing photoacoustic signals. It can rapidly detect the occurrence of AKI within 10 min after ischemia–reperfusion treatment in mice, significantly earlier than the times determined by most probes and routine blood tests. Simultaneously, the DNA nanofold structure demonstrates a remarkably high ROS clearance rate, mitigating local OS in AKI.

·OH play a crucial role in the occurrence and development of AKI. As shown in Fig. 15d, Tian et al. designed a ·OH-activatable fluorescence/photoacoustic (CDIA) probe for imaging in a mouse AKI model [238]. The CDIA probe is designed with two components: 1) a signal part consisting of NIR hemicyanine dye and 2) a target-responsive substrate, iodine salicylic acid, which is recognized and cleaved by ·OH. The probe exhibits no fluorescence and photoacoustic signals under normal conditions but is activated to produce NIRF and PA signals once exposed to a ·OH environment. The positive detection time using this probe is 12 h, superior to the 48-h detection time of typical clinical methods such as BUN and blood Crea detection. Additionally, when combined with puerarin, the probe alleviates AKI by activating the Sirt1/Nrf2/Keap1 signaling pathway, providing insights and strategies for the diagnosis and treatment of clinical AKI.

Summary and outlook

The annual morbidity and mortality rate of AKI is alarmingly high, primarily due to the current clinical challenge in early AKI diagnosis, resulting in delayed treatment initiation. Furthermore, the absence of specific drugs targeting AKI underscores the significance of exploring novel materials for both its diagnosis and treatment. Phototherapy has been utilized for over a century, leading to the development of nearly 1,000 phototherapy agents; however, only a limited number have gained approval for clinical use. Consequently, non-invasive and highly targeted light-based diagnostics and therapies hold immense promise as an effective approach towards disease management. In recent years, nanotechnology advancements have significantly facilitated the application of phototherapy in diagnosing and treating acute kidney injury. Despite encouraging progress observed in preclinical research on phototherapy nanomedicine, numerous challenges persist when translating these agents into clinical applications.

(1) The clinic should prioritize the assessment of nanomaterials' toxicity, biodegradability, and in vivo metabolism. Compared to small molecule drugs, nanomaterials exhibit prolonged retention within the body, which can result in systemic toxicity. Inorganic materials, particularly those containing heavy metal ions such as zinc and copper, pose additional concerns. While some current studies have demonstrated favorable biosafety of nanomaterials in the short term, uncertainties remain for patients requiring long-term treatment. Further exploration is needed regarding their potential chronic toxicity, accumulation patterns, and associated immune responses. However, while enhancing the biodegradability and clearance of nanomaterials may be achieved at the expense of stability and drug half-life reduction leading to diminished cellular uptake; striking a balance between these factors becomes crucial during clinical translation.

(2) The water solubility of phototherapy drugs is generally limited. PEG encapsulation is a commonly employed technique for drug delivery. However, prolonged use of PEG can result in the accumulation of anti-PEG antibodies in the human body. Phagocytes recognize and eliminate peg-modified carriers, leading to a significant reduction in their blood half-life. Therefore, there is an urgent need to develop a more biocompatible and water-soluble approach.

(3) Due to interference from the glomerular filtration threshold and the reticuloendothelial system's (liver and spleen) capture of NPs, there are significant limitations on the shape and size of nanomaterial designs for interference. Although strategies have been proposed to evade immune surveillance and pass through the glomerular filtration membrane, such as size control within 150 nm, sheet-like nanomaterials (BPNS), and designs incorporating kidney-targeting peptides on the material's outer layer to enhance targeting of the kidney and renal tubular epithelial cells, many nanomaterials are still captured by the liver. Even if they reach the kidneys, they may not precisely target renal tubular epithelial cells. Therefore, researching nanomaterials that are more reliable and effective, increasing their specificity for the kidneys and renal tubular epithelial cells, is of great significance.

(4) Currently, many NIR responsive nanomaterials exhibit unsatisfactory quantum yields and fluorescence intensity. The majority of NIR-II fluorescent molecules exhibit low cytotoxicity; however, they suffer from limited water solubility and a low quantum dot yield. Conversely, quantum dots with high yields present certain drawbacks such as sluggish metabolism and inadequate tissue targeting. Another issue lies in the limited depth of laser penetration. In clinical settings, patients typically possess thicker layers of adipose tissue compared to

mice, and the kidney is situated at a greater depth. These challenges further compromise fluorescence intensity and significantly constrain its potential biological applications. Therefore, it is imperative to develop nanomaterials exhibiting longer wavelengths in the NIR II or even III. In light of the aforementioned limitations, this paper proposes several potential solutions. Firstly, one approach could involve investigating novel elements, substrates, components or incorporating photothermally stabilized plasma structures to enhance absorption in the NIR-II for nanomaterials. Secondly, employing nuclear/shell or highly branched structures and preparing organic/inorganic hybrids or doping with heterogeneous ions like lanthanide ions can also augment light absorption and improve PCE.

(5) NIR responsive nanomaterials can distinguish between healthy and diseased states. However, in practical clinical applications, patients often have complex conditions, such as concurrent liver, lung, and kidney injuries. In recent material designs, most are based on ROS response, greatly restricting their clinical translation. Faced with intricate disease scenarios, this approach may lead to the failure of kidney-specificity. Thus, it is essential to design NIR responsive nanomaterials with greater kidney specificity, especially targeting new points for AKI.

(6) On the diagnostic front, many NIR responsive nanomaterials solely rely on fluorescence imaging as a diagnostic indicator. Due to the delayed and complex nature of AKI diagnosis, it is necessary to design materials that can perform multi-modal imaging for joint diagnostics. The integration of NIR light-responsive materials with a diverse range of imaging modalities, including photoacoustic imaging, MRI, CT, and PET, can be achieved.

(7) Currently, in the NIR diagnosis and treatment of AKI, at this stage, the brightness of fluorescence is only used to determine the occurrence of AKI as well as to monitor it, which is a qualitative judgment without a specific quantitative value. For example, when the fluorescence intensity exceeds 20% of the baseline, it is considered as mild AKI and when it exceeds 50%, it is considered as moderate AKI. Therefore, we need to promote clinical trials to obtain baseline data and reference values to obtain more accurate and quantitative NIR disease diagnosis. It will be more meaningful for the diagnosis and treatment of AKI in the clinic.

Overall, the current research is still in its early stages. Interdisciplinarity enhances the diagnosis and treatment of AKI, but it also poses challenges for researchers with diverse disciplinary backgrounds. This necessitates their familiarity with state-of-the-art knowledge across various fields and its integration. The advancement of interdisciplinary research often relies on collaborative efforts and cooperation among researchers from different disciplines and fields. Strengthening the collaboration and communication between nanomaterials and clinical medicine, conducting more comprehensive mechanistic research, and designing nanomaterials with enhanced clinical translational effects may represent potential future research directions.

Acknowledgements
Yu Cai thanks for the financial support from National Natural Science Foundation of China (62205094), Natural Science Foundation of Zhejiang Province (LQ22F050010), Zhejiang Medical Health Science and Technology Project (2023RC130, 2024KY693), Zhejiang TCM Science and Technology Project (2023ZR001), Basic Scientific Research Funds of Department of Education of Zhejiang Province (KYYB202213), Excellent research start-up fund of Zhejiang Provincial People's Hospital (ZRY2021A002, ZRY2022J001), Adjunct Talent Fund of Zhejiang Provincial People's Hospital.

Author contributions
Shijie Yao: Conceptualization, Investigation, Methodology, Roles/Writing–original draft; Writing–review & editing. Yinan Wang: Investigation, Methodology. Xiaozhou Mou: Funding acquisition, Project administration, Resources. Xianghong Yang: Funding acquisition, Project administration, Resources. Yu Cai: Conceptualization, Funding acquisition, Project administration, Resources. All authors reviewed and approved the final version for submission.

Funding
The work was supported by National Natural Science Foundation of China (62205094), Natural Science Foundation of Zhejiang Province (LQ22F050010), Zhejiang Medical Health Science and Technology Project (2023RC130, 2024KY693), Zhejiang TCM Science and Technology Project (2023ZR001), Basic Scientific Research Funds of Department of Education of Zhejiang Province (KYYB202213), Excellent research start-up fund of Zhejiang Provincial People's Hospital (ZRY2021A002, ZRY2022J001), Adjunct Talent Fund of Zhejiang Provincial People's Hospital.

Data availability
No datasets were generated or analysed during the current study.

Declarations

Ethics approval and consent to participate
Not applicable.

Consent for publication
All authors of this study agreed to publish.

Competing interests
The authors declare they have no competing interests.

Author details
[1]Emergency and Critical Care Center, Intensive Care Unit, Zhejiang Provincial People's Hospital (Affiliated People's Hospital), Hangzhou Medical College, Hangzhou 310014, Zhejiang, China. [2]The Second School of Clinical Medicine, Zhejiang Chinese Medical University, Hangzhou 310053, Zhejiang, China. [3]Center for Rehabilitation Medicine, Rehabilitation & Sports Medicine Research Institute of Zhejiang Province, Department of Rehabilitation Medicine, Zhejiang Provincial People's Hospital, (Affiliated People's Hospital), Hangzhou Medical College, Hangzhou 310014, Zhejiang, China. [4]Clinical Research Institute, Zhejiang Provincial People's Hospital, (Affiliated People's Hospital), Hangzhou Medical College, Hangzhou 310014, Zhejiang, China.

Received: 20 June 2024 Accepted: 4 October 2024
Published online: 05 November 2024

References

1. Vanmassenhove J, Kielstein J, Jörres A, Biesen WV. Management of patients at risk of acute kidney injury. Lancet. 2017;389:2139–51.
2. Vaara ST, Bhatraju PK, Stanski NL, McMahon BA, Liu K, Joannidis M, Bagshaw SM. Subphenotypes in acute kidney injury: a narrative review. Critical Care. 2022. https://doi.org/10.1186/s13054-022-04121-x.
3. Summary of recommendation statements. Kidney international supplements 2012, 2:8-12.
4. Kellum JA, Lameire N. Diagnosis, evaluation, and management of acute kidney injury: a KDIGO summary (part 1). Critical Care. 2013;17:204.
5. Kellum JA, Romagnani P, Ashuntantang G, Ronco C, Zarbock A, Anders HJ. Acute kidney injury. Nat Rev Dis Primers. 2021;7:52.
6. Chawla LS, Bellomo R, Bihorac A, Goldstein SL, Siew ED, Bagshaw SM, Bittleman D, Cruz D, Endre Z, Fitzgerald RL, et al. Acute kidney disease and renal recovery: consensus report of the acute disease quality initiative (ADQI) 16 Workgroup. Nat Rev Nephrol. 2017;13:241–57.
7. Levey AS. Defining AKD: the spectrum of AKI, AKD, and CKD. Nephron. 2022;146:302–5.
8. Lameire NH, Levin A, Kellum JA, Cheung M, Jadoul M, Winkelmayer WC, Stevens PE, Caskey FJ, Farmer CKT, Ferreiro Fuentes A, et al. Harmonizing acute and chronic kidney disease definition and classification: report of a kidney disease: improving global outcomes (KDIGO) Consensus Conference. Kidney Int. 2021;100:516–26.
9. Meersch M, Weiss R, Strauß C, Albert F, Booke H, Forni L, Pittet J-F, Kellum JA, Rosner M, Mehta R, et al. Acute kidney disease beyond day 7 after major surgery: a secondary analysis of the EPIS-AKI trial. Intensive Care Med. 2024;50:247–57.
10. Su C-C, Chen J-Y, Chen S-Y, Shiao C-C, Neyra JA, Matsuura R, Noiri E, See E, Chen Y-T, Hsu C-K, et al. Outcomes associated with acute kidney disease: a systematic review and meta-analysis. eClin Med. 2023;55:101760.
11. Vijayan A. Tackling AKI: prevention, timing of dialysis and follow-up. Nat Rev Nephrol. 2020;17:87–8.
12. Mehta RL, Cerda J, Burdmann EA, Tonelli M, Garcia-Garcia G, Jha V, Susantitaphong P, Rocco M, Vanholder R, Sever MS, et al. International society of nephrology's 0by25 initiative for acute kidney injury (zero preventable deaths by 2025): a human rights case for nephrology. Lancet. 2015;385:2616–43.
13 Harrois A, Soyer B, Gauss T, Hamada S, Raux M, Duranteau J. Prevalence and risk factors for acute kidney injury among trauma patients: a multicenter cohort study. Critical Care. 2018. https://doi.org/10.1186/s13054-018-2265-9.
14 Huber M, Ozrazgat-Baslanti T, Thottakkara P, Scali S, Bihorac A, Hobson C. Cardiovascular-specific mortality and kidney disease in patients undergoing vascular surgery. JAMA Surg. 2016;151:441.
15. Liu KD, Yang J, Tan TC, Glidden DV, Zheng S, Pravoverov L, Hsu C-Y, Go AS. Risk factors for recurrent acute kidney injury in a large population-based cohort. Am J Kidney Dis. 2019;73:163–73.
16. Legrand M, Clark AT, Neyra JA, Ostermann M. Acute kidney injury in patients with burns. Nat Rev Nephrol. 2023;20:188–200.
17. Mehta RL, Burdmann EA, Cerda J, Feehally J, Finkelstein F, Garcia-Garcia G, Godin M, Jha V, Lameire NH, Levin NW, et al. Recognition and management of acute kidney injury in the international society of nephrology 0by25 global snapshot: a multinational cross-sectional study. Lancet. 2016;387:2017–25.
18. Minami S, Nakamura S. Therapeutic potential of Beclin1 for transition from AKI to CKD: autophagy-dependent and autophagy-independent functions. Kidney Int. 2022;101:13–5.
19. Abebe A, Kumela K, Belay M, Kebede B, Wobie Y. Mortality and predictors of acute kidney injury in adults: a hospital-based prospective observational study. Sci Rep. 2021;11:15672.
20. Hoste EA, Bagshaw SM, Bellomo R, Cely CM, Colman R, Cruz DN, Edipidis K, Forni LG, Gomersall CD, Govil D, et al. Epidemiology of acute kidney injury in critically ill patients: the multinational AKI-EPI study. Intensive Care Med. 2015;41:1411–23.
21. McMahon GM, Waikar SS. Biomarkers in nephrology: core curriculum 2013. Am J Kidney Dis. 2013;62:165–78.
22. Ronco C, Bellomo R, Kellum JA. Acute kidney injury. Lancet. 2019;394:1949–64.
23. Chen Q, Nan Y, Yang Y, Xiao Z, Liu M, Huang J, Xiang Y, Long X, Zhao T, Wang X, et al. Nanodrugs alleviate acute kidney injury: manipulate RONS at kidney. Bioact Mater. 2023;22:141–67.
24. Lameire NH, Bagga A, Cruz D, De Maeseneer J, Endre Z, Kellum JA, Liu KD, Mehta RL, Pannu N, Van Biesen W, Vanholder R. Acute kidney injury: an increasing global concern. Lancet. 2013;382:170–9.
25. Lewington AJ, Cerda J, Mehta RL. Raising awareness of acute kidney injury: a global perspective of a silent killer. Kidney Int. 2013;84:457–67.
26 Turgut F, Awad AS, Abdel-Rahman EM. Acute kidney injury: medical causes and pathogenesis. J Clin Med. 2023;12:375.
27. Schrier RW, Wang W. Acute renal failure and sepsis. N Engl J Med. 2004;351:159–69.
28. Iwakiri Y. The molecules: mechanisms of arterial vasodilatation observed in the splanchnic and systemic circulation in portal hypertension. J Clin Gastroenterol. 2007;41(Suppl 3):S288-294.
29. Leithead JA, Hayes PC, Ferguson JW. Review article: advances in the management of patients with cirrhosis and portal hypertension-related renal dysfunction. Aliment Pharmacol Ther. 2014;39:699–711.
30. Uchino S, Kellum JA, Bellomo R, Doig GS, Morimatsu H, Morgera S, Schetz M, Tan I, Bouman C, Macedo E, et al. Acute renal failure in critically ill patients: a multinational, multicenter study. JAMA. 2005;294:813–8.
31. Arroyo V, Gines P, Gerbes AL, Dudley FJ, Gentilini P, Laffi G, Reynolds TB, Ring-Larsen H, Scholmerich J. Definition and diagnostic criteria of refractory ascites and hepatorenal syndrome in cirrhosis. Int Ascites Club Hepatol. 1996;23:164–76.
32. Boada-Romero E, Martinez J, Heckmann BL, Green DR. The clearance of dead cells by efferocytosis. Nat Rev Mol Cell Biol. 2020;21:398–414.
33. Hanna J, Hossain GS, Kocerha J. The potential for microRNA therapeutics and clinical research. Front Genet. 2019;10:478.
34. Rosner MH, Jhaveri KD, McMahon BA, Perazella MA. Onconephrology: the intersections between the kidney and cancer. CA Cancer J Clin. 2021;71:47–77.
35. Nang SC, Azad MAK, Velkov T, Zhou QT, Li J. Rescuing the last-line polymyxins: achievements and challenges. Pharmacol Rev. 2021;73:679–728.
36. Krishnan S, Suarez-Martinez AD, Bagher P, Gonzalez A, Liu R, Murfee WL, Mohandas R. Microvascular dysfunction and kidney disease: challenges and opportunities? Microcirculation. 2021;28: e12661.
37. Rani N, Singh S, Dhar P, Kumar R. Surgical importance of arterial segments of human kidneys: an angiography and corrosion cast study. J Clin Diagn Res. 2014;8:1–3.
38. Evans RG, Ince C, Joles JA, Smith DW, May CN, O'Connor PM, Gardiner BS. Haemodynamic influences on kidney oxygenation: clinical implications of integrative physiology. Clin Exp Pharmacol Physiol. 2013;40:106–22.
39. Vallon V, Thomson SC. The tubular hypothesis of nephron filtration and diabetic kidney disease. Nat Rev Nephrol. 2020;16:317–36.
40. Scholz H, Boivin FJ, Schmidt-Ott KM, Bachmann S, Eckardt KU, Scholl UI, Persson PB. Kidney physiology and susceptibility to acute kidney injury: implications for renoprotection. Nat Rev Nephrol. 2021;17:335–49.
41. Ergin B, Kapucu A, Demirci-Tansel C, Ince C. The renal microcirculation in sepsis. Nephrol Dial Transplant. 2015;30:169–77.
42. Tian Z, Liang M. Renal metabolism and hypertension. Nat Commun. 2021;12:963.
43. Mimura I, Nangaku M. The suffocating kidney: tubulointerstitial hypoxia in end-stage renal disease. Nat Rev Nephrol. 2010;6:667–78.
44. Rosin DL, Okusa MD. Dangers within: DAMP responses to damage and cell death in kidney disease. J Am Soc Nephrol. 2011;22:416–25.
45. Kroemer G, Galassi C, Zitvogel L, Galluzzi L. Immunogenic cell stress and death. Nat Immunol. 2022;23:487–500.
46. Vanpouille-Box C, Hoffmann JA, Galluzzi L. Pharmacological modulation of nucleic acid sensors - therapeutic potential and persisting obstacles. Nat Rev Drug Discov. 2019;18:845–67.
47. Daehn IS, Duffield JS. The glomerular filtration barrier: a structural target for novel kidney therapies. Nat Rev Drug Discov. 2021;20:770–88.

48. Cabrera LE, Schmotz C, Saleem MA, Lehtonen S, Vapalahti O, Vaheri A, Makela S, Mustonen J, Strandin T. Increased heparanase levels in urine during acute puumala orthohantavirus infection are associated with disease severity. Viruses. 2022;14:450.
49. Xu C, Chang A, Hack BK, Eadon MT, Alper SL, Cunningham PN. TNF-mediated damage to glomerular endothelium is an important determinant of acute kidney injury in sepsis. Kidney Int. 2014;85:72–81.
50. Jia Y, Pang C, Zhao K, Jiang J, Zhang T, Peng J, Sun P, Qian Y. Garcinol suppresses IL-1beta-induced chondrocyte inflammation and osteoarthritis via inhibition of the NF-kappaB signaling pathway. Inflammation. 2019;42:1754–66.
51. Chen Y, Lin L, Tao X, Song Y, Cui J, Wan J. The role of podocyte damage in the etiology of ischemia-reperfusion acute kidney injury and post-injury fibrosis. BMC Nephrol. 2019;20:106.
52. Zhu MM, Wang L, Yang D, Li C, Pang ST, Li XH, Li R, Yang B, Lian YP, Ma L, et al. Wedelolactone alleviates doxorubicin-induced inflammation and oxidative stress damage of podocytes by IkappaK/IkappaB/NF-kappaB pathway. Biomed Pharmacother. 2019;117: 109088.
53. Tomsa AM, Alexa AL, Junie ML, Rachisan AL, Ciumarnean L. Oxidative stress as a potential target in acute kidney injury. PeerJ. 2019;7: e8046.
54. Giam B, Kaye DM, Rajapakse NW. Role of renal oxidative stress in the pathogenesis of the cardiorenal syndrome. Heart Lung Circ. 2016;25:874–80.
55. Lushchak VI. Free radicals, reactive oxygen species, oxidative stress and its classification. Chem Biol Interact. 2014;224:164–75.
56. Kishi S, Nagasu H, Kidokoro K, Kashihara N. Oxidative stress and the role of redox signalling in chronic kidney disease. Nat Rev Nephrol. 2024;20:101–19.
57. Sies H, Belousov VV, Chandel NS, Davies MJ, Jones DP, Mann GE, Murphy MP, Yamamoto M, Winterbourn C. Defining roles of specific reactive oxygen species (ROS) in cell biology and physiology. Nat Rev Mol Cell Biol. 2022;23:499–515.
58. Zuk A, Bonventre JV. Acute kidney injury. Annu Rev Med. 2016;67:293–307.
59. Venkatachalam MA, Weinberg JM, Kriz W, Bidani AK. Failed tubule recovery, AKI-CKD transition, and kidney disease progression. J Am Soc Nephrol. 2015;26:1765–76.
60. Plotnikov E, Ciarimboli G. Editorial: mitochondria in renal health and disease. Front Physiol. 2021;12: 707175.
61. Nath KA, Grande JP, Croatt AJ, Likely S, Hebbel RP, Enright H. Intracellular targets in heme protein-induced renal injury. Kidney Int. 1998;53:100–11.
62. Bhargava P, Schnellmann RG. Mitochondrial energetics in the kidney. Nat Rev Nephrol. 2017;13:629–46.
63. Lan R, Geng H, Singha PK, Saikumar P, Bottinger EP, Weinberg JM, Venkatachalam MA. Mitochondrial pathology and glycolytic shift during proximal tubule atrophy after ischemic AKI. J Am Soc Nephrol. 2016;27:3356–67.
64. Shimada K, Crother TR, Karlin J, Dagvadorj J, Chiba N, Chen S, Ramanujan VK, Wolf AJ, Vergnes L, Ojcius DM, et al. Oxidized mitochondrial DNA activates the NLRP3 inflammasome during apoptosis. Immunity. 2012;36:401–14.
65. Paerewijck O, Lamkanfi M. The human inflammasomes. Mol Aspects Med. 2022;88: 101100.
66. Kelley N, Jeltema D, Duan Y, He Y. The NLRP3 inflammasome: an overview of mechanisms of activation and regulation. Int J Mol Sci. 2019;20:3328.
67. Bai B, Yang Y, Wang Q, Li M, Tian C, Liu Y, Aung LHH, Li PF, Yu T, Chu XM. NLRP3 inflammasome in endothelial dysfunction. Cell Death Dis. 2020;11:776.
68. Bedoui S, Herold MJ, Strasser A. Emerging connectivity of programmed cell death pathways and its physiological implications. Nat Rev Mol Cell Biol. 2020;21:678–95.
69. Galluzzi L, Vitale I, Aaronson SA, Abrams JM, Adam D, Agostinis P, Alnemri ES, Altucci L, Amelio I, Andrews DW, et al. Molecular mechanisms of cell death: recommendations of the nomenclature committee on cell death 2018. Cell Death Differ. 2018;25:486–541.
70. Wan J, Kalpage HA, Vaishnav A, Liu J, Lee I, Mahapatra G, Turner AA, Zurek MP, Ji Q, Moraes CT, et al. Regulation of respiration and apoptosis by cytochrome c threonine 58 phosphorylation. Sci Rep. 2019;9:15815.
71. Speidel D. Transcription-independent p53 apoptosis: an alternative route to death. Trends Cell Biol. 2010;20:14–24.
72. Harrington JS, Ryter SW, Plataki M, Price DR, Choi AMK. Mitochondria in health, disease, and aging. Physiol Rev. 2023;103:2349–422.
73. Wang S, Long H, Hou L, Feng B, Ma Z, Wu Y, Zeng Y, Cai J, Zhang DW, Zhao G. The mitophagy pathway and its implications in human diseases. Signal Transduct Target Ther. 2023;8:304.
74. Tang D, Kang R, Berghe TV, Vandenabeele P, Kroemer G. The molecular machinery of regulated cell death. Cell Res. 2019;29:347–64.
75. Ichim G, Tait SW. A fate worse than death: apoptosis as an oncogenic process. Nat Rev Cancer. 2016;16:539–48.
76. Gudipaty SA, Conner CM, Rosenblatt J, Montell DJ. Unconventional ways to live and die: cell death and survival in development, homeostasis, and disease. Annu Rev Cell Dev Biol. 2018;34:311–32.
77. Wu Y, Dong G, Sheng C. Targeting necroptosis in anticancer therapy: mechanisms and modulators. Acta Pharm Sin B. 2020;10:1601–18.
78. Fatemikia H, Seyedabadi M, Karimi Z, Tanha K, Assadi M, Tanha K. Comparison of 99mTc-DMSA renal scintigraphy with biochemical and histopathological findings in animal models of acute kidney injury. Mol Cell Biochem. 2017;434:163–9.
79. Rizk DV, Meier D, Sandoval RM, Chacana T, Reilly ES, Seegmiller JC, DeNoia E, Strickland JS, Muldoon J, Molitoris BA. A novel method for rapid bedside measurement of GFR. J Am Soc Nephrol. 2018;29:1609–13.
80. Yan J, Wang Y, Zhang J, Liu X, Yu L, He Z. Rapidly blocking the calcium overload/ros production feedback loop to alleviate acute kidney injury via microenvironment-responsive BAPTA-AM/BAC co-delivery nanosystem. Small. 2023;19: e2206936.
81. Weisbord SD, Palevsky PM, Kaufman JS, Wu H, Androsenko M, Ferguson RE, Parikh CR, Bhatt DL, Gallagher M, Investigators PT. Contrast-associated acute kidney injury and serious adverse outcomes following angiography. J Am Coll Cardiol. 2020;75:1311–20.
82. Prowle JR, Forni LG, Bell M, Chew MS, Edwards M, Grams ME, Grocott MPW, Liu KD, McIlroy D, Murray PT, et al. Postoperative acute kidney injury in adult non-cardiac surgery: joint consensus report of the acute disease quality initiative and perioperative quality initiative. Nat Rev Nephrol. 2021;17:605–18.
83. Nadim MK, Forni LG, Mehta RL, Connor MJ Jr, Liu KD, Ostermann M, Rimmele T, Zarbock A, Bell S, Bihorac A, et al. COVID-19-associated acute kidney injury: consensus report of the 25th acute disease quality initiative (ADQI) workgroup. Nat Rev Nephrol. 2020;16:747–64.
84. Jentzer JC, Bihorac A, Brusca SB, Del Rio-Pertuz G, Kashani K, Kazory A, Kellum JA, Mao M, Moriyama B, Morrow DA, et al. Contemporary management of severe acute kidney injury and refractory cardiorenal syndrome: JACC council perspectives. J Am Coll Cardiol. 2020;76:1084–101.
85. Wang L, Zhang Y, Li Y, Chen J, Lin W. Recent advances in engineered nanomaterials for acute kidney injury theranostics. Nano Res. 2020;14:920–33.
86. Messerer DAC, Halbgebauer R, Nilsson B, Pavenstadt H, Radermacher P, Huber-Lang M. Immunopathophysiology of trauma-related acute kidney injury. Nat Rev Nephrol. 2021;17:91–111.
87. Dixit M, Doan T, Kirschner R, Dixit N. Significant acute kidney injury due to non-steroidal anti-inflammatory drugs: inpatient setting. Pharmaceuticals. 2010;3:1279–85.
88. Bukowski RM. Amifostine (Ethyol): dosing, administration and patient management guidelines. Eur J Cancer. 1996;32A(Suppl 4):S46-49.
89. Rushworth GF, Megson IL. Existing and potential therapeutic uses for N-acetylcysteine: the need for conversion to intracellular glutathione for antioxidant benefits. Pharmacol Ther. 2014;141:150–9.
90. Hassanzadeh P, Atyabi F, Dinarvand R. Linkers: The key elements for the creation of efficient nanotherapeutics. J Control Release. 2018;270:260–7.
91. Choi HS, Liu W, Liu F, Nasr K, Misra P, Bawendi MG, Frangioni JV. Design considerations for tumour-targeted nanoparticles. Nat Nanotechnol. 2010;5:42–7.
92. Du B, Jiang X, Das A, Zhou Q, Yu M, Jin R, Zheng J. Glomerular barrier behaves as an atomically precise bandpass filter in a sub-nanometre regime. Nat Nanotechnol. 2017;12:1096–102.
93. Hua S, Wu SY. Editorial: advances and challenges in nanomedicine. Front Pharmacol. 2018;9:1397.

94. Chan Y, Wu XH, Chieng BW, Ibrahim NA, Then YY. Superhydrophobic nanocoatings as intervention against biofilm-associated bacterial infections. Nanomaterials. 2021;11:1046.
95. Kamaly N, He JC, Ausiello DA, Farokhzad OC. Nanomedicines for renal disease: current status and future applications. Nat Rev Nephrol. 2016;12:738–53.
96. Patra JK, Das G, Fraceto LF, Campos EVR, Rodriguez-Torres MDP, Acosta-Torres LS, Diaz-Torres LA, Grillo R, Swamy MK, Sharma S, et al. Nano based drug delivery systems: recent developments and future prospects. J Nanobiotechnology. 2018;16:71.
97. Williams RM, Shah J, Tian HS, Chen X, Geissmann F, Jaimes EA, Heller DA. Selective nanoparticle targeting of the renal tubules. Hypertension. 2018;71:87–94.
98. Han SJ, Williams RM, D'Agati V, Jaimes EA, Heller DA, Lee HT. Selective nanoparticle-mediated targeting of renal tubular Toll-like receptor 9 attenuates ischemic acute kidney injury. Kidney Int. 2020;98:76–87.
99. Jiang D, Ge Z, Im HJ, England CG, Ni D, Hou J, Zhang L, Kutyreff CJ, Yan Y, Liu Y, et al. DNA origami nanostructures can exhibit preferential renal uptake and alleviate acute kidney injury. Nat Biomed Eng. 2018;2:865–77.
100. Hou J, Wang H, Ge Z, Zuo T, Chen Q, Liu X, Mou S, Fan C, Xie Y, Wang L. Treating acute kidney injury with antioxidative black phosphorus nanosheets. Nano Lett. 2020;20:1447–54.
101. Ruggiero A, Villa CH, Bander E, Rey DA, Bergkvist M, Batt CA, Manova-Todorova K, Deen WM, Scheinberg DA, McDevitt MR. Paradoxical glomerular filtration of carbon nanotubes. Proc Natl Acad Sci USA. 2010;107:12369–74.
102. Du B, Yu M, Zheng J. Transport and interactions of nanoparticles in the kidneys. Nat Rev Mater. 2018;3:358–74.
103. Miner JH. The glomerular basement membrane. Exp Cell Res. 2012;318:973–8.
104. Huang Y, Wang J, Jiang K, Chung EJ. Improving kidney targeting: The influence of nanoparticle physicochemical properties on kidney interactions. J Control Release. 2021;334:127–37.
105. Liu J, Yu M, Zhou C, Zheng J. Renal clearable inorganic nanoparticles: a new frontier of bionanotechnology. Mater Today. 2013;16:477–86.
106. Balogh L, Nigavekar SS, Nair BM, Lesniak W, Zhang C, Sung LY, Kariapper MS, El-Jawahri A, Llanes M, Bolton B, et al. Significant effect of size on the in vivo biodistribution of gold composite nanodevices in mouse tumor models. Nanomedicine. 2007;3:281–96.
107. Dolman ME, Harmsen S, Storm G, Hennink WE, Kok RJ. Drug targeting to the kidney: advances in the active targeting of therapeutics to proximal tubular cells. Adv Drug Deliv Rev. 2010;62:1344–57.
108. Gu X-R, Liu K, Deng Y-X, Xiang B-X, Zhou L-Y, Yin W-J, Huang J-X, Meng Y-C, Li D-K, Que R-M, et al. A renal-targeted gene delivery system derived from spermidine for arginase-2 silencing and synergistic attenuation of drug-induced acute kidney injury. Chem Eng J. 2024;486:150125.
109. Hu JB, Kang XQ, Liang J, Wang XJ, Xu XL, Yang P, Ying XY, Jiang SP, Du YZ. E-selectin-targeted sialic acid-PEG-dexamethasone micelles for enhanced anti-inflammatory efficacy for acute kidney injury. Theranostics. 2017;7:2204–19.
110. Ding C, Wang B, Zheng J, Zhang M, Li Y, Shen HH, Guo Y, Zheng B, Tian P, Ding X, Xue W. Neutrophil membrane-inspired nanorobots act as antioxidants ameliorate ischemia reperfusion-induced acute kidney injury. ACS Appl Mater Interfaces. 2023;15:40292–303.
111. Yao S, Wu D, Hu X, Chen Y, Fan W, Mou X, Cai Y, Yang X. Platelet membrane-coated bio-nanoparticles of indocyanine green/elamipretide for NIR diagnosis and antioxidant therapy in acute kidney injury. Acta Biomater. 2024;173:482–94.
112. Shen Y, Yang F, Wu F, Zhang M, Deng B, Wu Z, Li J, Shen Y, Wang L, Ding F, Liu J. STING antagonist-loaded renal tubule epithelial cell-mimicking nanoparticles ameliorate acute kidney injury by orchestrating innate and adaptive immunity. Nano Today. 2024;55:102209.
113. Zhao S, Tian R, Wu J, Liu S, Wang Y, Wen M, Shang Y, Liu Q, Li Y, Guo Y, et al. A DNA origami-based aptamer nanoarray for potent and reversible anticoagulation in hemodialysis. Nat Commun. 2021;12:358.
114. Li J, Wei L, Zhang Y, Wu M. Tetrahedral DNA nanostructures inhibit ferroptosis and apoptosis in Cisplatin-induced renal injury. ACS Appl Bio Mater. 2021;4:5026–32.
115. Li W, Wang C, Lv H, Wang Z, Zhao M, Liu S, Gou L, Zhou Y, Li J, Zhang J, et al. A DNA nanoraft-based cytokine delivery platform for alleviation of acute kidney injury. ACS Nano. 2021;15:18237–49.
116. Li H, Fan R, Zou B, Yan J, Shi Q, Guo G. Roles of MXenes in biomedical applications: recent developments and prospects. J Nanobiotechnology. 2023;21:73.
117. Zhao X, Wang LY, Li JM, Peng LM, Tang CY, Zha XJ, Ke K, Yang MB, Su BH, Yang W. Redox-mediated artificial non-enzymatic antioxidant MXene Nanoplatforms for acute kidney injury alleviation. Adv Sci. 2021;8: e2101498.
118. Deng L, Xiao M, Wu A, He D, Huang S, Deng T, Xiao J, Chen X, Peng Y, Cao K. Se/Albumin nanoparticles for inhibition of ferroptosis in tubular epithelial cells during acute kidney injury. ACS Appl Nano Mater. 2022;5:227–36.
119. Qiu M, Wang D, Liang W, Liu L, Zhang Y, Chen X, Sang DK, Xing C, Li Z, Dong B, et al. Novel concept of the smart NIR-light-controlled drug release of black phosphorus nanostructure for cancer therapy. Proc Natl Acad Sci USA. 2018;115:501–6.
120. Li L, Yu Y, Ye GJ, Ge Q, Ou X, Wu H, Feng D, Chen XH, Zhang Y. Black phosphorus field-effect transistors. Nat Nanotechnol. 2014;9:372–7.
121. Zhou W, Cui H, Ying L, Yu XF. Enhanced cytosolic delivery and release of CRISPR/Cas9 by black phosphorus nanosheets for genome editing. Angew Chem Int Ed Engl. 2018;57:10268–72.
122. Wang H, Yang X, Shao W, Chen S, Xie J, Zhang X, Wang J, Xie Y. Ultrathin black phosphorus nanosheets for efficient singlet oxygen generation. J Am Chem Soc. 2015;137:11376–82.
123. Ethordevic L, Arcudi F, Cacioppo M, Prato M. A multifunctional chemical toolbox to engineer carbon dots for biomedical and energy applications. Nat Nanotechnol. 2022;17:112–30.
124. Wang H, Liu X, Yan X, Fan J, Li D, Ren J, Qu X. A MXene-derived redox homeostasis regulator perturbs the Nrf2 antioxidant program for reinforced sonodynamic therapy. Chem Sci. 2022;13:6704–14.
125. Wang H, Yu D, Fang J, Zhou Y, Li D, Liu Z, Ren J, Qu X. Phenol-like group functionalized graphene quantum dots structurally mimicking natural antioxidants for highly efficient acute kidney injury treatment. Chem Sci. 2020;11:12721–30.
126. Zhu Z, Liu X, Li P, Wang H, Zhang Y, Liu M, Ren J. Renal clearable quantum dot-drug conjugates modulate labile iron species and scavenge free radicals for attenuating chemotherapeutic drug-induced acute kidney injury. ACS Appl Mater Interfaces. 2023;15:21854–65.
127 Kang T, Kim YG, Kim D, Hyeon T. Inorganic nanoparticles with enzyme-mimetic activities for biomedical applications. Coord Chem Rev. 2020;403:213092.
128. Zandieh M, Liu J. Nanozymes: definition, activity, and mechanisms. Adv Mater. 2024;36: e2211041.
129. Xu C, Qu X. Cerium oxide nanoparticle: a remarkably versatile rare earth nanomaterial for biological applications. NPG Asia Materials. 2014;6:e90–e90.
130. Yang Y, Mao Z, Huang W, Liu L, Li J, Li J, Wu Q. Redox enzyme-mimicking activities of CeO(2) nanostructures: intrinsic influence of exposed facets. Sci Rep. 2016;6:35344.
131. Heckert EG, Karakoti AS, Seal S, Self WT. The role of cerium redox state in the SOD mimetic activity of nanoceria. Biomaterials. 2008;29:2705–9.
132. Gao X, Wang B, Li J, Niu B, Cao L, Liang XJ, Zhang J, Jin Y, Yang X. Catalytic tunable black phosphorus/ceria nanozyme: a versatile oxidation cycle accelerator for alleviating cisplatin-induced acute kidney injury. Adv Healthc Mater. 2023;12: e2301691.
133. Ni D, Jiang D, Kutyreff CJ, Lai J, Yan Y, Barnhart TE, Yu B, Im HJ, Kang L, Cho SY, et al. Molybdenum-based nanoclusters act as antioxidants and ameliorate acute kidney injury in mice. Nat Commun. 2018;9:5421.
134. Liu T, Xiao B, Xiang F, Tan J, Chen Z, Zhang X, Wu C, Mao Z, Luo G, Chen X, Deng J. Ultrasmall copper-based nanoparticles for reactive oxygen species scavenging and alleviation of inflammation related diseases. Nat Commun. 2020;11:2788.
135. Pan J, Wu T, Chen L, Chen X, Zhang C, Wang Y, Li H, Guo J, Jiang W. A bimetallic nanozyme coordinated with quercetin for efficient radical scavenging and treatment of acute kidney injury. Nanoscale. 2024;16:2955–65.
136. Meng L, Feng J, Gao J, Zhang Y, Mo W, Zhao X, Wei H, Guo H. Reactive oxygen species- and cell-free DNA-scavenging Mn(3)O(4)

nanozymes for acute kidney injury therapy. ACS Appl Mater Interfaces. 2022;14:50649–63.
137. Liu J, Huang X, Zhang F, Luo X, Yu W, Li C, Qiu Z, Liu Y, Xu Z. Metal-free multifunctional nanozymes mimicking endogenous antioxidant system for acute kidney injury alleviation. Chem Eng J. 2023;477:147048.
138. Zhao X, Sun J, Dong J, Guo C, Cai W, Han J, Shen H, Lv S, Zhang R. An auto-photoacoustic melanin-based drug delivery nano-platform for self-monitoring of acute kidney injury therapy via a triple-collaborative strategy. Acta Biomater. 2022;147:327–41.
139. Yin H, Kanasty RL, Eltoukhy AA, Vegas AJ, Dorkin JR, Anderson DG. Non-viral vectors for gene-based therapy. Nat Rev Genet. 2014;15:541–55.
140. Davis ME, Zuckerman JE, Choi CH, Seligson D, Tolcher A, Alabi CA, Yen Y, Heidel JD, Ribas A. Evidence of RNAi in humans from systemically administered siRNA via targeted nanoparticles. Nature. 2010;464:1067–70.
141. Castanotto D, Rossi JJ. The promises and pitfalls of RNA-interference-based therapeutics. Nature. 2009;457:426–33.
142. Kanasty R, Dorkin JR, Vegas A, Anderson D. Delivery materials for siRNA therapeutics. Nat Mater. 2013;12:967–77.
143. Alidori S, Akhavein N, Thorek DL, Behling K, Romin Y, Queen D, Beattie BJ, Manova-Todorova K, Bergkvist M, Scheinberg DA, McDevitt MR. Targeted fibrillar nanocarbon RNAi treatment of acute kidney injury. Sci Transl Med. 2016;8:331ra339.
144. Calin GA, Croce CM. MicroRNA signatures in human cancers. Nat Rev Cancer. 2006;6:857–66.
145. Hata A, Lieberman J. Dysregulation of microRNA biogenesis and gene silencing in cancer. Sci Signal. 2015;8:re3.
146. Selbach M, Schwanhausser B, Thierfelder N, Fang Z, Khanin R, Rajewsky N. Widespread changes in protein synthesis induced by microRNAs. Nature. 2008;455:58–63.
147. Zhang S, Sun H, Kong W, Zhang B. Functional role of microRNA-500a-3P-loaded liposomes in the treatment of cisplatin-induced AKI. IET Nanobiotechnol. 2020;14:465–9.
148. Liu S, Zhao M, Zhou Y, Li L, Wang C, Yuan Y, Li L, Liao G, Bresette W, Chen Y, et al. A self-assembling peptide hydrogel-based drug co-delivery platform to improve tissue repair after ischemia-reperfusion injury. Acta Biomater. 2020;103:102–14.
149. Liu D, Shu G, Jin F, Qi J, Xu X, Du Y, Yu H, Wang J, Sun M, You Y, et al. ROS-responsive chitosan-SS31 prodrug for AKI therapy via rapid distribution in the kidney and long-term retention in the renal tubule. Sci Adv. 2020. https://doi.org/10.1126/sciadv.abb7422.
150. Sun J, Zhao X, Shen H, Dong J, Rong S, Cai W, Zhang R. CD44-targeted melanin-based nanoplatform for alleviation of ischemia/reperfusion-induced acute kidney injury. J Control Release. 2024;368:1–14.
151. Nie Y, Wang L, Liu S, Dai C, Cui T, Lei Y, You X, Wang X, Wu J, Zheng Z. Natural ursolic acid based self-therapeutic polymer as nanocarrier to deliver natural resveratrol for natural therapy of acute kidney injury. J Nanobiotechnology. 2023;21:484.
152. Li Y, Wang G, Wang T, Li C, Zhang X, Li J, Wang Y, Liu N, Chen J, Su X. PEGylated gambogic acid nanoparticles enable efficient renal-targeted treatment of acute kidney injury. Nano Lett. 2023;23:5641–7.
153. Smith AM, Mancini MC, Nie S. Second window for in vivo imaging. Nat Nanotechnol. 2009;4:710–1.
154. Yan L, Gu Q-S, Jiang W-L, Tan M, Tan Z-K, Mao G-J, Xu F, Li C-Y. Near-infrared fluorescent probe with large stokes shift for imaging of hydrogen sulfide in tumor-bearing mice. Anal Chem. 2022;94:5514–20.
155. Ma X, Huang Y, Abedi SAA, Kim H, Davin TTB, Liu X, Yang W-C, Sun Y, Liu SH, Yin J, et al. Rational design and application of an indolium-derived heptamethine cyanine with record-long second near-infrared emission. CCS Chemistry. 2022;4:1961–76.
156. Liu H, Li C, Qian Y, Hu L, Fang J, Tong W, Nie R, Chen Q, Wang H. Magnetic-induced graphene quantum dots for imaging-guided photothermal therapy in the second near-infrared window. Biomaterials. 2020;232: 119700.
157. Geng B, Shen W, Fang F, Qin H, Li P, Wang X, Li X, Pan D, Shen L. Enriched graphitic N dopants of carbon dots as F cores mediate photothermal conversion in the NIR-II window with high efficiency. Carbon. 2020;162:220–33.
158. Gao P, Hui H, Guo C, Liu Y, Su Y, Huang X, Guo K, Shang W, Jiang J, Tian J. Renal clearing carbon dots-based near-infrared fluorescent super-small nanoprobe for renal imaging. Carbon. 2023;201:805–14.
159. Li J, Fu C, Feng B, Liu Q, Gu J, Khan MN, Sun L, Wu H, Wu H. Polyacrylic acid-coated selenium-doped carbon dots inhibit ferroptosis to alleviate chemotherapy-associated acute kidney injury. Adv Sci. 2024;11: e2400527.
160. Geng B, Shen W, Li P, Fang F, Qin H, Li XK, Pan D, Shen L. Carbon dot-passivated black phosphorus nanosheet hybrids for synergistic cancer therapy in the NIR-II window. ACS Appl Mater Interfaces. 2019;11:44949–60.
161. Zhang W, Shen Z, Wu Y, Zhang W, Zhang T, Yu BY, Zheng X, Tian J. Renal-clearable and biodegradable black phosphorus quantum dots for photoacoustic imaging of kidney dysfunction. Anal Chim Acta. 2022;1204: 339737.
162. Schröck E, du Manoir S, Veldman T, Schoell B, Wienberg J, Ferguson-Smith MA, Ning Y, Ledbetter DH, Bar-Am I, Soenksen D, et al. Multicolor spectral karyotyping of human chromosomes. Science (New York, NY). 1996;273:494–7.
163. Muhr V, Wilhelm S, Hirsch T, Wolfbeis OS. Upconversion nanoparticles: from hydrophobic to hydrophilic surfaces. Acc Chem Res. 2014;47:3481–93.
164. Ye M, Zhang J, Jiang D, Tan Q, Li J, Yao C, Zhu C, Zhou Y. A hemicyanine-assembled upconversion nanosystem for nir-excited visualization of carbon monoxide bio-signaling In Vivo. Small. 2022;18: e2202263.
165. Zhu H, Chen Y, Yan F-J, Chen J, Tao X-F, Ling J, Yang B, He Q-J, Mao Z-W. Polysarcosine brush stabilized gold nanorods for in vivo near-infrared photothermal tumor therapy. Acta Biomater. 2017;50:534–45.
166. Ding X, Liow CH, Zhang M, Huang R, Li C, Shen H, Liu M, Zou Y, Gao N, Zhang Z, et al. Surface plasmon resonance enhanced light absorption and photothermal therapy in the second near-infrared window. J Am Chem Soc. 2014;136:15684–93.
167 Zhao Z, He K, Liu B, Nie W, Luo X, Liu J. Intrarenal pH-responsive self-assembly of luminescent gold nanoparticles for diagnosis of early kidney injury. Angewandte Chem Int Edn. 2024;63:e202406016.
168. Wang Y, Yang F, Zhang HX, Zi XY, Pan XH, Chen F, Luo WD, Li JX, Zhu HY, Hu YP. Cuprous oxide nanoparticles inhibit the growth and metastasis of melanoma by targeting mitochondria. Cell Death Dis. 2013;4:e783–e783.
169. Hang Y, Wang A, Wu N. Plasmonic silver and gold nanoparticles: shape- and structure-modulated plasmonic functionality for point-of-caring sensing, bio-imaging and medical therapy. Chem Soc Rev. 2024;53:2932–71.
170. Panáček A, Kvítek L, Smékalová M, Večeřová R, Kolář M, Röderová M, Dyčka F, Šebela M, Prucek R, Tomanec O, Zbořil R. Bacterial resistance to silver nanoparticles and how to overcome it. Nat Nanotechnol. 2018;13:65–71.
171. Ding M, Zhang Y, Li X, Li Q, Xiu W, He A, Dai Z, Dong H, Shan J, Mou Y. Simultaneous biofilm disruption, bacterial killing, and inflammation elimination for wound treatment using silver embellished polydopamine nanoplatform. Small. 2024;10:e2400927.
172. Montaseri H, Kruger CA, Abrahamse H. Recent advances in porphyrin-based inorganic nanoparticles for cancer treatment. Int J Mol Sci. 2020;21:3358.
173. Pucelik B, Sułek A, Drozd A, Stochel G, Pereira MM, Pinto SMA, Arnaut LG, Dąbrowski JM. Enhanced cellular uptake and photodynamic effect with amphiphilic fluorinated porphyrins: the role of sulfoester groups and the nature of reactive oxygen species. Int J Mol Sci. 2020;21:2786.
174. Jin CS, Cui L, Wang F, Chen J, Zheng G. Targeting-triggered porphysome nanostructure disruption for activatable photodynamic therapy. Adv Healthcare Mater. 2014;3:1240–9.
175. Zhao H, Wang Y, Chen Q, Liu Y, Gao Y, Müllen K, Li S, Narita A. A nanographene-porphyrin hybrid for near-infrared-li phototheranostics. Adv Sci. 2024;11:e2309131.
176. Lin Y, Zhou T, Bai R, Xie Y. Chemical approaches for the enhancement of porphyrin skeleton-based photodynamic therapy. J Enzyme Inhib Med Chem. 2020;35:1080–99.
177. Cheng Y-Q, Yue Y-X, Cao H-M, Geng W-C, Wang L-X, Hu X-Y, Li H-B, Bian Q, Kong X-L, Liu J-F, et al. Coassembly of hypoxia-sensitive macrocyclic amphiphiles and extracellular vesicles for targeted kidney injury imaging and therapy. Journal of Nanobiotechnology. 2021;19:451.
178. Li J, Rao J, Pu K. Recent progress on semiconducting polymer nanoparticles for molecular imaging and cancer phototherapy. Biomaterials. 2018;155:217–35.

179. A DFT/TDDFT interpretation of the ground and excited states of porphyrin and porphyrazine complexes. *Coord Chem Rev*, 230: 5–27.
180. Korzdorfer T, Bredas JL. Organic electronic materials: recent advances in the DFT description of the ground and excited states using tuned range-separated hybrid functionals. Acc Chem Res. 2014;47:3284–91.
181. Verbeek FP, Schaafsma BE, Tummers QR, van der Vorst JR, van der Made WJ, Baeten CI, Bonsing BA, Frangioni JV, van de Velde CJ, Vahrmeijer AL, Swijnenburg RJ. Optimization of near-infrared fluorescence cholangiography for open and laparoscopic surgery. Surg Endosc. 2014;28:1076–82.
182. Frangioni JV. In vivo near-infrared fluorescence imaging. Curr Opin Chem Biol. 2003;7:626–34.
183. Li Q, Ding Q, Li Y, Zeng X, Liu Y, Lu S, Zhou H, Wang X, Wu J, Meng X, et al. Novel small-molecule fluorophores for in vivo NIR-IIa and NIR-IIb imaging. Chem Commun. 2020;56:3289–92.
184. Zhang Z, Fang X, Liu Z, Liu H, Chen D, He S, Zheng J, Yang B, Qin W, Zhang X, Wu C. Semiconducting polymer dots with dual-enhanced NIR-IIa fluorescence for through-skull mouse-brain imaging. Angew Chem Int Ed Engl. 2020;59:3691–8.
185. Troyan SL, Kianzad V, Gibbs-Strauss SL, Gioux S, Matsui A, Oketokoun R, Ngo L, Khamene A, Azar F, Frangioni JV. The FLARE intraoperative near-infrared fluorescence imaging system: a first-in-human clinical trial in breast cancer sentinel lymph node mapping. Ann Surg Oncol. 2009;16:2943–52.
186. Tummers QR, Schepers A, Hamming JF, Kievit J, Frangioni JV, van de Velde CJ, Vahrmeijer AL. Intraoperative guidance in parathyroid surgery using near-infrared fluorescence imaging and low-dose methylene blue. Surgery. 2015;158:1323–30.
187. Verbeek FP, van der Vorst JR, Schaafsma BE, Swijnenburg RJ, Gaarenstroom KN, Elzevier HW, van de Velde CJ, Frangioni JV, Vahrmeijer AL. Intraoperative near infrared fluorescence guided identification of the ureters using low dose methylene blue: a first in human experience. J Urol. 2013;190:574–9.
188. Tanaka E, Chen FY, Flaumenhaft R, Graham GJ, Laurence RG, Frangioni JV. Real-time assessment of cardiac perfusion, coronary angiography, and acute intravascular thrombi using dual-channel near-infrared fluorescence imaging. J Thorac Cardiovasc Surg. 2009;138:133–40.
189. Verbeek FP, Tummers QR, Rietbergen DD, Peters AA, Schaafsma BE, van de Velde CJ, Frangioni JV, van Leeuwen FW, Gaarenstroom KN, Vahrmeijer AL. Sentinel lymph node biopsy in vulvar cancer using combined radioactive and fluorescence guidance. Int J Gynecol Cancer. 2015;25:1086–93.
190. Hussain T, Nguyen QT. Molecular imaging for cancer diagnosis and surgery. Adv Drug Deliv Rev. 2014;66:90–100.
191. He X, Gao J, Gambhir SS, Cheng Z. Near-infrared fluorescent nanoprobes for cancer molecular imaging: status and challenges. Trends Mol Med. 2010;16:574–83.
192. de Boer E, Harlaar NJ, Taruttis A, Nagengast WB, Rosenthal EL, Ntziachristos V, van Dam GM. Optical innovations in surgery. Br J Surg. 2015;102:e56-72.
193. Wang F, Wan H, Ma Z, Zhong Y, Sun Q, Tian Y, Qu L, Du H, Zhang M, Li L, et al. Light-sheet microscopy in the near-infrared II window. Nat Methods. 2019;16:545–52.
194. Dang X, Bardhan NM, Qi J, Gu L, Eze NA, Lin CW, Kataria S, Hammond PT, Belcher AM. Deep-tissue optical imaging of near cellular-sized features. Sci Rep. 2019;9:3873.
195. Wang Z, Yu Y, Wu Y, Gao S, Hu L, Jian C, Qi B, Yu A. Dynamically monitoring lymphatic and vascular systems in physiological and pathological conditions of a swine model via a portable NIR-II imaging system with ICG. Int J Med Sci. 2022;19:1864–74.
196. Hu Z, Fang C, Li B, Zhang Z, Cao C, Cai M, Su S, Sun X, Shi X, Li C, et al. First-in-human liver-tumour surgery guided by multispectral fluorescence imaging in the visible and near-infrared-I/II windows. Nat Biomed Eng. 2020;4:259–71.
197. Cai Z, Zhu L, Wang M, Roe AW, Xi W, Qian J. NIR-II fluorescence microscopic imaging of cortical vasculature in non-human primates. Theranostics. 2020;10:4265–76.
198. Welsher K, Liu Z, Sherlock SP, Robinson JT, Chen Z, Daranciang D, Dai H. A route to brightly fluorescent carbon nanotubes for near-infrared imaging in mice. Nat Nanotechnol. 2009;4:773–80.
199. Hong G, Lee JC, Robinson JT, Raaz U, Xie L, Huang NF, Cooke JP, Dai H. Multifunctional in vivo vascular imaging using near-infrared II fluorescence. Nat Med. 2012;18:1841–6.
200. Hong G, Robinson JT, Zhang Y, Diao S, Antaris AL, Wang Q, Dai H. In vivo fluorescence imaging with Ag2S quantum dots in the second near-infrared region. Angew Chem Int Ed Engl. 2012;51:9818–21.
201 Bruns OT, Bischof TS, Harris DK, Franke D, Shi Y, Riedemann L, Bartelt A, Jaworski FB, Carr JA, Rowlands CJ, et al. Next-generation in vivo optical imaging with short-wave infrared quantum dots. Nat Biomed Eng. 2017. https://doi.org/10.1038/s41551-017-0056.
202. Bandi VG, Luciano MP, Saccomano M, Patel NL, Bischof TS, Lingg JGP, Tsrunchev PT, Nix MN, Ruehle B, Sanders C, et al. Targeted multicolor in vivo imaging over 1000 nm enabled by nonamethine cyanines. Nat Methods. 2022;19:353–8.
203. Wang S, Fan Y, Li D, Sun C, Lei Z, Lu L, Wang T, Zhang F. Anti-quenching NIR-II molecular fluorophores for in vivo high-contrast imaging and pH sensing. Nat Commun. 2019;10:1058.
204. Carr JA, Franke D, Caram JR, Perkinson CF, Saif M, Askoxylakis V, Datta M, Fukumura D, Jain RK, Bawendi MG, Bruns OT. Shortwave infrared fluorescence imaging with the clinically approved near-infrared dye indocyanine green. Proc Natl Acad Sci USA. 2018;115:4465–70.
205. Oliinyk OS, Ma C, Pletnev S, Baloban M, Taboada C, Sheng H, Yao J, Verkhusha VV. Deep-tissue SWIR imaging using rationally designed small red-shifted near-infrared fluorescent protein. Nat Methods. 2023;20:70–4.
206. Chen M, Feng Z, Fan X, Sun J, Geng W, Wu T, Sheng J, Qian J, Xu Z. Long-term monitoring of intravital biological processes using fluorescent protein-assisted NIR-II imaging. Nat Commun. 2022;13:6643.
207. Zhong Y, Ma Z, Wang F, Wang X, Yang Y, Liu Y, Zhao X, Li J, Du H, Zhang M, et al. In vivo molecular imaging for immunotherapy using ultra-bright near-infrared-IIb rare-earth nanoparticles. Nat Biotechnol. 2019;37:1322–31.
208. Wang R, Li X, Zhou L, Zhang F. Epitaxial seeded growth of rare-earth nanocrystals with efficient 800 nm near-infrared to 1525 nm short-wavelength infrared downconversion photoluminescence for in vivo bioimaging. Angew Chem Int Ed Engl. 2014;53:12086–90.
209. Wang R, Zhou L, Wang W, Li X, Zhang F. In vivo gastrointestinal drug-release monitoring through second near-infrared window fluorescent bioimaging with orally delivered microcarriers. Nat Commun. 2017;8:14702.
210. Baghdasaryan A, Wang F, Ren F, Ma Z, Li J, Zhou X, Grigoryan L, Xu C, Dai H. Phosphorylcholine-conjugated gold-molecular clusters improve signal for Lymph Node NIR-II fluorescence imaging in preclinical cancer models. Nat Commun. 2022;13:5613.
211. Ma H, Zhang X, Liu L, Huang Y, Sun S, Chen K, Xin Q, Liu P, Yan Y, Wang Y, et al. Bioactive NIR-II gold clusters for three-dimensional imaging and acute inflammation inhibition. Sci Adv. 2023;9:eadh7828.
212. Ji A, Lou H, Qu C, Lu W, Hao Y, Li J, Wu Y, Chang T, Chen H, Cheng Z. Acceptor engineering for NIR-II dyes with high photochemical and biomedical performance. Nat Commun. 2022;13:3815.
213. Antaris AL, Chen H, Cheng K, Sun Y, Hong G, Qu C, Diao S, Deng Z, Hu X, Zhang B, et al. A small-molecule dye for NIR-II imaging. Nat Mater. 2016;15:235–42.
214. Zhu S, Yang Q, Antaris AL, Yue J, Ma Z, Wang H, Huang W, Wan H, Wang J, Diao S, et al. Molecular imaging of biological systems with a clickable dye in the broad 800- to 1,700-nm near-infrared window. Proc Natl Acad Sci USA. 2017;114:962–7.
215. Tian R, Feng X, Wei L, Dai D, Ma Y, Pan H, Ge S, Bai L, Ke C, Liu Y, et al. A genetic engineering strategy for editing near-infrared-II fluorophores. Nat Commun. 2022;13:2853.
216. Hu X, Zhu C, Sun F, Chen Z, Zou J, Chen X, Yang Z. J-Aggregation Strategy toward potentiated NIR-II fluorescence bioimaging of molecular fluorophores. Adv Mater. 2024;36: e2304848.
217. Chen W, Cheng CA, Cosco ED, Ramakrishnan S, Lingg JGP, Bruns OT, Zink JI, Sletten EM. Shortwave infrared imaging with J-aggregates stabilized in hollow mesoporous silica nanoparticles. J Am Chem Soc. 2019;141:12475–80.
218. Zhong Y, Dai H. A mini-review on rare-earth down-conversion nanoparticles for NIR-II imaging of biological systems. Nano Res. 2020;13:1281–94.

219. Wang F, Jiang X, Xiang H, Wang N, Zhang Y, Yao X, Wang P, Pan H, Yu L, Cheng Y, et al. An inherently kidney-targeting near-infrared fluorophore based probe for early detection of acute kidney injury. Biosens Bioelectron. 2021;172: 112756.
220. Yang W, Liu R, Yin X, Jin Y, Wang L, Dong M, Wu K, Yan Z, Fan G, Tang Z, et al. Peroxynitrite activated near-infrared fluorescent probe for evaluating ferroptosis-mediated acute kidney injury. Sensors Actuators B Chem. 2023;393:134180.
221. Ding Y, Zhong R, Jiang R, Yang X, He L, Yuan L, Cheng D. Redox-reversible near-infrared fluorescent probe for imaging of acute kidney oxidative injury and remedy. ACS Sens. 2023;8:914–22.
222. Liu L, Jiang L, Yuan W, Liu Z, Liu D, Wei P, Zhang X, Yi T. Dual-Modality detection of early-stage drug-induced acute kidney injury by an activatable probe. ACS Sens. 2020;5:2457–66.
223. Ding F, Zhang S, Liu S, Feng J, Li J, Li Q, Ge Z, Zuo X, Fan C, Xia Q. Molecular visualization of early-stage acute kidney injury with a DNA framework nanodevice. Adv Sci. 2022;9: e2105947.
224. Weng J, Wang Y, Zhang Y, Ye D. An activatable near-infrared fluorescence probe for in vivo imaging of acute kidney injury by targeting phosphatidylserine and caspase-3. J Am Chem Soc. 2021;143:18294–304.
225. Tian Z, Yan F, Tian X, Feng L, Cui J, Deng S, Zhang B, Xie T, Huang S, Ma X. A NIR fluorescent probe for Vanin-1 and its applications in imaging, kidney injury diagnosis, and the development of inhibitor. Acta Pharm Sin B. 2022;12:316–25.
226. Jiang S, Hong J, Gong S, Li Q, Feng G. Kidney-targeted near-infrared fluorescence probe reveals that SO(2) is a biomarker for cisplatin-induced acute kidney injury. Anal Chem. 2023;95:12948–55.
227. Li S, Yang N, Ma Q, Li S, Tong S, Luo J, Song X, Yang H. Tailoring oxidation responsiveness of gold nanoclusters via ligand engineering for imaging acute kidney injury. Anal Chem. 2023;95:16153–9.
228. Zhao Z, Chen H, He K, Lin J, Cai W, Sun Y, Liu J. Glutathione-activated emission of ultrasmall gold nanoparticles in the second near-infrared window for imaging of early kidney injury. Anal Chem. 2023;95:5061–8.
229. Yi S, Hu Q, Chi Y, Qu H, Xiao Y. Bright and renal-clearable au nanoclusters with NIR-II excitation and emission for high-resolution fluorescence imaging of kidney dysfunction. ACS Materials Letters. 2023;5:2164–73.
230. Chen Y, Pei P, Lei Z, Zhang X, Yin D, Zhang F. A promising NIR-II fluorescent sensor for peptide-mediated long-term monitoring of kidney dysfunction. Angew Chem Int Ed Engl. 2021;60:15809–15.
231. Zeng C, Tan Y, Sun L, Long Y, Zeng F, Wu S. Renal-clearable probe with water solubility and photostability for biomarker-activatable detection of acute kidney injuries via NIR-II fluorescence and optoacoustic imaging. ACS Appl Mater Interfaces. 2023;15:17664–74.
232. Tan J, Yin K, Ouyang Z, Wang R, Pan H, Wang Z, Zhao C, Guo W, Gu X. Real-time monitoring renal impairment due to drug-induced AKI and diabetes-caused CKD using an NAG-activatable NIR-II nanoprobe. Anal Chem. 2021;93:16158–65.
233. Zhu D, Zhang H, Li J, Qian X, Guo M, Jiang G, Gu Y. Liposome-mediated biomimetic delivery of PLK3 inhibitor with NIR II-triggered release prevents renal ischemia-reperfusion injury. Adv Ther. 2022;5:2200087.
234. He K, Ding YF, Zhao Z, Liu B, Nie W, Luo X, Yu HZ, Liu J, Wang R. Cucurbit[7]uril-mediated organ-specific delivery of ultrasmall NIR-II luminescent gold nanocarriers for therapy of acute kidney injury. Adv Func Mater. 2023;34:2309949.
235. Huang Y, Chen K, Liu L, Ma H, Zhang X, Tan K, Li Y, Liu Y, Liu C, Wang H, Zhang XD. Single atom-engineered NIR-II gold clusters with ultrahigh brightness and stability for acute kidney injury. Small. 2023;19: e2300145.
236. Ge X, Su L, Yang L, Fu Q, Li Q, Zhang X, Liao N, Yang H, Song J. NIR-II fluorescent biodegradable nanoprobes for precise acute kidney/liver injury imaging and therapy. Anal Chem. 2021;93:13893–903.
237. Xu Y, Zhang Q, Chen R, Cao H, Tang J, Wu Y, Lu X, Chu B, Song B, Wang H, He Y. NIR-II photoacoustic-active DNA origami nanoantenna for early diagnosis and smart therapy of acute kidney injury. J Am Chem Soc. 2022;144:23522–33.
238. Gao H, Sun L, Li J, Zhou Q, Xu H, Ma XN, Li R, Yu BY, Tian J. Illumination of hydroxyl radical in kidney injury and high-throughput screening of natural protectants using a fluorescent/photoacoustic probe. Adv Sci. 2023;10: e2303926.

Publisher's Note